2000

Structure and Function Studies of De Novo Peptides Containing Novel Amino Acids.

Ted Joseph Gauthier
Louisiana State University and Agricultural & Mechanical College

INFORMATION TO USERS

This manuscript has been reproduced from the microfilm master. UMI films the text directly from the original or copy submitted. Thus, some thesis and dissertation copies are in typewriter face, while others may be from any type of computer printer.

The quality of this reproduction is dependent upon the quality of the copy submitted. Broken or indistinct print, colored or poor quality illustrations and photographs, print bleedthrough, substandard margins, and improper alignment can adversely affect reproduction.

In the unlikely event that the author did not send UMI a complete manuscript and there are missing pages, these will be noted. Also, if unauthorized copyright material had to be removed, a note will indicate the deletion.

Oversize materials (e.g., maps, drawings, charts) are reproduced by sectioning the original, beginning at the upper left-hand corner and continuing from left to right in equal sections with small overlaps.

Photographs included in the original manuscript have been reproduced xerographically in this copy. Higher quality 6" x 9" black and white photographic prints are available for any photographs or illustrations appearing in this copy for an additional charge. Contact UMI directly to order.

Bell & Howell Information and Learning
300 North Zeeb Road, Ann Arbor, MI 48106-1346 USA
800-521-0600

UMI®

STRUCTURE AND FUNCTION STUDIES OF *DE NOVO* PEPTIDES CONTAINING NOVEL AMINO ACIDS

A Dissertation

Submitted to the Graduate Faculty of the
Louisiana State University and
Agricultural and Mechanical College
in partial fulfillment of the
requirements for the degree of
Doctor of Philosophy

in

The Department of Chemistry

by
Ted Gauthier
B.S., Louisiana State University, 1985
M.S., Louisiana State University, 1988
B.S., Louisiana State University, 1995
December, 2000

Bell & Howell Information and Learning Company
300 North Zeeb Road
P.O. Box 1346
Ann Arbor, MI 48106-1346

Acknowledgements

I would like to thank my major professor, Dr. Mark McLaughlin, for his invaluable guidance and support throughout my studies at LSU. He always gave me the freedom to develop new ideas in my research and try them in the lab. I would also like to thank Dr. Robert Hammer for all the advice he has given me through the years.

None of the work I have done would have been possible without the help of Martha Juban. She was always there to help me with the synthesis and purification of my peptides. More importantly, she is as rabid an LSU fan as I am and was always willing to talk LSU sports. I will miss our chats greatly.

I would also like to thank Dr. Phil Elzer, Dr. Fred Enright and Sue Hagius for all the work done on the biological testing of the antimicrobial peptides; Dr. Tracy McCarley for the mass spectra; and Dr. Frank Fronczek for the crystal structure determinations.

I also greatly appreciated the contributions of past and present students in the McLaughlin group. Many thanks go to Dr. Scott Yokum for helping me with my laboratory work; to Lars Hammarström for assistance in the lab as well as immeasurable aid in solving crossword puzzles; and Umut Oguz for helping me complete my laboratory work. I would also like to thank my committee members: Dr. Mark McLaughlin, Dr. Robert Hammer, Dr. Paul Russo, Dr. Robert Strongin, and Dr. Witoon Prinyawiwatkul.

Finally, I would like to thank my family and friends for all their support. I could not have finished without their encouragement even though they thought I was nuts for going back to school, again!

Table of Contents

List of Tables

List of Figures

List of Abbreviations

ααAA	α,α-disubstituted amino acid
Aβ	Amyloid β-protein
AD	Alzheimer's Disease
Aib	α-Aminoisobutyric acid
Api	4-Aminopiperidine-4-carboxylic acid
ATCC	American Type Culture Collection
Ba	*Brucella abortus*
Boc	*tert*-Butyloxycarbonyl
BOP	Benzotriazolyloxy-tris(dimethylamino)phophonium hexafluorophosphate (BOP)
calcd	Calculated
CD	Circular Dichroism
cfu	Colony Forming Unit
CJD	Creutzfeldt-Jacob Disease
Cyh	1-Aminocyclohexane carboxylic acid
cm	Centimeter
d	Doublet
DBU	1,8-Diazobicyclo[4.5.0]undec-7-ene
DCE	1,2-Dichloroethane
DCM	Dichloromethane

deg	Degree
DIBAL	Diisobutyl aluminum hydride
DIEA	Diisopropylethylamine
DMAP	4-Dimehtylaminopyridine
DMEM	Dubelco's Modified Eagle Medium
DMF	*N,N*-dimethylformamide
dmol	Decimole
DMSO	Dimethylsulfoxide
DPU	Dipeptide unit
DTH	Delayed-type hypersensitivity
Et_3N	Triethylamine
Et_2O	Diethyl Ether
EtOAc	Ethyl Acetate
Equiv.	Equivalents
FAB	Fast atom bombardment
FCS	Fetal Calf Serum
Fmoc	9-Fluorenylmethyloxycarbonyl
GFP	Green fluorescent protein
h	Hour
HATU	*N*-[[(dimethylamino)-1*H*-1,2,3-triazolo[4,5-b]pyrindin-1-yl]methylene]-*N*-methylmethanaminium hexafluorophosphate *N*-oxide

HBTU	*O*-benzotriazolyl-*N,N,N',N'*-tetramethyluronium hexafluorophosphate
HOAt	1-Hydroxy-7-azabenzotriazole
HOBt	1-Hydroxybenzotriazole
HPLC	High Performance Liquid Chromatography
LCP	Left circularly polarized
m	Multiplet
Mϕ	Macrophage
MALDI	Matrix Assisted Laser Desorption Ionization
Mch	*Mycobacterium chelonei*
MHC	Major histocompatibility complex
MHz	Megahertz
MIC	Minimum Inhibitory Concentration
mL	Milliliter
mM	Millimolar
mmol	Millimole
MRW	Mean residue molecular weight
MS	Mass spectrometry
Mtb	*Mycobacterium tuberculosis*
μM	Micromolar
μg	Microgram
NCA	*N*-carboxyanhyride

nM	Nanomolar
NMR	Nuclear Magnetic Resonance
PAL	Peptide Amide Linker
PBS	Phosphate Buffered Saline
PEG	Polyethylene glycol
PrP	Prion protein
PS	Polystyrene
PyAOP	7-Azabenzotriazole-1-yloxytris(pyrrolindino)phosphonium hexafluorophosphate
RCP	Right circularly polarized
s	Singlet
SDS	Sodium Dodecyl Sulfate
SPPS	Solid-Phase Peptide Synthesis
t	Triplet
tb	Tuberculosis
TFA	Trifluoroacetic Acid
TFE	Trifluoroethanol
TFFH	Tetramethylfluoroformamidinium Hexafluorophosphate
THF	Tetrahydrofuran
TMS-Cl	Trimethylsilyl chloride
UV	Ultraviolet

Abstract

A series of amphipathic peptides rich in α, α-disubstituted amino acids (ααAA's) was synthesized and studied for antimicrobial activity and helix preferences in various solvent systems. In addition, a constrained lactam dipeptide amino acid was synthesized and incorporated into a peptide to examine β-sheet dimer formation.

Several short, amphipathic, 3_{10}- and α-helical peptides containing 80% ααAA's were synthesized using various combinations of 1-aminocyclohexane-1-carboxylic acid, α-aminoisobutyric acid, and 4-aminopiperidine-4-carboxylic acid. The peptides showed direct antimicrobial activity against *E. coli* and *S. aureus*. In addition, several of the peptides showed *in vivo* and *in vitro* activity against *Brucella abortus* and *Mycobacterium chelonei*. Studies were done with a strain of *B. abortus* expressing a green fluorescent protein to show the peptides selectively destroyed infected macrophages.

The series of amphipathic 3_{10}- and α-helical peptides were also studied, using circular dichroism spectroscopy, for their helix preference in organic and aqueous-organic solvent systems. The α-helical peptides showed the expected spectra in all solvents used. One designed 3_{10}-helical peptide exhibited a transition from a 3_{10}-helix to an α-helix as the water content was increased. The other designed 3_{10}-helical

peptide exhibited a spectrum indicative of an α-helix in all solvents tested, presumably due to steric interactions of the amino acid side-chains.

A constrained lactam dipeptide amino acid, 3-(R)-*N'*-[(9H-fluoren-9-ylmethoxy)carbonyl]-amino-1-[1-(S)-methylethylethanoic acid]-2-piperidinone, was synthesized from D-glutamic acid and incorporated into a peptide. The starting material was esterified with allyl alcohol and the α-nitrogen was doubly protected with Boc protecting groups. Selective DIBAL reduction of the side-chain ester yielded the semi-aldehyde. Reductive amination with valine followed by removal of the remaining allyl ester and intramolecular amide bond formation yielded the fully protected constrained lactam dipeptide amino acid. Treatment with TFA and introduction of the Fmoc protecting group resulted in the amino acid ready for peptide coupling. A peptide using the constrained amino acid was synthesized and studied for β-sheet dimer formation.

Chapter 1

Introduction

1.1 Introduction

The basic component of all proteins and peptides is the amino acid. There are approximately twenty encoded and hundreds of post-translationally modified amino acids in nature that have the general structure shown in Figure 1.1

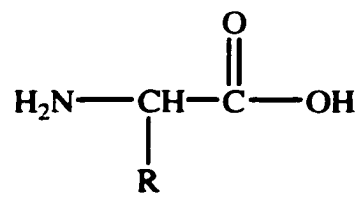

Figure 1.1. General structure of an amino acid.

As can be seen in Figure 1.1, the proteinogenic amino acids, with the exception of glycine, exist as enantiomers. In nature, the L-amino acid is the most common. The structures of the side chains of the twenty encoded amino acids are the distinguishing feature. The carbon atom bonded to the carbonyl carbon depicted in Figure 1.1 is designated as α and the atoms of the side chains are commonly designated as β, γ, δ, ε, ζ, in order away from the α carbon.

Amino acids that can be incorporated into proteins and peptides are not limited to the twenty encoded ones. Synthetic amino acids are routinely included in many protein and peptide sequences. Side chains that do not occur in biological systems distinguish synthetic amino acids from their natural counterparts. As a result, many synthetic amino

acids are incorporated into peptides to study their effects on the peptide's secondary structure.

1.2 Secondary Structures in Peptides

Amino acids can be chemically bonded to each other to form peptides and proteins. A peptide is generally considered a short chain of residues with a defined sequence. There is no maximum number of residues but if the physical properties of the chain are those expected from the sum of the residues and no fixed three-dimensional conformation exists, the term peptide is appropriate. The term protein is usually used for those polypeptides that occur in nature and have definite three-dimensional structure under physiological conditions.[1.1] This volume of work will focus on peptides.

The backbone of a peptide chain consists of a repeated sequence of three atoms of each residue in the chain – the amide N, the C^{α}, and the carbonyl C. These atoms are represented as N_i, C_i^{α}, and C_i', respectively, where i is the number of the residue starting from the amino end of the chain.

Peptides can adopt defined 3-D structures that are primarily stabilized by hydrogen bonds and secondarily by hydrophobic, electrostatic and steric interactions.[1.1-1.4] Helices and turns depend on intramolecular hydrogen bonds in the peptide chain for structural stability. β-sheets form as a result of either inter or intramolecular hydrogen bonds between peptide segments. Hydrophobic interactions further stabilize the β-sheet. Secondary structures that are not included above are classified as random coil. The random coil has no regular, repeating structure in significant stretches of the peptide chain.[1.4] The β-sheet results from two or more β-strands forming interchain hydrogen

bonds. Two types of β-sheet are known: anti-parallel and parallel.[1.1-1.4] The N→C sequence of the participating strands occur in the same direction in the parallel β-sheet. In the anti-parallel β-sheet, the N→C sequence is opposite in the participating strands. The β-strands comprising the β-sheet are almost fully extended with hydrogen bonds occurring between every other carbonyl oxygen and amide proton in the opposing strands. The hydrogen bonding patterns of the two types are shown in Figure 1.2.

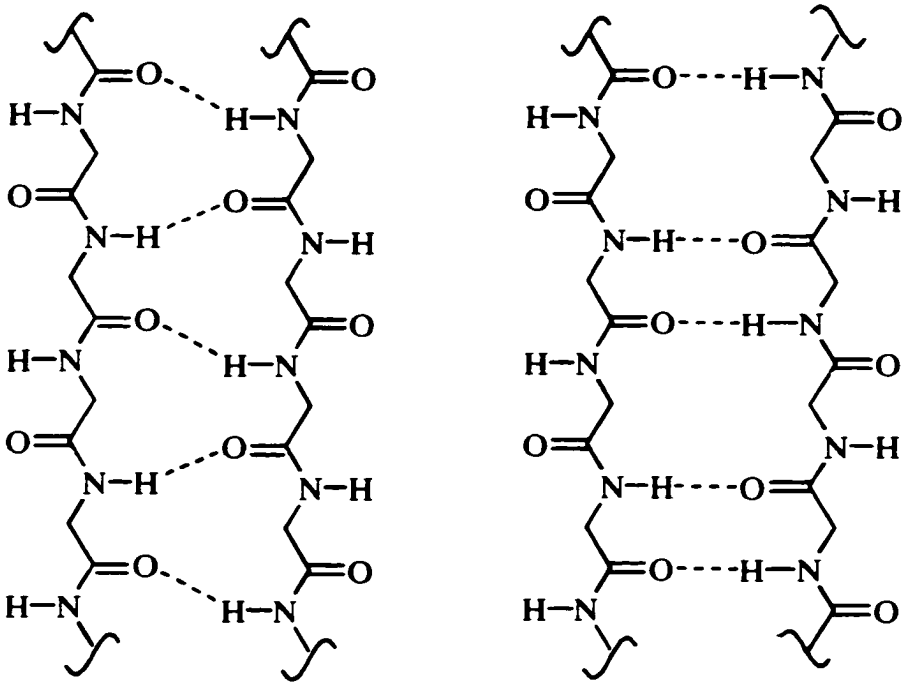

Figure 1.2. Hydrogen bonding patterns of the beta sheet structures.

Turns are types of secondary structures that help promote a change in direction of a peptide chain.[1.1, 1.3] Incorporation of a turn allows helices and β-sheets to fold back on themselves. Turns are distinguished by the number of residues they contain. β-Turns have four residues and a hydrogen bond between the carbonyl of the *i*th residue and the amide proton of the i^{th} + 3 residue. γ-Turns contain three residues and a hydrogen bond between the i^{th} and i^{th} + 2 residues. The types of turns are defined by the conformations of the i^{th} + 1 residue in the γ-turn and the i^{th} + 1 and i^{th} + 2 torsional angles in the β-turns.[1.3]

The most common secondary structure is the helix. Helices are stabilized by hydrogen bonds that are almost parallel to the helix axis. The hydrogen bond acceptors are the carbonyl oxygens while the hydrogen bond donors are the amide hydrogens. Side chain interactions, such as salt bridges, hydrophobic interactions and steric constraints, may further stabilize the helix.[1.1-1.4] The right-handed helix, promoted by L-amino acids, is the most common form of helix found in nature. The left-handed helix is promoted by D-amino acids and is far less common in nature. The two most common helices are the α-helix and the 3_{10}-helix. The α-helix comprises approximately 90% of all helices found in nature. In this helix type, the amide proton of the *i*th residue is the hydrogen bond donor while the carbonyl oxygen of the i^{th} + 4 residue is the hydrogen bond acceptor. There are 3.6 residues per turn and a pitch of 1.5Å per residue. The α-helix is also known as a 3.6_{13}-helix with 3.6 being the number of residues per turn and 13 being the number of atoms between the hydrogen bond donor and acceptor.[1.1-1.4]

The 3_{10}-helix comprises approximately 10% of all helical structures found in nature.[1.5, 1.6] The amide proton of the *i*th residue acts as the hydrogen bond donor while the carbonyl oxygen of the i^{th} + 3 residue acts as the hydrogen bond acceptor. This hydrogen bonding pattern results in a 10-membered ring. As a result, the 3_{10}- helix is more compact and longer than the α-helix.[1.3, 1.6] Figure 1.3 shows the hydrogen bonding patterns of the α-helix and 3_{10}-helix.

Determining secondary structure *a priori* from the amino acid sequence (known as primary structure) is the ultimate goal of peptide and protein chemistry. Ideally, if one wishes to design a peptide or protein with a particular secondary structure, we would only need to include those amino acids known to promote the desired structure. Unfortunately, this task is not so simple as many factors (i.e., hydrogen bonding, electrostatic and hydrophobic interactions) affect secondary structure. However, one can gain much information by studying the conformational restrictions placed on the peptide backbone.

Figure 1.4 shows the conventions used in describing peptide conformation. Rotations about bonds are defined as torsion or dihedral angles that lie from -180° to +180°. Rotation about the N-C^{α} bond is denoted by φ; rotation about the C^{α}-C′ bond by ψ; and rotation about C′-N by ω. Table 1.1 shows the ideal φ and ψ angles for the right-handed α-helix, antiparallel β-sheet, parallel β-sheet and 3_{10}-helix. Table 1.2 shows the dihedral angles for the residues in the γ-turn and several representative β-turns. Often, these values vary slightly in natural proteins, depending on the environment. These variations in the dihedral angles maximize hydrogen bonding, hydrophobic/electrostatic

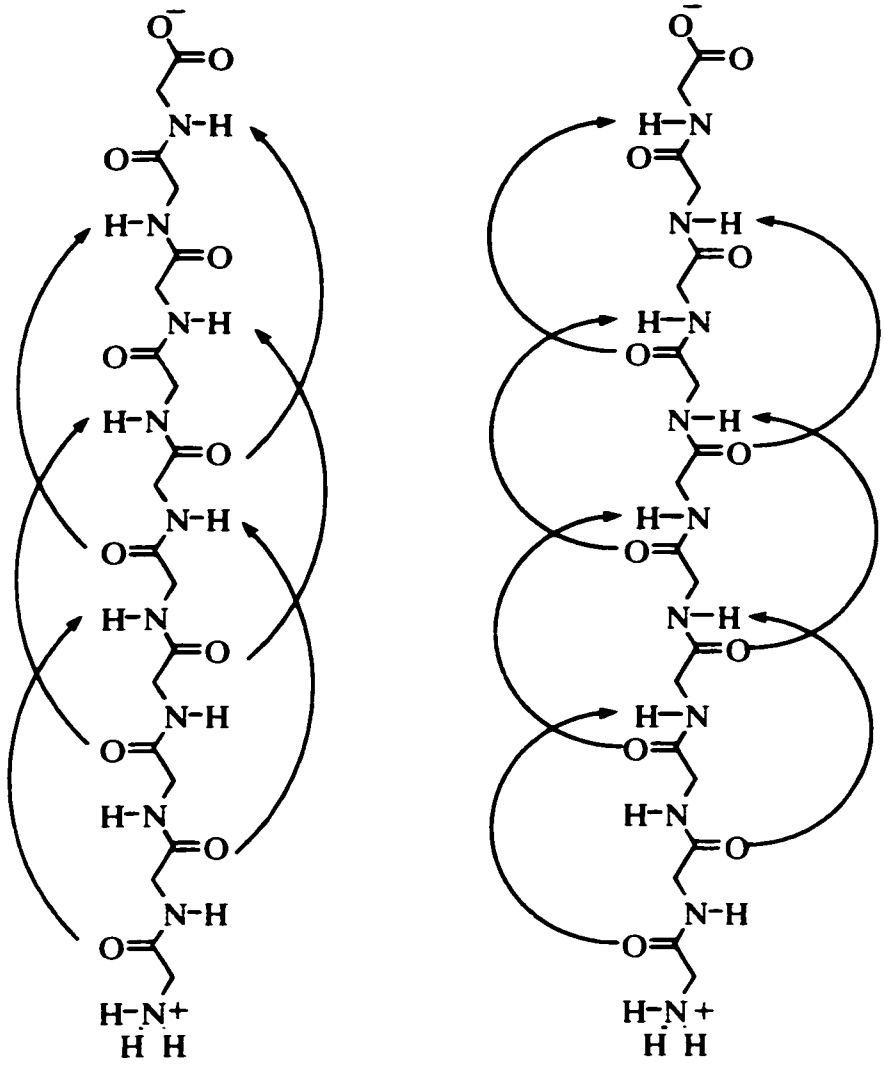

Figure 1.3. Hydrogen bonding patterns in helices.

Table 1.1

Dihedral angles for common secondary structures.[1.1]

	Bond Angle (deg)		
	ϕ	ψ	ω
Right-handed α-helix	-57	-47	180
Antiparallel β-sheet	-139	+135	-178
Parallel β-sheet	-119	+113	180
3_{10}-helix	-49	-26	180

Table 1.2

Common dihedral angles of selected γ and β turns.[1.1]

	Dihedral Angles of Central Residues (deg)[a]			
Bend type	ϕ_{i+1}	ψ_{i+1}	ϕ_{i+2}	ψ_{i+2}
Classical γ	70 to 85	-60 to –70	--	--
Type I′ β	60	30	90	0
Type II′ β	60	-120	-80	0

[a] The central residue of a γ turn is numbered $i + 2$; the two central residues of a β turn are $i + 2$ and $i + 3$.

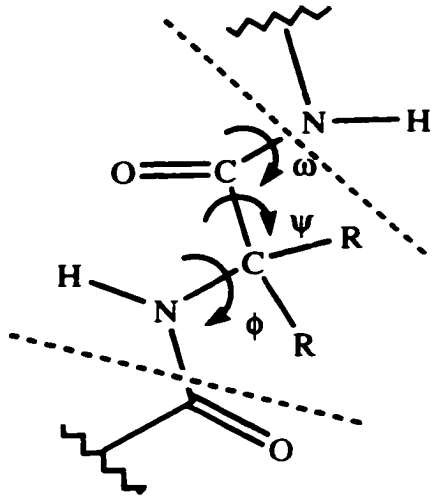

Figure 1.4. Torsion angles of the peptide bond.

interactions within the protein and interactions between the protein and the aqueous solvent. The values of ϕ and ψ available to amino acid residues in a particular secondary structure are indicated on a two-dimensional map of the ϕ-ψ plane known as a Ramachandran plot.[1.1]

1.3 Antimicrobial Peptides

Antimicrobial peptides have been isolated from many different organisms including insects, mammals, amphibians, bacteria and plants.[1.7] Antimicrobial peptides contain many structural similarities. While most are unstructured in aqueous media, many adopt an amphipathic α-helix in membrane environments.[1.8-1.10] Amphipathic alpha helices possess a hydrophobic or non-polar face and a hydrophilic or polar face. Peptides that contain an amphipathic α-helix tend to self-associate allowing the hydrophobic regions to interact while exposing polar regions to the polar media. Figure 1.5 shows a Schiffer-

Edmunson helical wheel diagram of the α-helix.[1.11] The wheel is shown looking down the helix axis from the C-terminus to the N-terminus. P represents the polar residues while N represents the non-polar residues.

Antimicrobial peptides are usually smaller than 40 residues long and contain virtually equal numbers of polar and non-polar residues. As a result, the polar face is usually less than 180°.[1.10] Cationic residues occur more often than anionic residues resulting in an overall positive charge at physiological pH.[1.12] Three classes of antimicrobial peptides have been extensively studied: melittin, magainins, and cecropins.[1.10, 1.13]

Isolated from the venom of the honeybee, *Apis mellifera*, melittin is a twenty-six residue antimicrobial peptide.[1.13] Like most antimicrobial peptides, melittin assumes no observable secondary structure in aqueous media at low concentrations but adopts an amphipathic α-helix at high concentrations or membrane environments.[1.10] Melittin exhibits broad spectrum antimicrobial activity with minimum inhibitory concentrations (MICs) in the μM range.[1.12] Melittin's highly hemolytic nature limits its therapeutic use.[1.10]

Cecropin A is a 37 residue antimicrobial peptide isolated form the North American silk moth, *Hyalophora cecropia*.[1.10] Cecropin A consists of two helical regions. Helix 1 adopts an amphipathic α-helix structure while helix 2 remains largely hydrophobic. This peptide exhibits high antimicrobial activity against representative

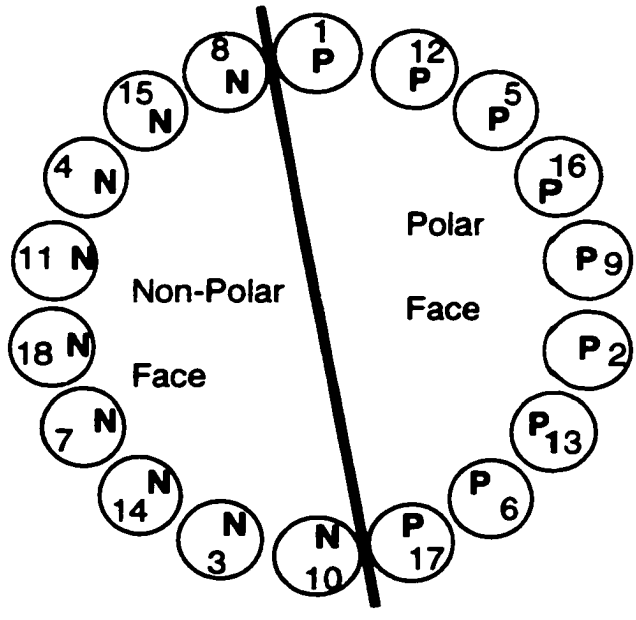

Figure 1.5. Helical wheel diagram of an amphipathic α-helix.

Gram-negative and Gram-positive bacteria while showing no hemolysis at these concentrations.[1.10]

Magainin 2 is a twenty-three residue antimicrobial peptide isolated from the skin of the frog *Xenopus laevis*. It too adopts an amphipathic α-helix in membrane environments. Magainin 2 possesses broad spectrum antimicrobial activities and is non-hemolytic at concentrations that are effective for antimicrobial activity.[1.14]

1.4 Mechanisms of Action of Antimicrobial Peptides

The target of antimicrobial peptides is the phospholipid bilayer of bacteria. The exact mechanism of action is not known. It is thought that the initial interaction between

the peptide and bacteria is an electrostatic interaction.[1.15] Two mechanisms of action on membranes have been proposed: the raft or carpet model and the barrel-stave or pore model.[1.15, 1.16] Figure 1.6 shows each. In the raft model, the amphipathic α-helical peptides first bind onto the surface of the target membrane. The target membrane can only be disrupted after a threshold peptide concentration has been reached. The peptide does not insert into the hydrophobic core of the membrane but binds to the phospholipid headgroups. The process of cell disruption via this method consists of four steps: (a) preferential binding of positively charged peptide monomers to the negatively charged phospholipid headgroups; (b) orientation of amphipathic α-helical monomers on the surface of the membrane so that the positively charged monomers can interact with the negatively charged phospholipid headgroups or water molecules; (c) partial insertion of the peptide into the membrane so that the hydrophobic residues interact with the hydrophobic core of the membrane; and (d) destroying the membrane by disrupting the bilayer curvature leading to micellization.[1.16] In the pore model, transmembrane amphipathic α-helices form bundles, in which their hydrophobic surfaces interact with the lipid core of the membrane. In this orientation, the hydrophilic surfaces point inward, producing a pore. In this model, the peptide binding to the membrane is driven by hydrophobic interactions. As a result, the peptide can bind to both zwitterionic and charged phospholipid membranes. Membrane destruction via this mechanism involves four steps: (a) binding of the helical peptide monomers to the membrane; (b) aggregation of the membrane bound monomers; (c) insertion of at least two assembled monomers into the membrane to begin the pore formation; and (d) recruitment of

additional monomers to increase the pore size leading to membrane disruption. Initial assembly of the monomers must occur before insertion into the cell membrane as it is energetically unfavorable for a single amphipathic α-helix to span the membrane as a monomer.[1.16]

1.5 Protein Structure and Amyloid Disorders

Many diseases are characterized by the presence of protein aggregates that form as fibrillar structures known amyloid plaques. These plaques are rich in beta sheet structures and insoluble under physiological conditions. Their presence may result from genetic anomalies, accumulation of over the lifetime of the individual or exposure to exogenous prion proteins. Among these diseases are Alzheimer's disease (AD), type II diabetes, Creutzfeldt-Jacob disease (CJD), Parkinson's and Huntington's diseases, kuru and bovine spongiform encephalopathy (mad cow disease). There has been much speculation about what role the fibrillar structures play in the pathology of these diseases. Two theories have evolved to explain the presence of the structures. One posits that the fibrillar structures are the causative agent of the diseases. The other suggests that the fibrils are a result linked to the disease but are not the causative agent.[1.17-1.20]

Many believe that the fibrils are the result of a normal protein misfolding to an abnormal isoform. This abnormal isoform is rich in beta sheet structures resulting in the formation of insoluble fibrils and protofibrils. Several proteins can misfold, each resulting in a different disease. For example, the protein associated with AD is the amyloid β -peptide (Aβ) while the protein for CJD and other encepholapathies is the prion protein (PrP).[1.17-1.19] Since the amyloid plaques associated with all of these

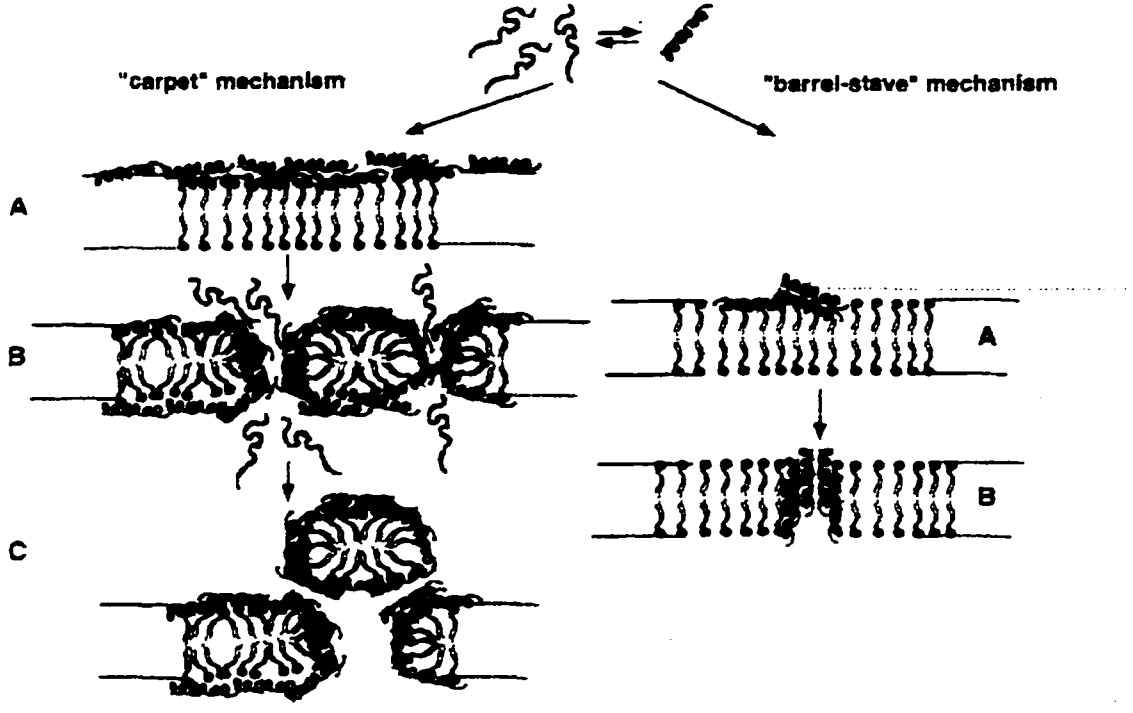

Figure 1.6. Mechanisms of action of antimicrobial peptides.[1.16]

diseases are comprised largely of beta sheets, it would be beneficial to study the factors that form and stabilize this secondary structure. If these factors can be elucidated, it may be possible to inhibit or even reverse the formation of the fibrillar structures linked to many of these degenerative diseases.

The beta sheet is the second most common secondary structure found in peptides and proteins, but relatively little is known about the factors that stabilize this structure. Very few beta sheet models lend themselves to detailed study.[1.21] Much of the recent work done to study beta sheets has centered around synthesizing unnatural amino acids to act as a turn thus nucleating beta sheet formation.[1.21-1.25] These amino acids are successful in promoting beta sheets because they effectively tie the strands together, thus overcoming entropy. As a result, the beta sheet formed is an intramolecular structure. Kelly reports that while the entropy barrier is significant, the resulting hydrogen bonds alone are insufficient to maintain the beta sheet structure.[1.22] It is believed that hydrophobic interactions are also necessary to stabilize the structure.[1.22] To date, there are no known peptides that have been synthesized to reversibly form an intermolecular beta sheet.

1.6 Peptide Synthesis

The synthesis of helical peptides requires amino acids that promote this secondary structure. The many studies that have investigated the helix-promoting capacity of the natural amino acids have focused on the frequency of these amino acids in helical regions of proteins and peptides or on the effects of substituting a proteinogenic amino

acid in the helical region of a peptide or protein.[1.26-1.28] These studies found that alanine, leucine, and lysine promote helical structures while proline and glycine break helical structures.[1.26, 1.27]

As peptide length decreases, the proteinogenic amino acids that promote helicity do so to the extent required. Other non-natural amino acids were then investigated for their helix promoting ability. The first discovered was α-aminoisobutyric acid (Aib). Its presence in the peptide, alamethicin, prompted investigators to postulate that Aib was a strong helix promoter. Alamethicin was found to be more helical than was predicted based on the natural amino acids.[1.29]

It has been shown that residues that are disubstituted at the α-carbon like Aib, where the R groups are not very large, promote helical structures. The presence of the additional R group limits the possible conformations of the residue in the peptide. As a result, the rotation of the ϕ, ψ angles is restricted. In the case of Aib, the angles are limited to $\phi \cong$ -60°/60° and $\psi \cong$ -30°/30° for the left-handed and right-handed 3_{10}-helices. For α-helices, $\phi \cong$ -55°/55° and $\psi \cong$ -45°/45° for the left-handed and right-handed helices.[1.30, 1.31]

Many other α,α-disubstituted amino acids (ααAA's) have been synthesized and their effects on secondary structure studied.[1.31-1.40] A series of ααAA's have been studied in which the R groups on the α-carbon are identical and are not in a ring system. Examples are diethylglycine, di-n-propylglycine, di-n-butylglycine, diphenylglycine and dibenzylglycine. These amino acids, unlike Aib, promote extended conformations.[1.31]

While larger, acyclic R groups promote extended conformations, cyclic, aliphatic ααAA's can promote helical structures. 1-Aminocyclobutane carboxylic acid, 1-aminocyclopentane carboxylic acid, 1-aminocyclohexane carboxylic acid and 1-amino cycloheptane carboxylic acid promote helical formation. 1-Aminocyclooctane carboxylic acid forms a 3_{10}-helix or β-bend structure while 1-aminocyclopropane carboxylic acid forms a distorted 3_{10}-helix.[1.31, 1.33]

In order to study amphipathic peptides containing ααAA's, several polar ααAA's have been synthesized.[1.37-1.40] These polar ααAA's are believed to promote the same secondary structures as their non-polar counterparts. Orthogonal protection of the side chain with respect to the α-amine or carboxylic acid is necessary for the incorporation of the amino acid into a peptide. As a result, incorporation of polar ααAA's allows one to synthesize water-soluble peptides that contain high percentage of ααAA's. In turn, these peptides can be designed to be amphipathic and used for biological studies.

1.7 Incorporation of α,α-Disubstituted Amino Acids Into Peptides

Incorporating ααAA's into a peptide has proven difficult.[1.32] The additional R group on the α-carbon substantially increases steric bulk, making ααAA couplings difficult.[1.41] Traditional coupling reagents such as carbodiimides (i.e. dicyclohexyl carbodiimide or diisopropyl carbodiimide) or 1-hydroxybenzotriazole (HoBT) rarely improve the yields of ααAA couplings.[1.42] In addition, (benzotriazolyloxy)-tris-(dimethylamino) phosphonium hexafluorophosphate or *O*-benzotriazolyl-*N*, *N*, *N'*, *N'*-tetramethyluronium hexafluorophosphate have not improved coupling yields.[1.41]

As a result of the limited success in ααAA couplings, new methods have been pursued to improve coupling yields. Acid chlorides, oxazolones, N-carboxyanhydrides (NCA's) and 2-(dimethylamino)-3,3′-dimethylozirine are a few of the methods used.[1.41, 1.43, 1.44] Each of these methods has improved ααAA coupling yields but each suffers disadvantages. Acid chloride use is limited because of harsh conditions for its formation and its tendency to form oxazolones.[1.43] NCA's and oxazolones suffer from side product formation accompanying the couplings. Hydrolysis following azirine coupling severely limits its usefulness in peptide synthesis.[1.41, 1.44]

Some degree of success has been recently achieved in improving ααAA coupling yields. The most noted are the use of acid fluorides or other coupling reagents such as 7-azabenzotriazole-1-yloxytris(pyrrolindino)phosphonium hexafluorophosphate (PyAOP) or N-[[dimethyl amino-)-1H-1,2,3-triazole[4,5-b]pyrindin-1-yl]methylene]-N-methylmethanaminium hexafluorophosphate N-oxide (HATU).[1.41, 1.45-1.48] The acid fluoride method developed by Carpino can give high ααAA couplings under mild conditions and is useful in either solution phase synthesis or solid phase peptide synthesis (SPPS).[1.41, 1.45, 1.46] The preformed acid fluorides are reacted with the free amine of another amino acid in the presence of base (e.g., N, N-diisopropylethylamine, DIEA). The acid fluoride can be prepared by treating the amino protected amino acid with cyanuric fluoride and pyridine or *in situ* with tetramethylfluorformamidinium hexafluorophosphate (TFFH).[1.49-1.51]

1.8 Effects of α,α-Disubstituted Amino Acids on Secondary Structure

As mentioned previously, the three major secondary structures are the α-helix, 3_{10}-helix and beta sheet. ααAA's have been shown to promote each of these structures. The beta sheet is usually promoted by ααAA's that have large, bulky α-substitutents.[1.31] Cyclic ααAA's, with 8-membered or smaller rings, and ααAA's with a methyl group as one of the α-substitutents promote 3_{10}-helices or α-helices. The preference for which helix type depends on the peptide design, the environment, location and number of ααAA's.

Many groups have studied the equilibrium between 3_{10}- and α-helices because the 3_{10}-helix is thought to be a folding intermediate to the α-helix and is thought to play a role in receptor binding.[1.52-1.55] Several studies have been done which characterize both helix types in short peptides containing ααAA's.[1.53-1.55] Until recently, the use of hydrophobic amino acids has prevented studies in aqueous media.

Many factors have been postulated for the prediction of the type of helix formed in short peptides rich in ααAA's. The length of the peptide, percentage of ααAA's, location of monosubstituted amino acids, and the solvent effects are among the major factors believed to be involved in the 3_{10}/α-helix equilibrium.[1.44, 1.52-1.59] Peptide length is believed to play an important role in helix preference. Karle reported that Aib rich peptides with five residues or less form 3_{10}-helices, while peptides with ten or more residues form α-helices.[1.53] Aib rich peptides between five and ten residues do not

appear to have a helix preference but many still believe peptide length is an important factor in preferential helix formation.[1.31, 1.53]

The percentage of ααAA's incorporated in a peptide is also believed to have an influence on helix formation. This factor is significant for medium length peptides (7-10 residues) which can form either a 3_{10}-helix or an α-helix. Peptides with at least seven residues and 50% or more ααAA's form a 3_{10}-helix while those containing less than 50% ααAA content favor an α-helix.[1.53]

It has been suggested that the location of monosubstituted amino acids in ααAA rich peptides is more important on the helix preference than the percentage of ααAA's.[1.44] This factor was studied using peptides containing 75% Aib residues. Incorporating two monosubstituted amino acids consecutively in the peptide sequence resulted in 3_{10}-helix formation.[1.44]

Helix preference may also be influenced by the media surrounding the peptide. The polarity of organic solvents used in crystallization and NMR studies has influenced helix preference.[1.55, 1.57-1.59] One experiment performed on an Aib rich peptide showed α-helix formation in dimethyl sulfoxide (DMSO) while the helix type shifted to a 3_{10}-helix when chloroform was used.[1.57] Another experiment with Aib rich peptides showed an α-helix is preferred when water is present and a 3_{10}-helix is preferred under anhydrous conditions.[1.58, 1.59] In crystallization experiments, an α-helix and 3_{10}-helix was obtained using methanol and methanol/ethyl ether solvent systems respectively.[1.55]

Based on these studies, it appears that polar solvents favor an α-helix while less polar solvents favor a 3_{10}-helix.

Theoretical calculations have been performed to further probe the effects of solvent polarity on helix preference. The α-helix appears to be favored thermodynamically while the 3_{10}-helix is favored entropically. The theoretical studies confirm what has been observed experimentally. Specifically, the 3_{10}-helix is favored in short, Aib-rich peptides while the α-helix is favored in longer peptides. In addition, the two helix types have the same energy in peptides with a length of 7.5 residues. This agrees with the observed data presented by Karle and others who report an equal helix preference for peptides between seven and ten residues.[1.53, 1.56] For peptides of this length, the solvent significantly affects the 3_{10}-/α-helix equilibrium.

To study the solvent effects on 3_{10}-/α-helix equilibrium, four media, vacuum, methylene chloride, acetonitrile, and water were examined using a poly-Aib 10-mer peptide. In lower polarity environments, the 3_{10}-helix is slightly more stable. As the polarity of the media increases, the α-helix becomes more stable. The correlation of α-helix stability to increasing solvent polarity can be attributed to peptide-solvent interactions. In a ten-residue peptide, the α-helix forms six intramolecular hydrogen bonds. This leaves three N-terminal amide hydrogens and four C-terminal carbonyl oxygens without internal hydrogen bonding partners. In a ten residue 3_{10}-helix, seven intramolecular hydrogen bonds are possible. This leaves two N-terminal amide protons and three C-terminal carbonyl oxygens without hydrogen bonding partners (Figure 1.3). As a result of the additional exposed carbonyl and amide protons, the α-helix has more

favorable interactions with the solvent thereby increasing stability. In non-polar environments, the 3_{10}-helix gains stability form the extra intramolecular hydrogen bonds present as compared to the α-helix.[1.56]

1.9 Characterization of Peptide Secondary Structure

There are several techniques, such as X-ray crystallography and NMR for the characterization of secondary structure. However, neither is as convenient and reliable as circular dichroism (CD). In ultraviolet-visible light spectroscopy, organic molecules absorb radiation via the promotion of electrons to higher energy molecular orbitals. Circular dichroism takes advantage of this phenomenon and carries it one step further.

Optically active (i.e., chiral) organic molecules rotate plane-polarized light. Plane polarized light can be resolved into its two circularly polarized components: left circularly polarized light (LCP) and right circularly polarized light (RCP). The electric vector of LCP rotates counterclockwise about the axis perpendicular to the direction of travel of the light beam while the electric vector of RCP rotates clockwise. A chiral molecule produces a circular dichroism spectrum because its absorption of LCP is not equal to its absorption of RCP. After passing through a chiral medium, the electric vectors describe an ellipse whose major axis lies along a new angle of rotation. The measured eccentricity of the ellipse represents the unequal absorption of LCP and RCP referred to as circular dichroism. Analogous to Beer's law, the experimentally measured ellipticity is equal to θcd where θ is the molar value in radians, c is the molar concentration and d is the cell path length in centimeters. A circular dichroism spectrum plots the molar ellipticity versus wavelength.[1.60-1.62]

CD is useful in determining the secondary structure of peptides because in the absence of aromatic amino acid residues, only the peptide backbone contributes significantly in the far UV region as the spectrum reflects the spatial arrangement of chiral units in the peptide chain. The presence of aromatic amino acids induces a positive CD signal, causing significant errors in ellipticity values.[1.63-1.65] The three main classes of secondary structure, the alpha helix, 3_{10}-helix, and beta sheet as well as the random coil, can be distinguished by their CD spectra. Figure 1.7 shows the typical CD spectrum for each of these secondary structures.[1.61]

Helical peptides, the α-helix and 3_{10}-helix, exhibit two minima near 208 nm ($\pi \rightarrow \pi^*_{\parallel}$) and 222 nm ($n \rightarrow \pi^*_{\parallel}$) and a positive band near 195 nm ($\pi \rightarrow \pi^*_{\perp}$). The 3_{10}-helix and the α-helix spectra are very similar but can be easily distinguished. The ratio, R, of the intensity of the 222 nm band divided by the intensity of the minimum near 208 nm is used to differentiate between the 3_{10}-helix and the α-helix. The ratio is approximately 1 for the α-helix, while the ratio is 0.4 or less for the 3_{10}-helix. Also, the positive band near 195 nm is much weaker for the 3_{10}-helix as compared to the α-helix. Few CD spectra of 3_{10}-helices have been reported. To date, experimental spectra reported agree well with the theoretically calculated 3_{10}-helix CD spectra.[1.60, 1.66-1.69]

The β-sheet and random coil, are easily distinguished from each other. The β-sheet exhibits a negative band near 217 nm representing an $n \rightarrow \pi^*$ transition and a positive band near 195 nm representing a $\pi \rightarrow \pi^*$ transition. The random coil exhibits a strong negative band near 197 nm ($\pi \rightarrow \pi^*$) and a small positive band at 217 nm ($n \rightarrow \pi^*$).[1.60]

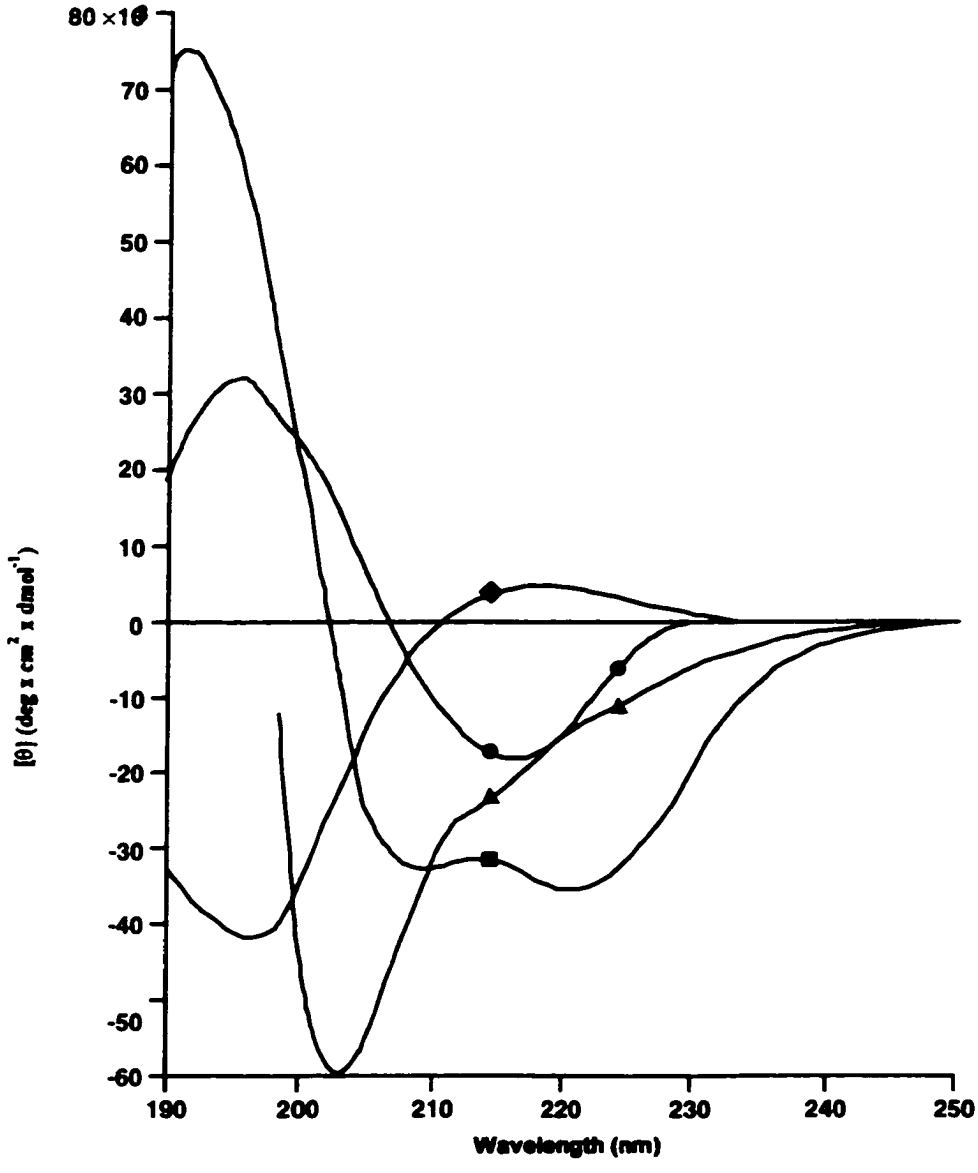

Figure 1.7. Typical CD spectra for the α-helix (■), 3_{10}-helix (▲), β-sheet (●) and random coil (◆).[1.60, 1.70]

Peptide conformation is highly sensitive to solution variables; a peptide may be insoluble in one condition, but well behaved under others. In characterizing the secondary structure of peptides by CD, the effect of pH, ionic strength of the buffer and peptide concentration should be examined. As a general rule, aggregation increases with peptide concentration, ionic strength or pH. Concentration dependence reveals whether the peptide is monomeric or self-associating. For example, a shift from random coil to beta sheet as the peptide concentration increases indicates an association equilibrium. Self-association may be obtained by changing pH (usually increasing) to titrate the amino groups present in the peptide sequence or by changing the ionic strength of the buffer to optimize charge screening. Variations in these parameters are examined systematically in an effort to determine the number and type of species present in the solution. Stable equilibrium between only two states are identified by the presence of an isodichroic point.[1.60, 1.61]

1.10 References

1.1 Creighton, T.E., *Proteins: Structure and Molecular Properties*. 2nd ed. 1993, New York: W.H. Freeman and Co.

1.2 Gutte, B., ed. *Peptides: Synthesis, Structures and Applications*. 1995, Academic Press: New York.

1.3 Moore, M.L., ed. *Synthetic Peptides: A User's Guide*., 1992, W. H. Freeman and Co.: USA.

1.4 Walton, A.G., *Polypeptides and Protein Structure*. 1981, New York: Elsevier.

1.5 Smythe, M.L., Huston, S.E., and Marshall, G.R., *J. Am. Chem. Soc.*, **1995,** *117*, 5445-5452.

1.6 Toniolo, C. and Benedetti, E., *Trends Biochem. Sci.*, **1991,** *16*, 350-353.

1.7 Zhong, L., Putnam, R.J., Johnson, W.C., and Rao, A.G., *Int. J. Pept. Protein Res.*, **1995,** *45*, 337-347.

1.8 Mchaourab, H.S., Hyde, J.S., and Feix, J.B., *Biochemistry*, **1993,** *32*, 11895-11902.

1.9 Marion, D., Zasloff, M., and Bax, A., *FEBS Lett.*, **1988,** *227*, 21-26.

1.10 Saberwal, G. and Nagaraj, R., *Biochim. Biophys. Acta*, **1994,** *1197*, 109-131.

1.11 Schiffer, M. and Edmunson, A.B., *Biophys. J.*, **1967,** *7*, 121-135.

1.12 Javadpour, M.M., Juban, M.M., Lo, W.J., Bishop, S.M., Alberty, J.B., Cowell, S.M., Becker, C.L., and McLaughlin, M.L., *J. Med. Chem.*, **1996,** *39*, 3107-3113.

1.13 Dempsey, C.E., *Biochim. Biophys. Acta*, **1990,** *1031*, 143-161.

1.14 Tyler, E.M., Anantharamaiah, G.M., Walker, D.E., Mishra, V.K., Palgunachari, M.N., and Segrest, J.P., *Biochemistry*, **1995,** *34*, 4393-4401.

1.15 Bessalle, R., Gorea, A., Shalit, I., Metzger, J.W., Dass, C., Desiderio, D.M., and Fridkin, M., *J. Med. Chem.*, **1993,** *36*, 1203-1209.

1.16 Oren, Z. and Shai, Y., *Biopolymers (Peptide Science)*, **1999,** *47*, 451-463.

1.17 Horwich, A.L. and Weissman, J.S., *Cell*, **1997,** *89*, 499-510.

1.18 Pan, K.M., Baldwin, M., Nguyen, J., Gasset, M., Serban, A., Groth, D., Mehlhorn, I., Huang, Z., Gletterick, R.J., Cohen, F.E., and Prusiner, S.B., *Proc. Natl. Acad. Sci. USA*, **1993,** *90*, 10962-10966.

1.19 Nguyen, J., Baldwin, M.A., Cohen, F.E., and Prusiner, S.B., *Biochemistry*, **1996,** *34*, 4186-4192.

1.20 Lansbury, P.T., *Proc. Natl. Acad. Sci. USA*, **1999,** *96*, 3342-3344.

1.21 Diaz, H.D., Tsang, K.Y., Choo, D., and Kelly, J.W., *Tetrahedron*, **1993,** *49*, 3533-3545.

1.22 McWilliams, K. and Kelly, J.W., *J. Org. Chem.*, **1996,** *61*, 7408-7414.

1.23 Doig, A.J., *Chem. Commun.*, **1997**, 2153-2154.

1.24 Tsang, K.Y., Diaz, H., Graciani, N., and Kelly, J.W., *J. Am. Chem. Soc.*, **1994,** *116*, 3988-4005.

1.25 Kemp, D.S. and Li, Z.Q., *Tetrahedron Lett.*, **1995,** *36*, 4175-4178.

1.26 O'Neil, K.T. and DeGrado, W.F., *Science*, **1990,** *250*, 646-651.

1.27 Scholtz, J.M. and Baldwin, R.L., *Annu. Rev. Biophys. Biomol. Struct.*, **1992,** *21*, 95-118.

1.28 Chou, P.Y. and Fasman, G.D., *Adv. Enzymol. Rel. Areas Mol. Biol.*, **1978,** *47*, 45-148.

1.29 Nagaraj, R. and Balaram, P., *Acc. Chem. Res.*, **1981,** *14*, 356-362.

1.30 Karle, I.L. and Balaram, P., *Biochemistry*, **1990,** *29*, 6747-6756.

1.31 Benedetti, E., *Biopolymers (Peptide Sci.)*, **1996,** *40*, 3-44.

1.32 Balaram, P., *Curr. Opin. Struct. Biol.*, **1992,** *2*, 845-851.

1.33 Toniolo, C., Crimsa, M., Formaggio, F., Benedetti, E., Santini, A., Iacovino, R., Diblasio, B., Pedone, C., and Kamphuis, J., *Biopolymers (Peptide Sci.)*, **1996,** *40*, 519-522.

1.34 Burgess, K., Ho, K., and Pettitt, B.M., *J. Am. Chem. Soc.*, **1995,** *117*, 54-65.

1.35 Burgess, K., Ho, K., and Pal, B., *J. Am. Chem. Soc.*, **1995,** *117*, 3808-3819.

1.36 Formaggio, F., Toniolo, C., Crisma, M., Valle, G., Kaptein, B., Schoemaker, H.E., Kamphuis, J., DiBlasio, B., Maglio, O., Fattorusso, R., Benedetti, E., and Santini, A., *Int. J. Pept. Protein Res*, **1995,** *45*, 70-77.

1.37 Gershonov, E., Granoth, R., Tzehoval, E., Gaoni, Y., and Fridkin, M., *J. Med. Chem.*, **1996,** *39*, 4833-4843.

1.38 Curry, K., Peet, M.J., Magnuson, D.S.K., and McLennan, H.J., *J. Med. Chem.*, **1988,** *31*, 864-867.

1.39 Kozikowski, A.P. and Fauq, A.H., *Synlett*, **1991**, 783-784.

1.40 Alonso, F., Mico, I., Najera, C., Sansano, J.M., and Yus, M., *Tetrahedron*, **1995,** *51*, 10259-10280.

1.41 Wenschuh, H., Beyermann, M., Krause, E., Brudel, M., Winter, R., Schumann, M., Carpino, L.A., and Bienert, M., *J. Org. Chem.*, **1994,** *59*, 3275-3280.

1.42 Ferot, E., Coste, J., Pantaloni, A., Dufour, M., and Jouin, P., *Tetrahedron*, **1991,** *47*, 259-270.

1.43 Carpino, L.A., Chao, H.G., Beyermann, M., and Bienert, M., *J. Org. Chem.*, **1991,** *56*, 2635-2642.

1.44 Basu, G., Bagchi, K., and Kuki, A., *Biopolymers*, **1991,** *31*, 1763-1774.

1.45 Wenschuh, H., Beyermann, M., El-Faham, A., Ghassemi, S., Carpino, L.A., and Bienert, M., *J. Chem. Soc., Chem. Commun.*, **1995**, 669-670.

1.46 Wenschuh, H., Beyermann, M., Haber, H., Seydel, J.K., Krause, E., Bienert, M., Carpino, L.A., El-Faham, A., and Albericio, F., *J. Org. Chem.*, **1995,** *60*, 405-410.

1.47 Carpino, L.A., El-Faham, A., Minor, C.A., and Albericio, F., *J. Chem. Soc., Chem. Commun.*, **1994**, 201-203.

1.48 Albericio, F., Cases, M., Alsina, J., Triolo, S.A., Carpino, L.A., and Kates, S.A., *Tetrahedron Lett.*, **1997,** *38*, 4853-4856.

1.49 Carpino, L.A., Sadat-Aalaee, D., Chao, H.C., and DeSelms, R.H., *J. Am. Chem. Soc.*, **1990,** *112*, 9651-9652.

1.50 Carpino, L.A., Mansour, E.M.E., and Sadat-Aalaee, D., *J. Org. Chem.*, **1991,** *56*, 2611-2614.

1.51 Carpino, L.A. and El-Faham, A., *J. Am. Chem. Soc.*, **1995,** *117*, 5401-5402.

1.52 Smythe, M.L., Huston, S.E., and Marshall, G.R., *J. Am. Chem. Soc.*, **1993,** *115*, 11594-11595.

1.53 Karle, I.L., Flippen-Andersen, J.L., Gurunath, R., and Balaram, P., *Protein Sci.*, **1994,** *3*, 1547-1555.

1.54 Basu, G. and Kuki, A., *Biopolymers*, **1992,** *32*, 61-71.

1.55 Otoda, K., Kitagawa, Y., Kimura, S., and Imanishi, Y., *Biopolymers*, **1993,** *33*, 1337-1345.

1.56 Myers, A.G., Gleason, J.L., Yoon, T., and Kung, D.W., *J. Am. Chem. Soc.*, **1997,** *119*, 656-673.

1.57 Vijayakumar, E.K.S. and Balaram, P., *Biopolymers*, **1983,** *22*, 2133-2140.

1.58 Karle, I.L., Sukumar, M., and Balaram, P., *Proc. Natl. Acad. Sci. USA*, **1986,** *83*, 9284-9288.

1.59 Karle, I.L., Flippen-Andersen, J.L., Sukumar, M., and Balaram, P., *Int. J. Pept. Protein Res.*, **1988,** *31*, 567-576.

1.60 Fasman, G.D., ed. *Circular Dichroism and the Conformational Analysis of Biomolecules.*. 1996, Plenum Press: New York.

1.61 Johnson, W.C., *Proteins: Structure, Function and Genetics*, **1990,** *7*, 205-214.

1.62 Purdle, N. and Swallows, K.A., *Analytical Chemistry*, **1989,** *61*, 77A-89A.

1.63 Manning, M.C. and Woody, R.W., *Biochemistry*, **1989,** *28*, 8609-8613.

1.64 Chakrabartty, A., Kortemme, T., Padmanabhan, S., and Baldwin, R.L., *Biochemistry*, **1993,** *32*, 5560-5565.

1.65 Krittanai, C. and Johnson, W.C., *Analytical Biochemistry*, **1997,** *253*, 57-64.

1.66 Toniolo, C., Polese, A., Formaggio, F., Crimsa, M., and Kamphius, J., *J. Am. Chem. Soc.*, **1996,** *118*, 2744-2745.

1.67 Manning, M.C. and Woody, R.W., *Biopolymers*, **1991,** *31*, 569-586.

1.68 Iwata, T., S., L., Oishi, O., Aoyagi, H., Ohno, M., Anzai, K., Kirino, Y., and Sugihara, G., *J. Biol. Chem.*, **1994,** *269*, 4928-4933.

1.69 Hungerford, G., Martinez-Insua, M., Birch, D.J.S., and Moore, B.D., *Angew. Chem. Int. Ed. Engl.*, **1996,** *35*, 326-329.

1.70 Rossi, P., Felluga, F., Tecilla, P., Formaggio, F., Crisma, M., Toniolo, C., and Scrimin, P., *J. Am. Chem. Soc.*, **1999,** *121*, 6948-6949.

Chapter 2

α, α-Disubstituted Amino Acid Rich Peptides Active Against Intracellular Pathogens

2.1 Introduction

While antibiotics have saved countless lives by fighting bacterial infections, bacteria are increasingly resistant to their effects.[2.1-2.3] This has stimulated the search for new antimicrobial agents with modes of action different from those of known antibiotics. Antimicrobial peptides are thought to be one solution to this problem.[2.4] Though the mechanism of action of these peptides is still debated, there is agreement that they disrupt the cell membranes of susceptible cells.[2.5-2.7] The reason for this selectivity is also unclear but it has been postulated that exterior membrane charge differences, membrane potential differences, cholesterol content and differences in the rate of membrane repair contribute to the selective activity of the peptides.[2.8-2.12] There is also evidence that there is a distinction between antimicrobial peptides (those with direct action against bacteria) and cytotoxic peptides. Cytotoxic peptides, as well as antimicrobial peptides, have activity against altered mammalian cells.[2.11, 2.13] This result is intriguing as it suggests the possibility of using cytotoxic peptides to treat intracellular pathogens, which are especially difficult to eliminate because conventional antibiotic therapy and the host's immune response are ineffective.[2.14] *Brucella abortus* (*Ba*) and *Mycobacterium tuberculosis* (*Mtb*) are intracellular pathogens that live and replicate within the macrophages of their hosts.[2.15]

The veterinary pathogenic brucella species, *B. abortus, B. melitensis, B. suis* and *B. canis* are also pathogenic for man.[2.16, 2.17] They are short, non-motile, non-sporulating and non-encapsulated Gram-negative aerobic rods. In animals, brucella localizes in the reproductive organs, supramammary lymph nodes and other reticuloendothelial tissues resulting in abortion and infertility.[2.18] In humans, infection leads to a chronic, debilitating disease known as undulant fever.[2.19] Human infection may result from exposure to infected animals or infected animal products.[2.20] As a result, brucellosis is an occupational hazard for veterinarians, abattoir workers, animal handlers and laboratory staff.[2.21] The brucella species is easily spread via aerosolization, making them good candidates for biological weapons.[2.22]

Undulant fever is characterized by general malaise, fever, anorexia, muscular weakness, arthritis and dementia.[2.19] Other disorders associated with the disease include cardiac and neurologic disorders. If untreated, undulant fever is fatal in about 10% of the cases. Current treatment consists of lengthy antibiotic therapy with one or more drugs for 30 to 45 days. Relapses often occur after the treatment is stopped and the antibiotics do not relieve the symptoms. The vaccines used to control brucellosis in animals are not available for use in humans as they are virulent to man.

Brucella abortus is an intracellular pathogen that lives and replicates in a host's macrophages.[2.23-2.25] The ability to survive in a host's macrophages is a key element in allowing the organism to cause disease.[2.26] Intracellular brucellae are hidden from the

immune responses of the host and are not directly exposed to the complement cascade, neutrophils, brucella specific antibodies or conventional antibiotics.[2.27] Brucellosis requires alternative treatments.

Diseases caused by other intracellular pathogens would be potential targets for treatments developed for brucellosis. For example, the mycobacterium species of bacteria are intracellular pathogens that cause diseases that have etiologies similar to brucellosis. *Mycobacterium tuberculosis*, the causative agent of tuberculosis (Tb), infects about a third of the world's population and kills more people than any other infectious agent.[2.28] *Mtb* is a rod-shaped, acid-fast bacterium that localizes mainly in the respiratory systems of animals. The symptoms of tuberculosis include low-grade fever, night sweats, fatigue, weight loss and persistent cough. Tuberculosis is spread via aerosolization of the bacteria as a result of a cough or sneeze.[2.28] Like *Ba*, *Mtb* can live and replicate within a host's macrophages, making it especially difficult to treat. Current treatment consists of a prolonged regimen of multiple antibiotics. Many strains of mycobacterium now resist antibiotics, making the development of alternative treatments critical.

2.2 Cell Mediated Immune Responses to Intracellular Pathogens

Antimicrobial peptides have mechanisms of action different from that of antibiotics, thus making them interesting targets for drug design. Infection of mammalian cells by intracellular pathogens is particularly difficult to treat with conventional antibiotics alone due to the body's inability to completely eliminate the pathogens. In order to understand the significance of a novel mechanism of action by an

antimicrobial peptide, a review of the immunology of intracellular pathogen infection is warranted.

One of the body's responses to an infection is to engulf the invading bacteria using macrophages (Mϕ). Some of the macrophages kill the bacteria and process bacterial antigens for display on the major histocompatibility complex (MHC). CD4+ T-cells differentiate into T_{DTH}-cells (DTH = delayed-type hypersensitivity) within two to several weeks after infection. Figure 2.1 shows how the T_{DTH}-cells target infected macrophages. The T_{DTH}-cells recognize the infected macrophages presenting the bacterial antigen, which results in the invasion of a large number of activated macrophages. The activated macrophages sequester the infection inside a granuloma consisting of a few T_{DTH}-cells and many activated macrophages. The macrophages may differentiate into epitheloid cells or multinucleated giant cells. Figure 2.2 shows the anatomy of a granuloma. The activated macrophages usually repress the infection. Cytokines produced by T_{DTH}-cells inhibit further spread of the infection. IFN-γ is important in the body's response to mycobacterium infection. Knockout mice lacking IFN-γ died even when infected with an attenuated strain of *Mycobacterium sp.* (Bacillus Calmette-Guerin). Normal mice possessing IFN-γ survive this infection. Macrophages presenting bacterial antigens are also attacked by CD8+ T-cells that differentiate into cytolytic T-cells. Figure 2.3 shows the development and killing mechanism of cytolytic T-cells. The cytolytic T-cells release granules near the cell marked for eradication. The granules contain perforin monomers that oligomerize into large pores on the cell membrane, resulting in lysis of the cell. These immune responses are effective only against macrophages that process the intracellular pathogen and present bacterial

antigens. Infected cells that fail to process the intracellular pathogen will harbor the infection. The infection becomes asymptomatic after the development of hypersensitivity in most people. Furthermore, quiescent granuloma can also harbor viable intracellular pathogens, especially in the case of tuberculosis.[2.29]

2.3 Results

Table 2.1 lists the *de novo* amphipathic peptides used in this study. They are comprised of 80% α,α-disubstituted amino acids (ααAA's) and a natural amino acid residue. The design is based on antimicrobial peptides that occur in nature with the incorporation of the ααAA's to promote helicity. Table 2.2 lists several naturally occurring antimicrobial peptides. Studies have shown that amphipathic peptides with at least eighteen residues can have high cytotoxicity. [2.30, 2.31] Shortening the peptides to fourteen residues reduces cytotoxicity but maintains most of the antimicrobial activity.[2.30, 2.31] The peptides under discussion were part of a series of peptides synthesized in our lab to test the hypothesis that α-aminoisobutyric acid, Aib and Aib-like residues would stabilize helical conformations and maintain biological activity as the peptide length was decreased.[2.32] Various combinations of lysine with Aib, 1-amino-1-cyclohexanecarboxylic acid, Cyh, and 4-aminopiperidine-4-carboxylic acid, Api, were used in the peptides. Figure 2.4 shows the structures of these amino acids. The peptides were synthesized using acid fluorides developed by Carpino.[2.33-2.35]

The peptides were synthesized on a Milligen 9050 peptide synthesizer using PAL-PEG-PS support. The reactions were carried out in N,N-dimethylformamide

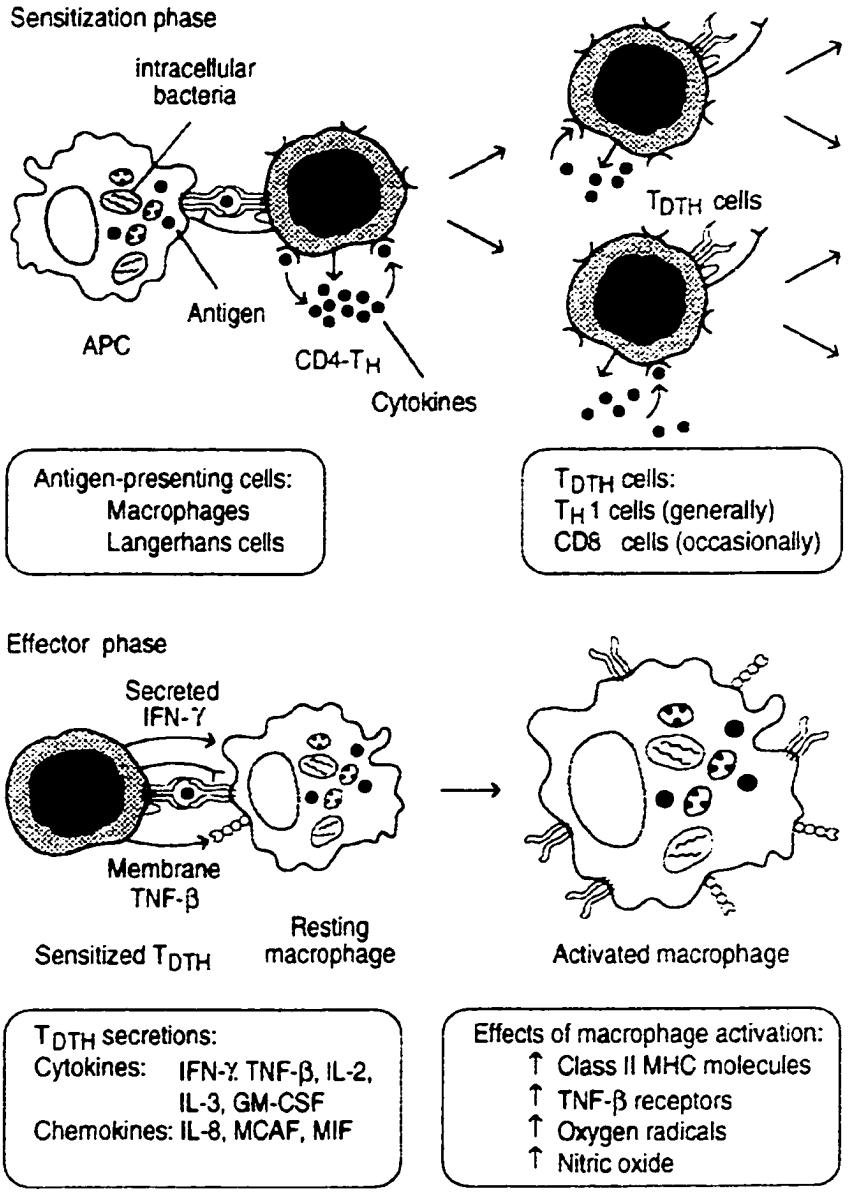

Figure 2.1. Delayed-type hypersensitivity (DTH) immune response.[2.29]

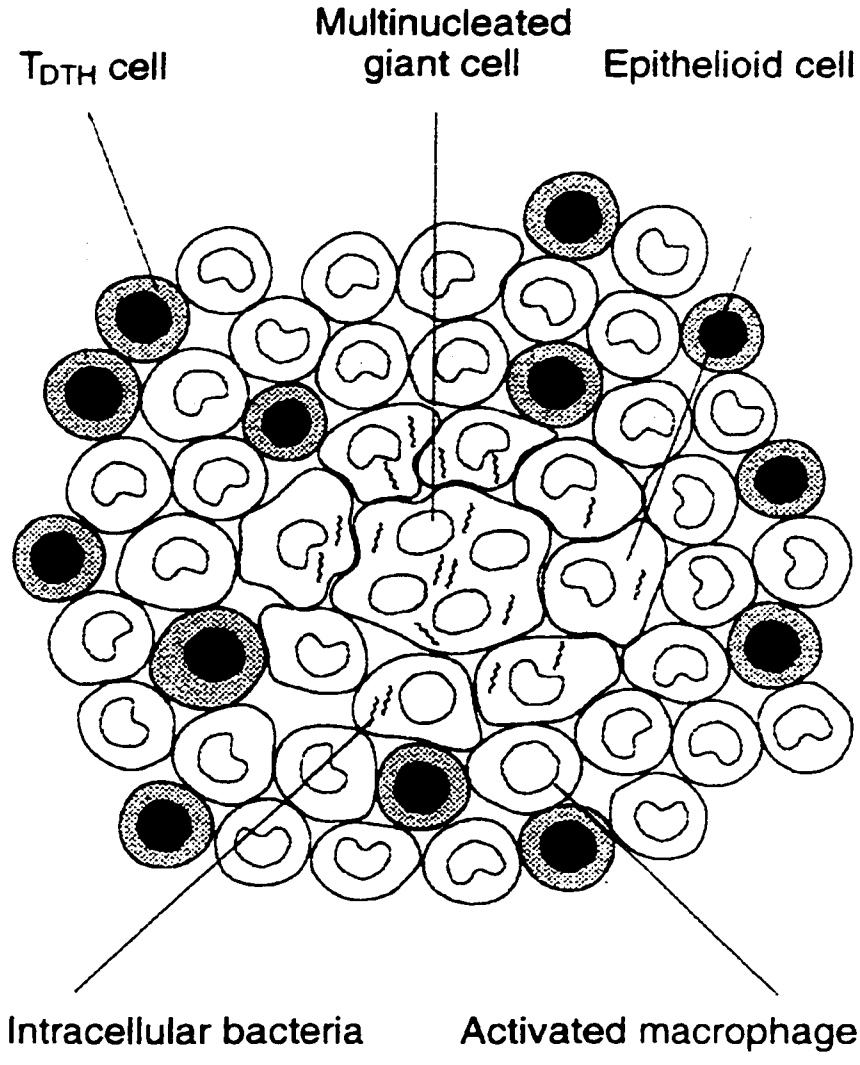

Figure 2.2. Anatomy of a granuloma.[2.29]

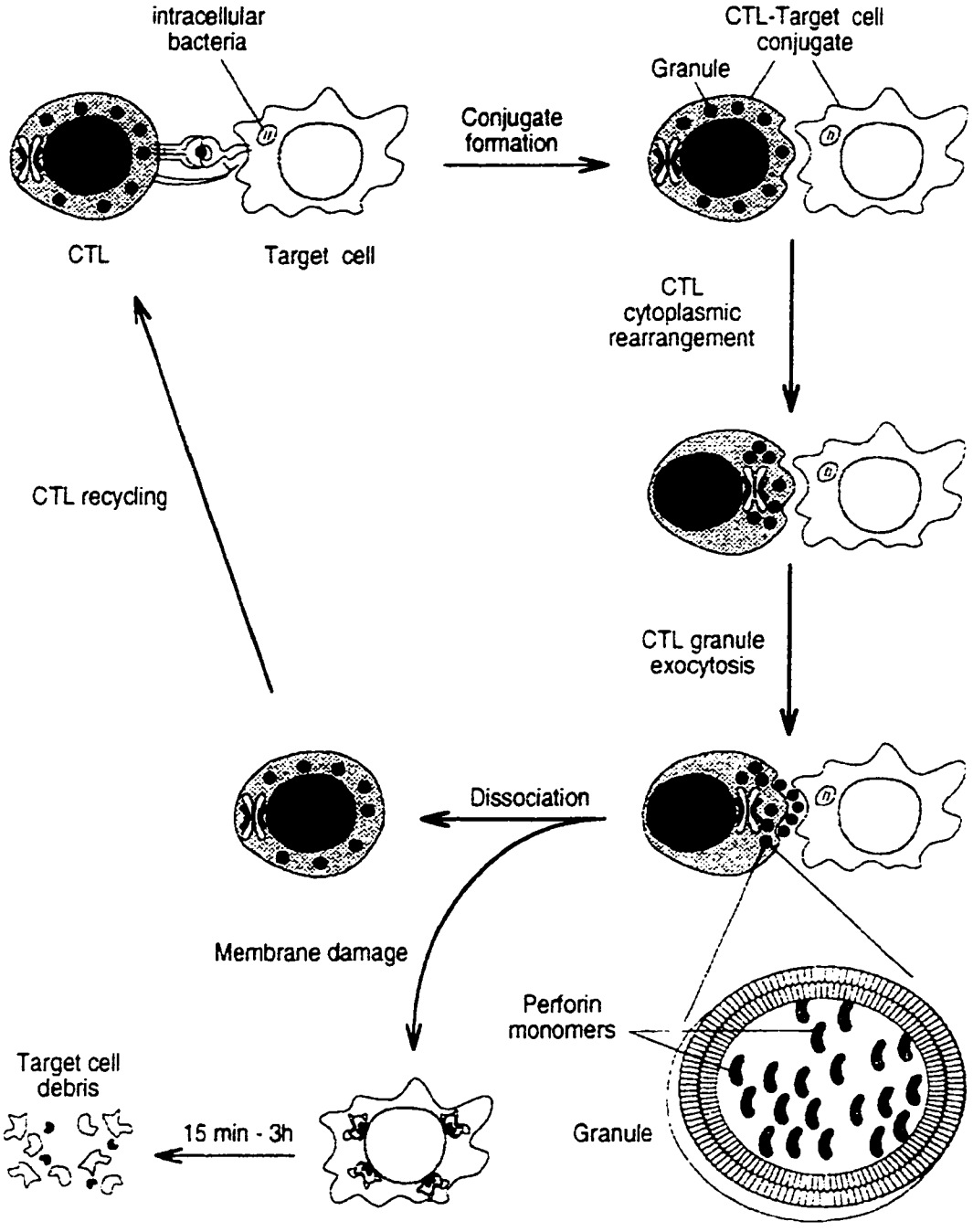

Figure 2.3. Development and killing mechanism of cytolytic T cells.[2.29]

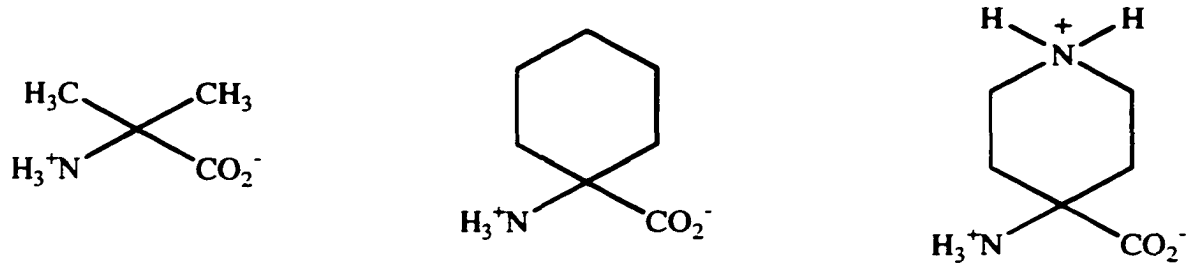

Aib **Cyh** **Api**

Figure 2.4. Structures of Aib, Cyh and Api amino acids.

Table 2.1

Sequences of *de novo* peptides.

Peptide	Sequence
Pi-10	Aib-Aib-Api-Lys-Aib-Aib-Api-Lys-Aib-Aib-NH_2
Ipi-10	Api-Aib-Aib-Lys-Aib-Aib-Lys-Aib-Aib-Api-NH_2
Cyh-10	Cyh-Cyh-Api-Lys-Cyh-Cyh-Api-Lys-Cyh-Cyh-NH_2
Ich-10	Api-Cyh-Cyh-Lys-Cyh-Cyh-Lys-Cyh-Cyh-Api-NH_2

Table 2.2

Sequences of naturally occurring antimicrobial peptides.

Peptide	Sequence
Melittin	Gly-Ile-Gly-Ala-Val-Leu-Lys-Val-Leu-Thr-Thr-Gly-Leu-Pro-Ala-Leu-Ile-Ser-Trp-Ile-Lys-Arg-Lys-Arg-Gln-Gln-NH_2
Cecropin B amide	Lys-Trp-Lys-Val-Phe-Lys-Lys-Ile-Glu-Lys-Met-Gly-Arg-Asn-Ile-Arg-Asn-Gly-Ile-Val-Lys-Ala-Gly-Pro-Ala-Ile-Ala-Val-Leu-Gly-Glu-Ala-Lys-Ala-Leu-NH_2
Magainin 2 amide	Gly-Ile-Gly-Lys-Phe-Leu-His-Ser-Ala-Lys-lys-Phe-Gly-Lys-Ala-Phe-Val-Gly-Glu-Ile-Met-Asn-Ser-NH_2

(DMF) using 8 equivalents of the 9-fluorenylmethyloxycarbonyl (Fmoc)-amino acid fluorides, and 3 equivalents of diisopropylethylamine (DIEA). The amino acids were allowed to couple for 1.5 hours. Removal of the Fmoc protecting group was done using a solution of 2% 1,8-diazobicyclo[4.5.0]undec-7-ene (DBU), and 20% piperdine in DMF. Deprotection of the side chains and cleavage from the resin was accomplished simultaneously by treatment with trifluoroacetic acid (TFA), triisopropylsilane, water, and phenol (8.8:0.2:0.5:0.5) (reagent B) for 2 hours.[2.36] Purification of the peptides was done by preparative reverse-phase HPLC on a C_4 column using a gradient of water and acetonitrile with 0.05% TFA in each. Molecular weight and amino acid composition were verified by MALDI mass spectrometry and amino acid analysis, respectively. The peptides were synthesized by manually coupling the first three residues on PAL-PEG-PS resin using eight equivalents of the amino acid fluoride and two equivalents of DIEA in gently refluxing methylene chloride (DCM). The reaction was monitored by removal of small aliquots of resin followed by work-up to determine the level of Fmoc-piperidine

adduct present relative to the expected amounts.[2.37] After the first three couplings were completed, the remainder of the sequences was synthesized on the Milligen 9050. The direct antimicrobial activities of the peptides were tested against representative Gram-positive (*S. aureus*) and Gram-negative (*E. coli*) bacteria. Table 2.3 summarizes the results.

Table 2.3

Peptide antimicrobial activity.

Peptide	**MIC (μM) vs. *E. coli***	**MIC (μM) vs. *S. aureus***
Pi-10	8	123
Ipi-10	4	Not active
Cyh-10	6	6
Ich-10	13	3
Melittin	3	3
Cecropin B amide	1	12
Magainin 2 amide	10	19

Chronically infected mice are susceptible to peptide toxicity at lower doses than healthy mice. For melittin, the highest non-lethal dose was 25 μg. For Aib containing peptides (Pi-10 and Ipi-10), the highest non-lethal dose was 500 μg. For Ich-10, the highest non-lethal dose was 25 μg. The toxicity estimations were grouped into three categories: none, stress and toxic. None meant the peptide showed no apparent effect on the peptide-treated, non-infected mice as compared to the saline-treated infected mice.

Stress was used to indicate that the mouse showed signs of distress: i.e. tremors, temporary paralysis, etc. Toxic meant that some of the mice in that treatment group died at the lowest dose that still reduced spleenic brucella levels.

Peptide doses were titrated to the lowest effective dose; however, several of the infected mice died at peptide doses that were harmless to the control mice. The mice usually died within 1-2 minutes of injection from massive internal bleeding. Table 2.4 shows the indirect *in vivo* activity of the peptides against *Brucella abortus* in BALB/c mice.

Table 2.5 shows percent normal murine macrophage survival versus peptide concentration. Pi-10 shows little toxicity at all concentrations tested while Ich-10 was very toxic at 100 μM and less so at 10 μM. For comparison, melittin is very toxic at 10 μM. For the *in vitro* studies, doses that showed ≥ 70% macrophage survival were used as the starting dosages to determine if infected macrophages are selectively destroyed relative to non-infected macrophages. The data is shown in Table 2.6.

Murine macrophages were incubated with *B. abortus*, which infects approximately 40% of the macrophages.[2.24] The survival rate (90%) of this partially infected macrophage population was the same as the normal non-infected macrophage survival rate over a 48-hour period. Melittin shows slightly lower survival of infected macrophages while the remaining peptides show significantly lower survival of the infected macrophages. Pi-10 shows an approximately 40% lower macrophage survival rate of the partially infected population. This agrees with the maximum expected since about 40% of the macrophages are infected. Ipi-10 and Ich-10 kill less and more than the expected ideal value of 40%, respectively.

Table 2.4

Indirect *in vivo* activity against *Brucella abortus* in BALB/c mice.

Peptide	Dose (μg)	% Brucella Reduction	Toxicity
Pi-10	500	90	None
Ipi-10	500	55	Stress
Cyh-10	ND	ND	ND
Ich-10	25	82	None
Melittin	25	50	None
Cecropin B amide	500	53	None
Magainin 2 amide	500	54	None

Table 2.5

Normal macrophage survival versus peptide concentration.

Peptide	100 μM	10 μM	1 μM
Pi-10	91	96	97
Ich-10	0	77	100
Melittin	ND	< 2	ND

Table 2.6

In vitro peptide toxicity against normal and infected murine macrophages.

Peptide	Conc (μM)	% Survival Normal Mϕ's	% Survival Infected Mϕ's	Statistical Significance[a]
Pi-10	10	90	55	S
Ipi-10	50	90	80	S
Ich-10	25	95	20	S
Melittin	0.1	85	78	S

[a] Independent student's t-test at a 95% confidence level.

To test the hypothesis that these peptides selectively destroy infected macrophages over non-infected macrophages, *in vitro* studies were performed using a strain of *Ba* containing a green fluorescent protein (GFP) and a strain of *Mycobacterium chelonei* (*Mch*). *Ba* is too small to be seen at the magnification levels used to visualize the macrophages; therefore, the strain expressing the GFP allows the infected macrophages to be identified. *Mch* is a relatively large microorganism and is easily seen inside the macrophages. Table 2.7 summarizes the results using Pi-10 and Ich-10.

Figures 2.5 to 2.15 are photomicrographs of the macrophages used in this portion of the study. Trypan blue exclusion was used to visualize dead macrophages. Figure 2.5 is a photograph of normal, healthy macrophages. Figure 2.6 shows a fluorescence

Table 2.7

In vitro peptide activity against control and infected macrophages.

Peptide	Dose (μM)	% Survival *Ba* Infected Mϕ	% Survival *Mch* Infected Mϕ	Statistical Significance[a]
Pi-10	--	99.6 ± 0.6	97.0 ± 3.0	
Ich-10	--	95.0 ± 2.0	N/A	
Pi-10	100 μM	80.3 ± 3.5	72.8 ± 5.1	S
Ich-10	50 μM	81.0 ± 1.0	N/A	S

[a] Independent student's t-test at a 95% confidence level

photograph of healthy macrophages. Figure 2.7 shows a Nomarski photograph of macrophages infected with *Ba*-GFP. Figure 2.8 is a fluorescence photograph of the macrophages infected with *Ba*-GFP. Figure 2.9 shows uninfected macrophages treated with 100 μM Pi-10. Figure 2.10 shows a fluorescence photograph of uninfected macrophages treated with 100 μM Pi-10. Figure 2.11 is a Nomarski photograph of macrophages infected with *Ba*-GFP and treated with 100 μM Pi-10. Figure 2.12 shows a fluorescence photograph of the macrophages infected with *Ba*-GFP and treated with 100 μM Pi-10.

To test the theory that the peptides are active against macrophages infected with a different intracellular pathogen, studies were carried out using *Mycobacterium chelonei*. *Mch* was used instead of *Mtb* as it is less virulent to man than *Mtb*. Figures 2.13 to 2.15 show the results of this study. Figure 2.13 shows macrophages that have been infected

Figure 2.5. Nomarski photomicrograph of healthy macrophages.

Figure 2.6. Fluorescence photomicrograph of healthy macrophages.

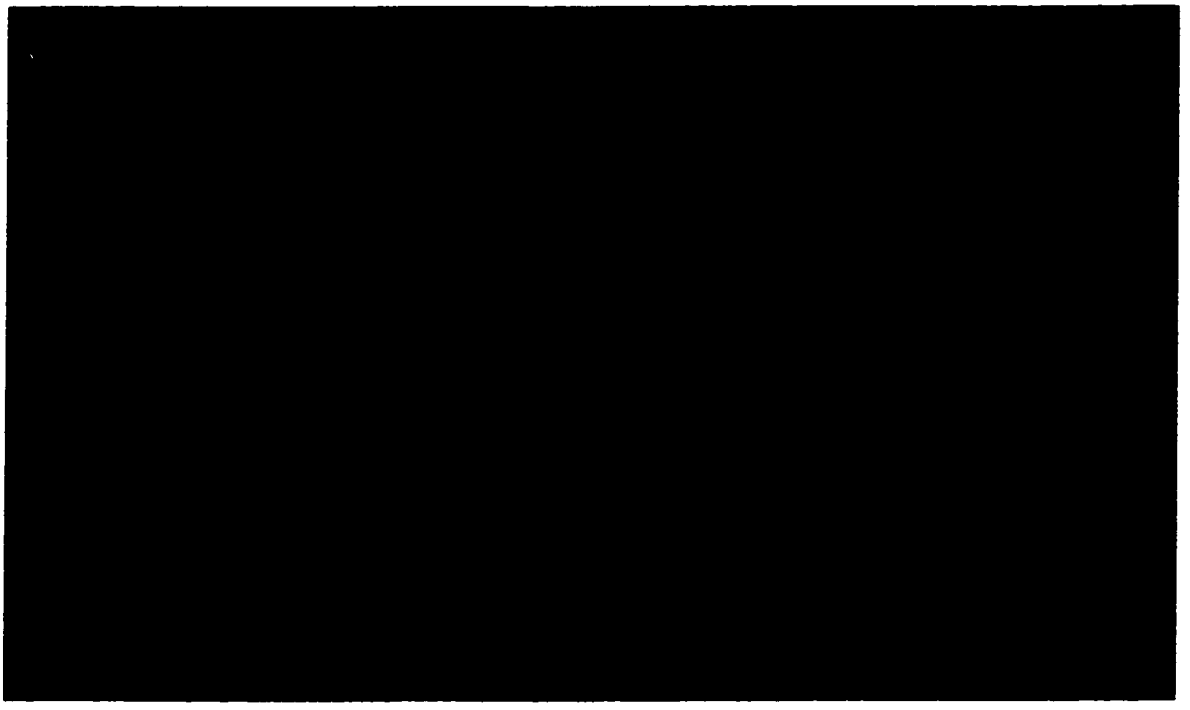

Figure 2.7. Nomarski photomicrograph of untreated macrophages infected with *Ba*-GFP.

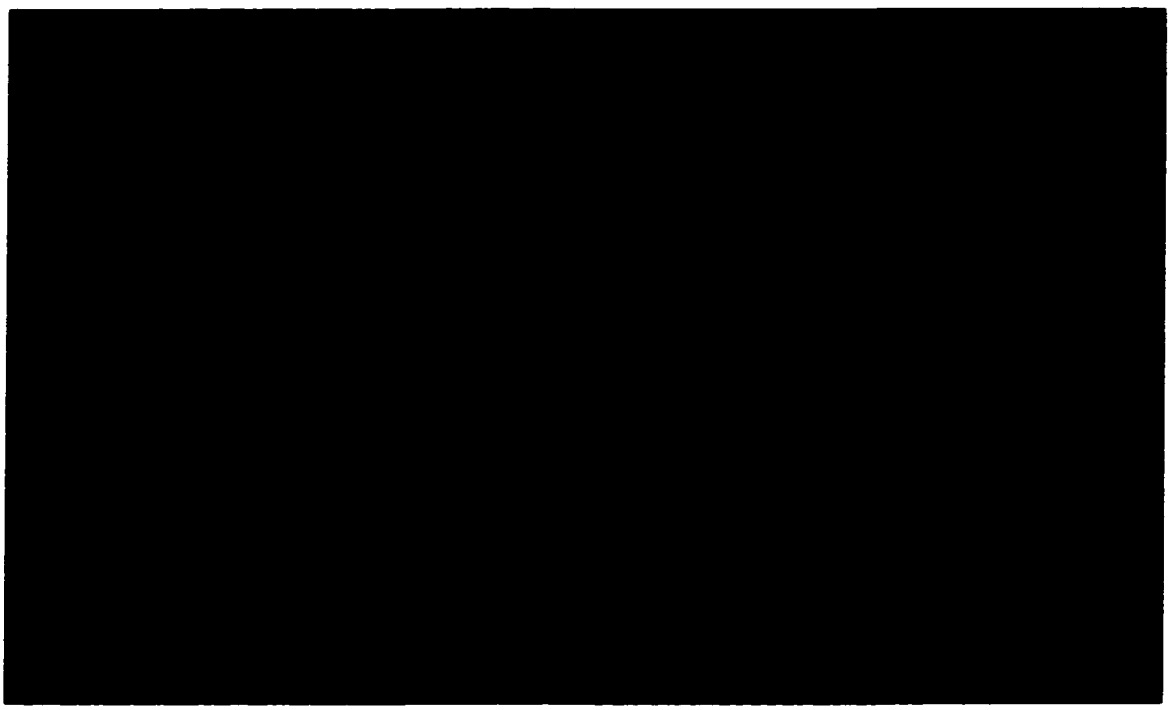

Figure 2.8. Fluorescence photomicrograph of untreated macrophages infected with *Ba*-GFP.

Figure 2.9. Nomarski photomicrograph of treated, uninfected macrophages.

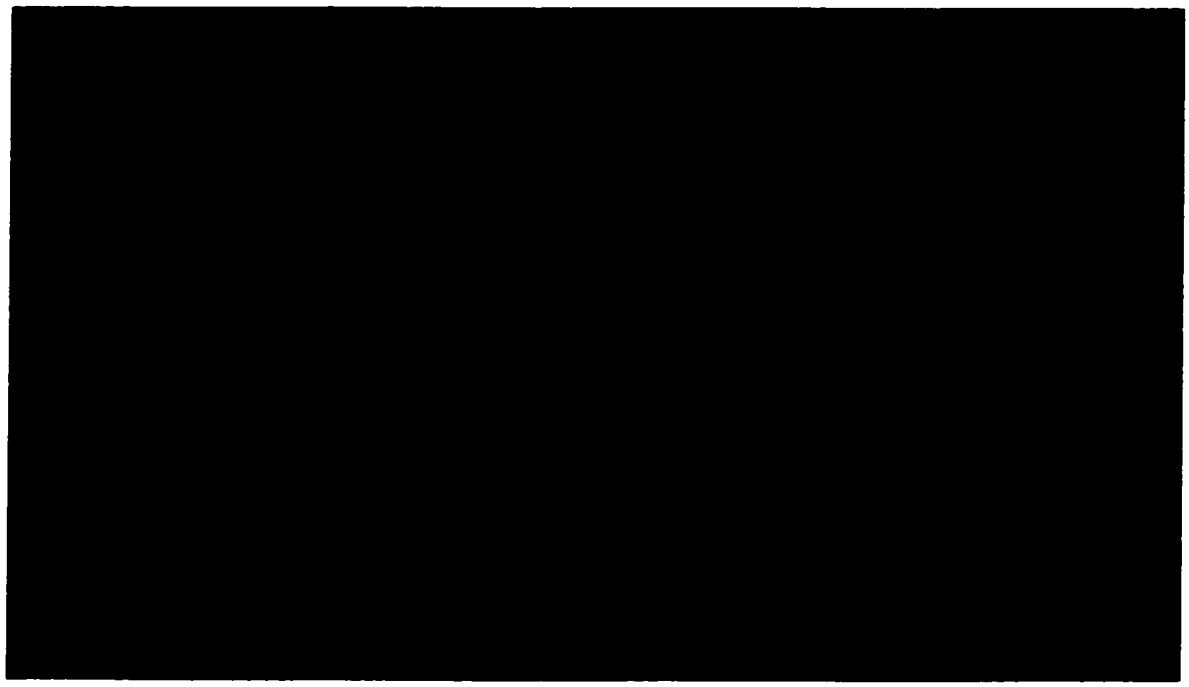

Figure 2.10. Fluorescence photomicrograph of treated, uninfected macrophages.

Figure 2.11. Nomarski photomicrograph of peptide treated macrophages infected with *Ba*-GFP.

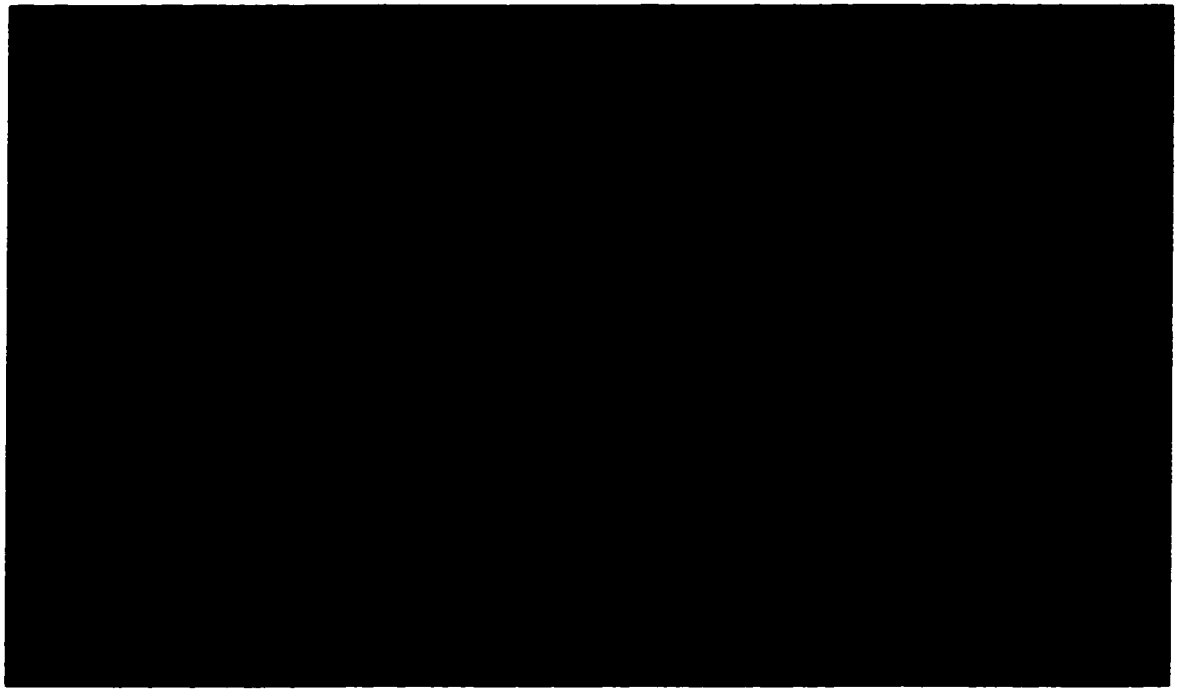

Figure 2.12. Fluorescence photomicrograph of peptide treated macrophages infected with *Ba*-GFP.

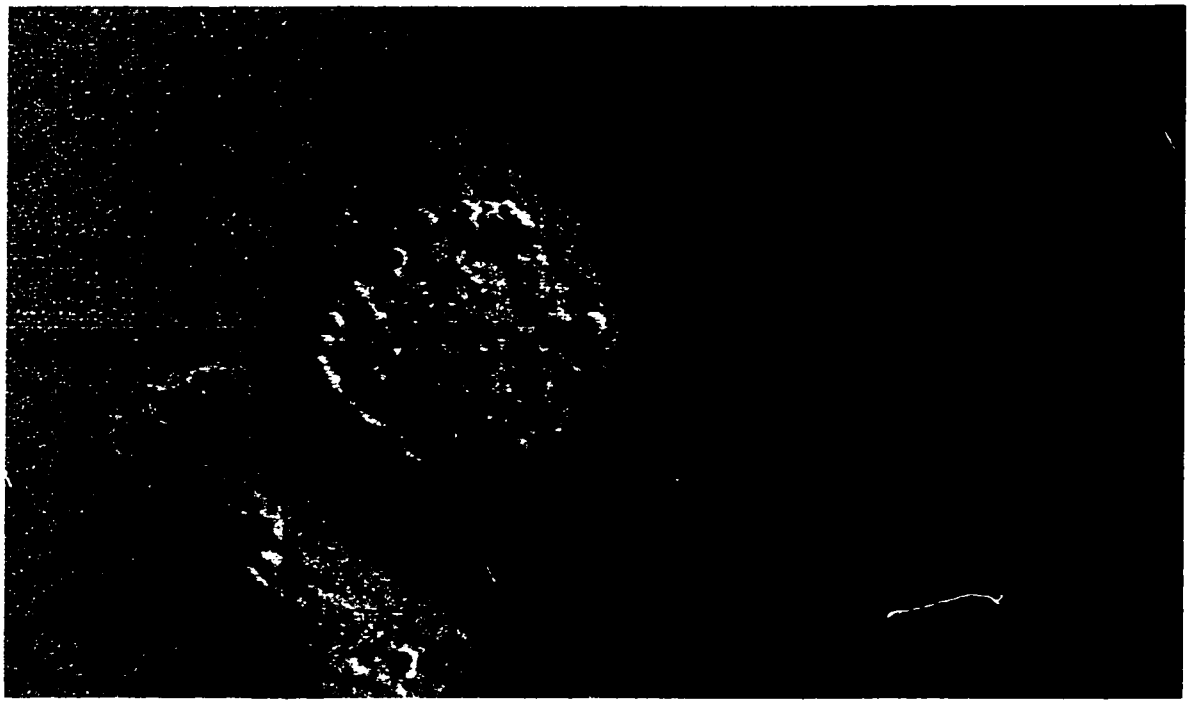

Figure 2.13. Nomarski photomicrograph of untreated macrophages infected with *Mch*.

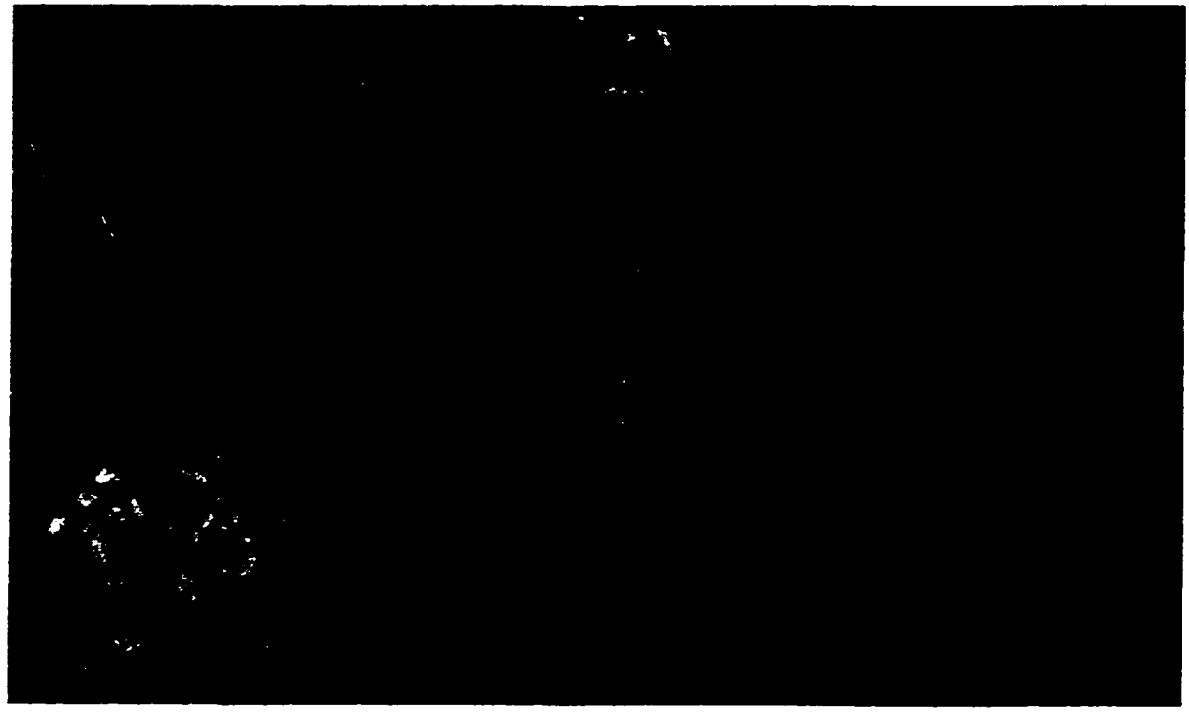

Figure 2.14. Nomarski photomicrograph of peptide treated macrophages infected with *Mch.*

Figure 2.15. Nomarski photomicrograph of peptide treated macrophages infected with *Mch* which shows cell membrane disruption.

with *Mch*. Figures 2.14 and 2.15 show macrophages infected with *Mch* that have been treated with 100 μM Pi-10.

2.4 Discussion

It is well known that basic amphipathic α-helical peptides exhibit *in vitro* antimicrobial activity at μM concentrations. The hydrophobic peptides in this class usually display high mammalian cell toxicity. A good example of this class of peptides is melittin. It is an amphipathic peptide with a relatively narrow polar face and possesses high cytotoxicity.[2.38] *De novo* peptides have been designed to mimic melittin and those containing hydrophobic and hydrophilic residues such as leucine and lysine are among the most cytotoxic known.[2.39] It has been shown that cytotoxicity depends on the length of the peptide as well as hydrophobicity. As the peptide length is decreased, cytotoxicity also decreases. Our group has demonstrated this phenomenon using a series of *de novo* hydrophobic, amphipathic peptides. Cytotoxicity was almost eliminated when the peptides were shortened from 21 residues to 14 residues. Interestingly, direct *in vitro* antimicrobial activity was essentially retained in the shorter peptides.[2.31]

Using the knowledge that shorter, more hydrophobic helical peptides could retain biological activity with reduced cytotoxicity, it was hypothesized that ααAA's could be used to design shorter, helical peptides. Since ααAA's promote helicity, their incorporation into very short hydrophobic peptides should lead to more selective and more biologically active peptides.[2.40-2.43] A problem with this approach is the difficulty associated with incorporation of ααAA's using conventional peptide coupling

reagents.[2.43] This problem has been solved with Carpino's development of acid fluorides for amino acid couplings. This method allows for the mild and efficient solid-phase synthesis of peptides containing multiple ααAA's.[2.33] Despite the improved coupling method, difficulties in the synthesis of the peptides were still encountered. The second residue in Pi-10, Ipi-10, Cyh-10 and Ich-10 did not couple efficiently. This is presumably due to steric difficulties in coupling two ααAA's together near the resin. The problem was resolved by gently refluxing the first three couplings in methylene chloride with DIEA. Each coupling was monitored by quantitative Fmoc tests until at least 95% coupling efficiency was indicated. Once the third residue was satisfactorily coupled, the remaining residues were coupled using the Milligen 9050.

A maximum number of ααAA's was desired in each peptide to promote helicity. To achieve this and maintain a high number of positive charges on the polar face, the ααAA, Api, was used.[2.33] A peptide consisting only of ααAA's would be difficult to synthesize and would present problems in our spectroscopic studies. Since the ααAA's are achiral, the resulting peptides would have no preference for a right-handed or left-handed helix. As a result, two L-lysine residues are used in each peptide.

It has been shown that peptides that contain Aib residues are significantly more helical than peptides that are comprised only of natural amino acids. The replacement of natural amino acids with Aib also substantially improved antimicrobial activity against *E. coli* and *S. aureus*.[2.31] Pi-10 shows a significant improvement in activity over peptides containing only proteinogenic amino acids.[2.32] This increase in activity is

attributed not only to the improved helicity but the increase in hydrophobicity that Aib gives the peptide. Ipi-10, a sequence permutation isomer of Pi-10, shows similar activity. To study the effects of hydrophobicity on peptide activity, Cyh-10 and Ich-10 were synthesized. In these peptides, the Aib residues are replaced with Cyh residues. As can be seen in Table 2.3, these peptides have similar activity against *E. coli* but are up to 41 times more active against *S. aureus.*

The *in vitro* studies provided us with some background regarding what to expect in the *in vivo* studies. Melittin proved to be the most cytotoxic peptide in the *in vitro* studies. It is the most active peptide *in vivo* with effective dosages at 25 μg per mouse. The *in vivo* studies were carried out by injecting the peptides in the lateral tail vein which should rapidly carry the peptide to the primary site of infection, the spleen. It was thought that melittin would indiscriminately attack all cells in the blood but in normal, non-infected mice, this did not occur. However, when similar doses of melittin were administered to infected mice, they died within 1 to 2 minutes of injection. Necropsy of these mice showed massive internal bleeding with the lungs filled with blood. Apparently, the mice died of sepsis associated with the simultaneous lysis of a large number of macrophages releasing nitric oxide and cytokines. Similar behavior was noted for Ich-10, which is expected due to its increased hydrophobicity. An injection of 50 μg into an infected mouse resulted in death.

The *de novo* peptides were tested *in vitro* against normal and infected murine macrophages. Macrophages were harvested from the spleens of normal mice and plated out in 96 well plates. Trypan blue exclusion was used as an indicator of macrophage viability. About 90% of the plated out macrophages survived the stress of this

manipulation, so only survival percentages less than 90% indicate peptide toxicity. These experiments were performed to determine the peptide concentrations to be used against the infected macrophages. Pi-10 and Ich-10 were tested at 1 to 100 μM. Pi-10 was non-toxic at 10 μM whereas Ich-10 was non-toxic at 1 μM. Melittin is non-toxic at 0.1 μM owing to its length and hydrophobicity. The macrophages plated out as above were infected with *B. abortus* for one hour. The excess brucellae were washed away leaving behind intracellular brucellae. Brucella counts indicated that approximately 40% of the macrophages were infected. This percentage of experimental brucellae infection is consistent with literature values.[2.20] The macrophages had the same viability pre- and 1 to 48 hours post infection as determined by trypan blue exclusion. Peptide effects on macrophage survival at the doses determined above were assayed. Table 2.6 shows that melittin, Ich-10 and Pi-10 are effective in selectively killing infected macrophages over non-infected macrophages. Ich-10 and melittin are effective at much lower concentrations than Pi-10 presumably due to their increased hydrophobicity. Ich-10 deviates slightly from the ideal value of 55%, suggesting that the optimal dose is lower than that tested.

To further test the hypothesis that the peptides selectively destroy infected over non-infected macrophages, the above *in vitro* studies were repeated using a strain of *B. abortus* containing a green fluorescent protein. In addition, *in vitro* studies were carried out using *M. chelonei* to verify that these peptides were effective against a different intracellular pathogen. Pi-10 was the only peptide used in this study since it showed the most selectivity for killing infected macrophages. The macrophages were harvested and plated out as before. Infection with *Ba*-GFP and *Mch* were also carried out as before.

Macrophage assays reveal that a similar percentage of macrophages were infected with both intracellular pathogens. The intracellular brucellae are too small to visualize with conventional light microscopy. The *Ba* containing the green fluorescent protein allows them to be visualized inside the macrophages using fluorescence microscopy. *Mch* is large enough to be seen inside the macrophages using conventional light microscopy. Each study was repeated as before to show that there was no difference in using the normal strain of *Ba* vs. *Ba*-GFP or *Mch*. The data on the non-infected peptide treated and infected non-peptide macrophages was within experimental error of that done for previous studies. Figures 2.5 to 2.15 show photomicrographs of these results. The infected macrophages were then treated with 100 μM of Pi-10 for one hour. Excess peptide was washed away, trypan blue was added and allowed to stand for 5 minutes. The excess trypan blue was removed and the macrophages were assayed. Figures 2.11 and 2.12 show the Nomarski and fluorescence photographs of the same region of a 96 well plate. As can be seen in Figure 2.11, the blue cells are dead. Figure 2.12 reveals that these cells were infected with *Ba*-GFP, making them susceptible to the peptide. There appears to be several cells that exhibit fluorescence and are not dead. This may be the result of slight auto-fluorescence of the cell that is not infected or insufficient peptide dose to kill the macrophage, which is infected. Figure 2.13 reveals several macrophages that are infected with *Mch*. The bacteria appear as rod-like structures. Figures 2.14 and 2.15 show that the macrophages possessing these organisms have been destroyed by the peptide, leaving other macrophages intact.

2.5 Experimental

2.5.1 Peptide Synthesis

Cyh-10 and Ich-10 were synthesized by manually coupling the first three residues onto a PAL-PEG-PS solid support. The couplings were done by refluxing 8 equivalents of the Fmoc-acid fluoride, 3 equivalents of DIEA and the resin in methylene chloride. The couplings were allowed to reflux until an acceptable yield was determined by quantitative Fmoc tests.[2.37] After the first three residues were coupled to the resin, the resin was placed on the Milligen 9050 synthesizer and the synthesis was continued. Eight equivalents of preformed Fmoc-acid fluorides, three equivalents of DIEA and a 1.5 h recycling time were used for the couplings. A solution of 20% piperidine/2% 1,8-diazobicyclo[4.5.0]undec-7-ene (DBU) in DMF was used for Fmoc removal. The peptides were simultaneously cleaved from the resin and side-chain deprotected using reagent B (8.8:0.2:0.5:0.5, trifluoroacetic acid (TFA), triisipropylsilane, water, phenol).[2.36] The resulting solution was diluted with cold 30% acetic acid, washed with diethyl ether (4 x 50 mL) and lyophilized. The crude peptides were purified by preparative reverse-phase HPLC on a Waters 15 μm Deltapak C_4 column using a water (0.05% TFA) and acetonitrile (0.05% TFA) gradient system. The gradient was run from 10% to 50% organic and the absorption was monitored at 222 nm. Peptide purity was verified on a Vydac 5 μm C_{18} column using the same conditions. Matrix assisted laser desorption ionization (MALDI) mass spectrometry was used to verify peptide mass. Ich-10 and Cyh-10 1276 $(M+H)^+$.

2.5.2 Amino Acid Analysis

Amino acid analyses were performed according to reference 2.21 using a Beckman 6300 Amino Acid Analyzer. In short, the peptides were hydrolyzed in 6N HCl and 0.01% phenol for 24 h at 110°C. The samples were analyzed on a cation exchange column at 65°C with post-column ninhydrin derivitization at 130°C.

2.5.3 MIC Assays

E. coli American type culture collection (ATCC) 25922 and *S. aureus* ATCC 25922 were used as representative Gram-positive and Gram-negative bacteria in the MIC assays. The bacterial cultures were grown in nutrient broth to midlog phase and standardized using McFarland standard before dilution. A 512 μg/mL peptide stock solution was prepared and 1:2 serial dilutions were prepared and added to the culture media to give final peptide concentrations of 256 μg/mL.

Fifty microliters of cells (5×10^4) and 50 μL of the peptide solution were added to a sterile well and the MIC was determined by the lowest concentration that inhibited cell growth. The inhibition of cell growth was indicated by the absence of turbidity after four hours. Turbidity in the wells was visualized manually. The MIC values are reported as the median value for at least three experiments.

2.5.4 *In vivo B. Abortus* Studies

Stock cultures of virulent *B. abortus* strain 2308 were passaged in BALB/c mice and isolated in pure culture from spleens. Stock cultures were prepared from 48 hour growth on Schaedler blood agar plates and stored at -80°C. For infections, the contents were freshly thawed, pooled and diluted in sterile phosphate buffered saline (PBS) to a concentration of 5×10^5 colony forming units (cfu) per mL. Exact numbers were

established by subsequent viable counts. Stock cultures for macrophage assays were derived from the stocks above from a single solid passage.

Mice. Female BALB/c mice were purchased at 10 weeks of age from the Department of Laboratory Animal Medicine at the LSU School of Veterinary Medicine breeding colony. The animals were held 1 week prior to use.

Challenge infection of mice with B. abortus and peptide treatment. Mice were infected via the lateral tail vein with approximately $5x10^4$ cfu of *B. abortus* in 100 µL of PBS. Approximately 4-6 weeks post infection, the mice were injected with a sublethal dose of peptide and a control group was injected with diluent. After 24 h, the peptide treatment group mice were sacrificed by CO_2 asphyxiation and their spleens and livers aseptically removed. The tissues were homogenized in 10 mL of PBS, serially diluted, and plated in triplicate. Colonies were counted after 3 days of incubation at 37°C under an atmosphere of 10% CO_2. Bacterial loads in the peptide treated animals were compared to the diluent controls.

2.5.5 *In Vitro* Biological Studies

Preparation of cells. Modifications of the procedures described previously were used to harvest and infect murine resident peritoneal macrophages with *B. abortus*-GFP and *M. chelonei*.[2.20, 2.22] Following euthanasia, cells were harvested by lavage from the peritoneal cavity of ten-week old BALB/c mice using 8 mL of DMEM (Dulbecco's Modified Eagle Medium) + 5% fetal calf serum (FCS). The cells were cultured in 96 well plates at a concentration of $1.5x10^5$ per well in 200 µL of DMEM + 5% FCS at 37°C in 5% CO_2. Cell cultures were enriched for macrophages by washing away non-

adherent cells after overnight incubation with PBS + 5% FCS and 200 µL of fresh media was added to the cultures.

Determination of non-cytotoxic concentration of peptides. Normal macrophage cultures were treated with 0 to 200 µM of the test peptide. The peptides were incubated with the cells for 1 hour at 37°C in 5% CO_2. The cells were washed 3 times with PBS + 5% FCS to remove any residual peptide. Peptide treated cells were stained with 0.04% trypan blue in DMEM + 5% FCS. One to two hundred cells per well were counted using an inverted microscope and the number of stained cells was recorded. Five wells were examined per peptide concentration. Percent survival was calculated by subtracting the number of blue (dead) cells from the total cells and normalized.

Infection of cells with *B. abortus*-GFP and *M. chelonei*. *B. abortus*-GFP or *M. chelonei* opsonized with a sub-agglutinating dilution (1:2000) of hyperimmune BALB/c mouse sera in DMEM + 5% FCS was added to the macrophages at a ratio of approximately 100 bacteria per macrophage. Phagocytosis proceeded for 2 h at 37°C. Extracellular organisms were removed by washing 3 times with PBS + 5% FCS and fresh DMEM.

In vitro peptide treatment. Using non-cytotoxic concentrations, peptides were added to infected and non-infected cell cultures for 1 hour at 37°C, 5% CO_2. The cells were washed 3 times with PBS + 5% FCS to remove any residual peptide. Percent viability was determined as described above.

2.5.6 Statistical Analysis

A mean value for each spleen count was obtained by averaging the triplicate values. Data was expressed as percent bacterial reduction compared to the appropriate

controls. Percent bacterial reduction was determined by subtracting the total number of organisms in the treated spleens from the total number of organisms in the control spleens. This difference was divided by the total number of organisms in the control spleens and multiplied by 100. Statistical comparisons between experimental groups were performed using the two-tailed independent Student's t test with ρ values less than 0.05 considered significant.[2.44]

2.5.7 Biological Containment and Animal Use

All procedures involving live Brucellae and Mycobacteria were performed in a Biological Level 3 (BL-3) containment facility at the LSU-SVM following Centers for Disease Control/National Institutes of Health guidelines.[2.45] In conducting research using animals, the investigators adhered to the "Guide for the Care and Use of Laboratory Animals" prepared by the Committee on Care and Use of Laboratory Animals of the Institute of Laboratory Animal Resources, National Research Council.[2.46]

2.6 References

2.1 Williams, R. J., Heymann, D. L., *Science*, **1998**, *279*, 1153-1154.

2.2 Morell, V., *Science*, **1997**, *278*, 575-576.

2.3 Novak, R., Henriques, B., Charpentier, E., Normark, S., Tuomanen, E., *Nature*, **1999**, *399*, 590-593.

2.4 Maloy, W.L. and Kari, U.P., *Biopolymers (Peptide Science)*, **1995**, *37*, 105-122.

2.5 Kaiser, E.T. and Kezdy, F.J., *J. Ann. Rev. Biophys. Chem.*, **1987**, *16*, 561-581.

2.6 Epand, R., Shai, Y., Segrest, J.P., and Anantharamaiah, G.M., *Biopolymers (Peptide Science)*, **1995**, *37*, 319-338.

2.7 He, K., Ludtke, S.J., Worchester, L., and Huang, H.W., *Biochemistry*, **1995,** *34*, 16764-16769.

2.8 Matsuzaki, K., Harada, M., Handa, T., Munakoshi, S., Fuji, N., Yajima, H., and Miyajima, K., *Biochem. Biophys. Acta*, **1989,** *981*, 130-134.

2.9 Matsuzaki, K., Sugishita, K., Fuji, N., and Miyajima, K., *Biochemistry*, **1995,** *34*, 3423-3429.

2.10 Tyler, E.M., Anantharamaiah, G.M., Walker, D.E., Mishra, V.K., Palgunachari, M.N., and Segrest, J.P., *Biochemistry*, **1995,** *34*, 4393-4401.

2.11 Jaynes, J.M., Julian, G.R., Jeffers, G.W., White, K.L., and Enright, F.M., *Peptide Res.*, **1989,** *2*, 157-160.

2.12 Jaynes, J.M., *Drug & News Perspectives*, **1990,** *3*, 69-78.

2.13 Cruciani, R.A., Barker, J.L., Zasloff, M., Chen, H.-C., and Colamonici, O., *Proc. Natl. Acad. Sci., USA*, **1991,** *88*, 3792-3796.

2.14 Moulder, J.W., *Microbiol. Rev.*, **1985,** *49*, 298-337.

2.15 Araya, L.N., Elzer, P.H., Rowe, G.E., Enright, F.M., and Winter, A.J., *J. Immunol.*, **1989,** *53*, 3330-3337.

2.16 Timoney, J.F., Gillespie, J.H., Scott, F.W., and Barlough, J.E., *The Genus Brucella. Hagan's and Brunner's Microbiology and Infectious Diseases of Domestic Animals*. 8th ed. 1988, Ithaca, New York: Cornell Univ. Press, Comstock Publishing Assoc.

2.17 Burrows, W., *Brucella*, in *Textbook of Microbiology*. 1968, W. B. Saunders Co.: Philadelphia.

2.18 Nicoletti, P., *Adv. Vet. Sci. Compar. Med.*, **1980,** *24*, 70-98.

2.19 Young, E.J., *Clinical Manifestations of Human Brucellosis*, in *Brucellosis: Clinical and Laboratory Aspects*, E.J.C. Young, M. J., Editor. 1989, CRC Press: Boca Raton, FL. p. 97-126.

2.20 Nicoletti, P., in *Brucellosis: Clinical and Laboratory Aspects*, E.J.C. Young, M. J., Editor. 1989, CRC Press: Boca Raton, FL. p. 41-67.

2.21 Sansom, M.S.P., *Prog. Biophys. Mol. Biol.*, **1991,** *55*, 139-236.

2.22 Huxsoll, D.L., Patrick, W.C.I., and Parrott, C.D., *J. Am. Vet. Med. Assoc.*, **1987,** *190*, 714-722.

2.23 Detilleux, P.G., Deyoe, B.L., and Cheville, N.F., *In Vitro. Infect. Immun.*, **1990,** *58*, 2320-2328.

2.24 Jiang, X. and Baldwin, C.L., *Infect. Immun.*, **1993,** *61*, 124-134.

2.25 Jones, S.M. and Winter, A.J., *Infect. Immun.*, **1992,** *60*, 3011-3014.

2.26 Enright, F.M., Araya, L.N., Elzer, P.H., Rowe, G.E., and Winter, A.J., *J. Vet. Immunol. Immunopathol.*, **1990,** *26*, 171-182.

2.27 Corbeil, L.B., Blau, K., Inzana, T.J., Neilsen, K.H., Jacobson, R.H., and Corbeil, R.R., *Infect. Immun.*, **1988,** *56*, 3251-3261.

2.28 Bloom, B.R., *Tuberculosis: Pathogenesis, Protection and Control.* 1994, Washington, DC: ASM Press.

2.29 Kuby, J., *Immunology*. Third ed. 1997, New York: W. H. Freeman and Company.

2.30 Cornut, I., Buttner, K., Dasseux, J.-L., and Dufourcq, J., *FEBS Lett.*, **1994,** *349*, 29-33.

2.31 Javadpour, M.M., Juban, M.M., Lo, W.-C.J., Bishop, S.M., Alberty, J.B., Cowell, S.M., Becker, C.L., and McLaughlin, M.L., *J. Med. Chem.*, **1996,** *39*, 3107-3113.

2.32 Yokum, T.S., Elzer, P.H., and McLaughlin, M.L., *J. Med. Chem.*, **1996,** *39*, 3603-3605.

2.33 Wysong, C.L., Yokum, T.S., Morales, G.A., Gundry, R.L., McLaughlin, M.L., and Hammer, R.P., *J. Org. Chem.*, **1996,** *61*, 7650-7651.

2.34 Wenschuh, H., Beyermann, M., Krause, E., Brudel, M., Winter, R., Schumann, M., Carpino, L., and Bienert, M., *J. Org. Chem.*, **1994,** *59*, 3275-3280.

2.35 Wenschuh, H., Beyermann, M., Haber, H., Seydel, J.K., Krause, E., Bienert, M., Carpino, L., El-Faham, A., and Albericio, F., *J. Org. Chem.*, **1995,** *60*, 405-410.

2.36 Van Abel, R.J., Tang, Y., Rao, V.S.V., Dobbs, C.H., Tran, D., Barany, G., and Selsted, M.E., *Int. J. Pept. Protein Res.*, **1995,** *45*, 401-409.

2.37 Fields, G.B., Tian, Z., and Barany, G., *Synthetic Peptides: A User's Guide*, ed. G.A. Grant. 1992, USA: W. H. Freeman and Co.

2.38 Saberwal, G. and Nagaraj, R., *Biochim. Biophys. Acta*, **1994,** *1197*, 109-131.

2.39 Prasad, B.V.V. and Balaram, P., *CRC Crit. Rev. Biochem.*, **1984,** *16*, 307-348.

2.40 Marshall, G.R., Hodgkin, E.E., Langs, D.A., Smith, G.D., Zabrocki, J., and Leplawy, M.T., *Proc. Natl. Acad. Sci. USA*, **1990,** *87*, 487-491.

2.41 Augspurger, J.D., Bindra, V.A., Scheraga, H.A., and Kuki, A., *Biochemistry*, **1995,** *34*, 2566-2576.

2.42 Wysong, C.L., Yokum, T.S., McLaughlin, M.L., and Hammer, R.P., *CHEMTECH*, **1997,** *27*, 26-33.

2.43 Yokum, T.S., Gauthier, T.J., Hammer, R.P., and McLaughlin, M.L., *J. Am. Chem. Soc.*, **1997,** *119*, 1167-1168.

2.44 Snedecor, G.W. and Cochran, W.G., *Statistical Methods*. 1985, Ames, IA: Iowa State University Press.

2.45 United States Department of Health and Human Services. *Biosafety in Microbiological and Biomedical Laboratories*. H.H.S. Publication No. (NIH) 86-23. 1993, Washington, DC: U.S. Government Printing Office.

2.46 United States Department of Health and Human Services. *Guide for the Care and Use of Laboratory Animals*. H.H.S. Publication No. (NIH) 86-23. 1985, Washington, DC: U.S. Government Printing Office.

Chapter 3

Structural Studies of Peptides Rich in α,α-Disubstituted Amino Acids

3.1 Introduction

The holy grail of *de novo* protein design is the ability to predict secondary structure (i.e. α-helix, β-sheet, or 3_{10}-helix) from the amino acid sequence.[3.1-3.3] By far, the α-helix is the most common and most studied secondary structure. Relatively little is known about the factors favoring formation of the 3_{10}-helix.[3.4-3.8] The 3_{10}-helix comprises approximately 10% of all helical structures and is thought to be a folding intermediate to the α-helix.[3.5, 3.9-3.13] Small sections of 3_{10}-helices often occur in globular proteins and are thought to be important in protein recognition.[3.4-3.15] Thus efforts to study the 3_{10}-/α-helix equilibrium are important in increasing our knowledge of the protein folding process. Most studies exploring this equilibrium have been concentrated on short, hydrophobic peptides containing several α,α-disubstituted amino acids (ααAA's).[3.16-3.19] As a result, spectroscopic studies of these peptides have been limited to organic solvents such as dimethylsulfoxide (DMSO), methanol, trifluoroethanol (TFE) and acetonitrile. Structures of these peptides have also been obtained by X-ray analysis of crystals grown from organic solvents.[3.20-3.23] The α-helix has been studied extensively in water and organic solvent systems.[3.24-3.26] Recently, Toniolo and co-workers have reported spectroscopic studies of a peptide exhibiting 3_{10}-helical structure in water.[3.27] We have synthesized a series of amphipathic, water-

soluble peptides comprised of 80% ααAA's. Here we report the helical structure of these peptides using circular dichroism spectroscopy (CD).

3.2 Results

Each peptide was designed to form an amphipathic helix either in an α-helix or a 3_{10}-helix. The amphipathic helices have their charged residues along one side creating a polar face and have their uncharged residues along the other side, creating a non-polar face.[3.28, 3.29] Pi-10 and Cyh-10 were designed to be perfectly amphipathic as an α-helix while Ipi-10 and Ich-10 were designed to be perfectly amphipathic as a 3_{10}-helix. Figures 3.1 to 3.4 show each peptide in its amphipathic helical form as well as it's less perfectly amphipathic alternative form. The large percentages of ααAA's are used to promote helicity. Amphipathy is used as the design tool to control which helix type is formed. All peptides were synthesized and purified as previously reported.[3.30, 3.31]

In CD spectroscopy, helical peptides are characterized by two minima. The $n\rightarrow\pi^*$ transition is centered around 222 nm and the $\pi\rightarrow\pi^*$ transition is centered near 207 nm.[3.32] Since both the 3_{10}- and α-helices exhibit these minima, the intensities of the minima are used to distinguish between these helical structures. The ratio, R, where $R = [\theta]_{n\rightarrow\pi^*}/[\theta]_{n\rightarrow\pi^*}$, has been proposed as the factor to distinguish a 3_{10}-helix from an α-helix. In 3_{10}-helices, $R \leq 0.4$ while for α-helices $R \equiv 1$.[3.32-3.35] Tables 3.1 to 3.4 show the % α-helicity and R for Pi-10, Cyh-10 and Ich-10 and the % 3_{10}-helicity and R for Ipi-10 in various solvent systems. It was expected that the peptides would adopt the helical structure that allowed them to be most amphipathic. In SDS micelles, all

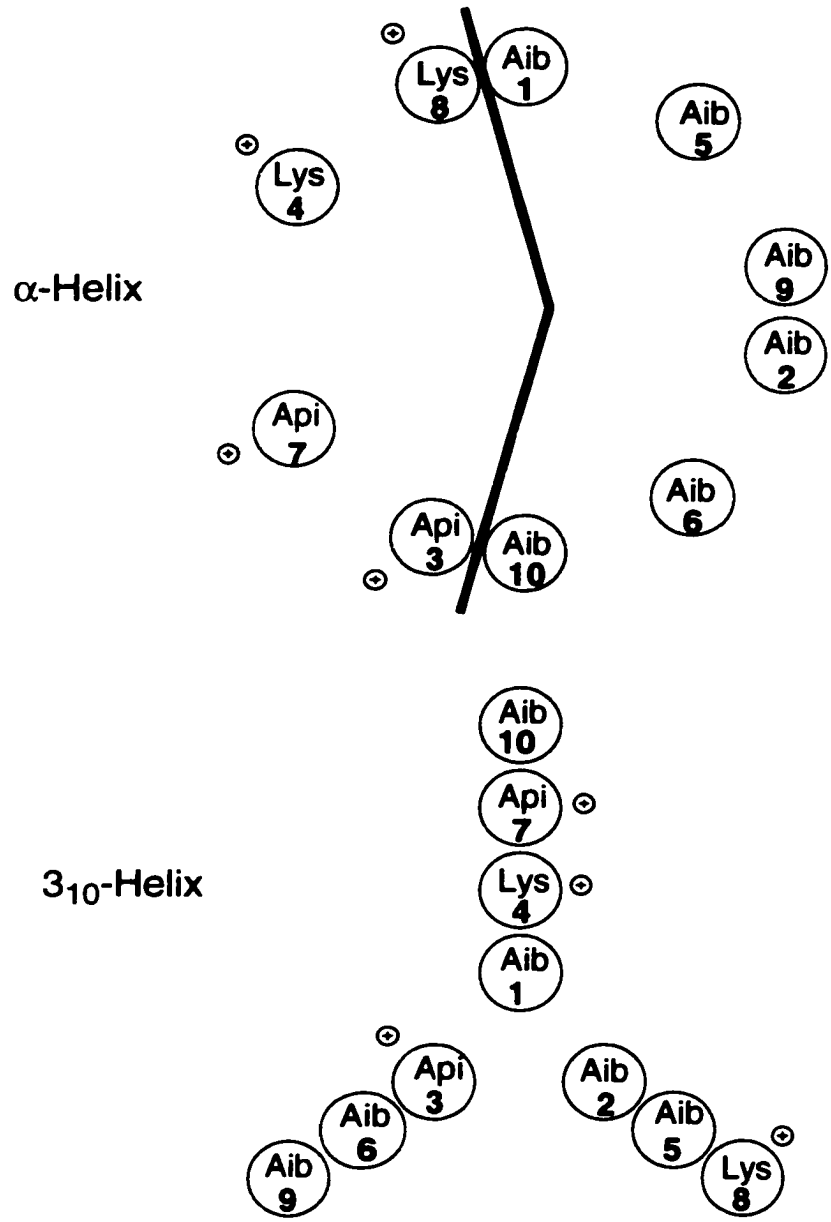

Pi-10 H-Aib-Aib-Api-Lys-Aib-Aib-Api-Lys-Aib-Aib-NH_2

Figure 3.1. Sequence and α- and 3_{10}-helical wheel diagrams of Pi-10.

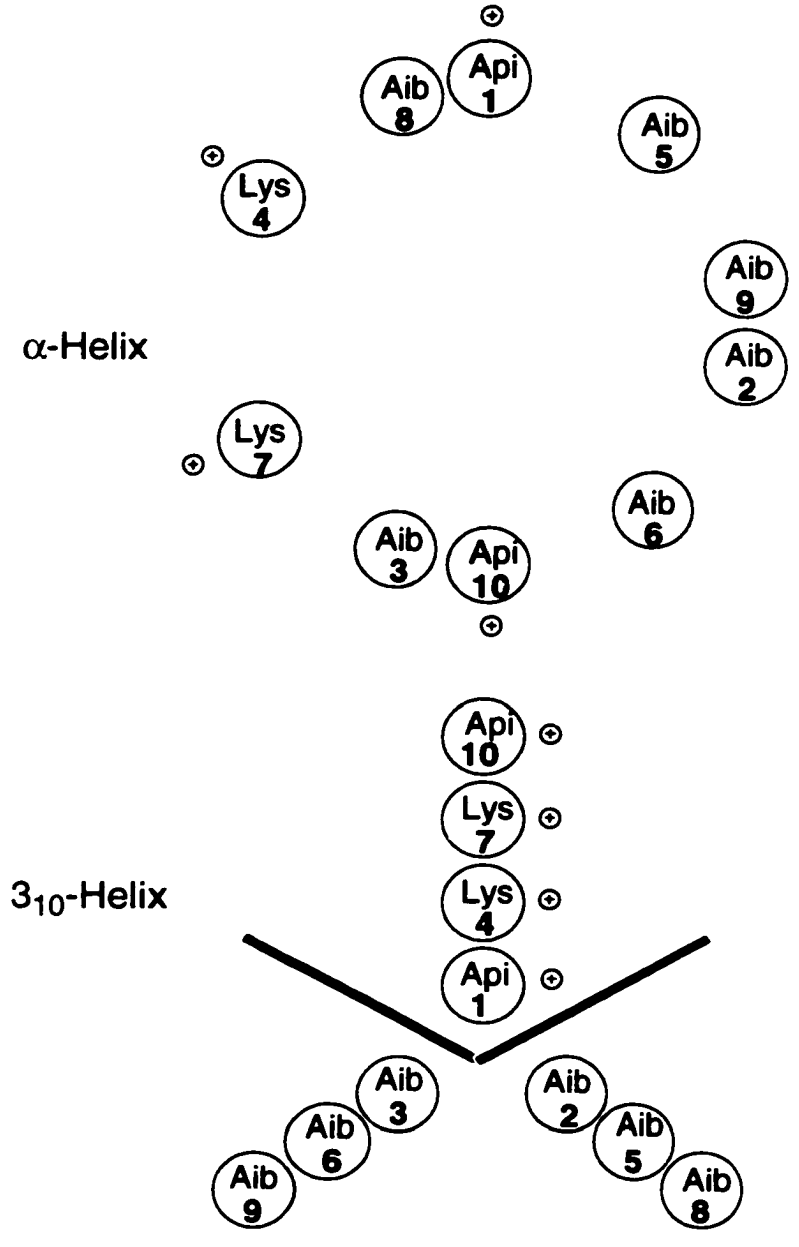

Ipi-10 H-Api-Aib-Aib-Lys-Aib-Aib-Lys-Aib-Aib-Api-NH_2

Figure 3.2. Sequence and α- and 3_{10}-helical wheel diagrams of Ipi-10.

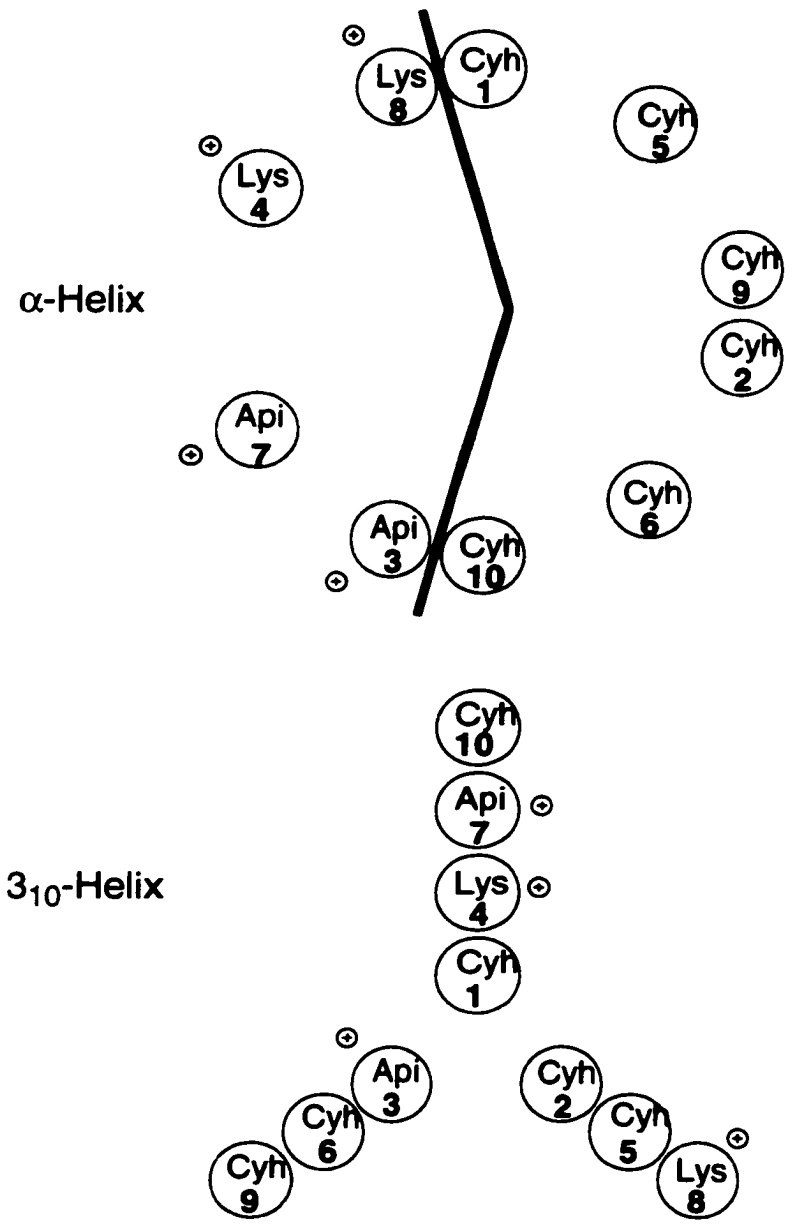

Cyh-10 H-Cyh-Cyh-Api-Lys-Cyh-Cyh-Api-Lys-Cyh-Cyh-NH_2

Figure 3.3. Sequence and α- and 3_{10}-helical wheel diagrams of Cyh-10.

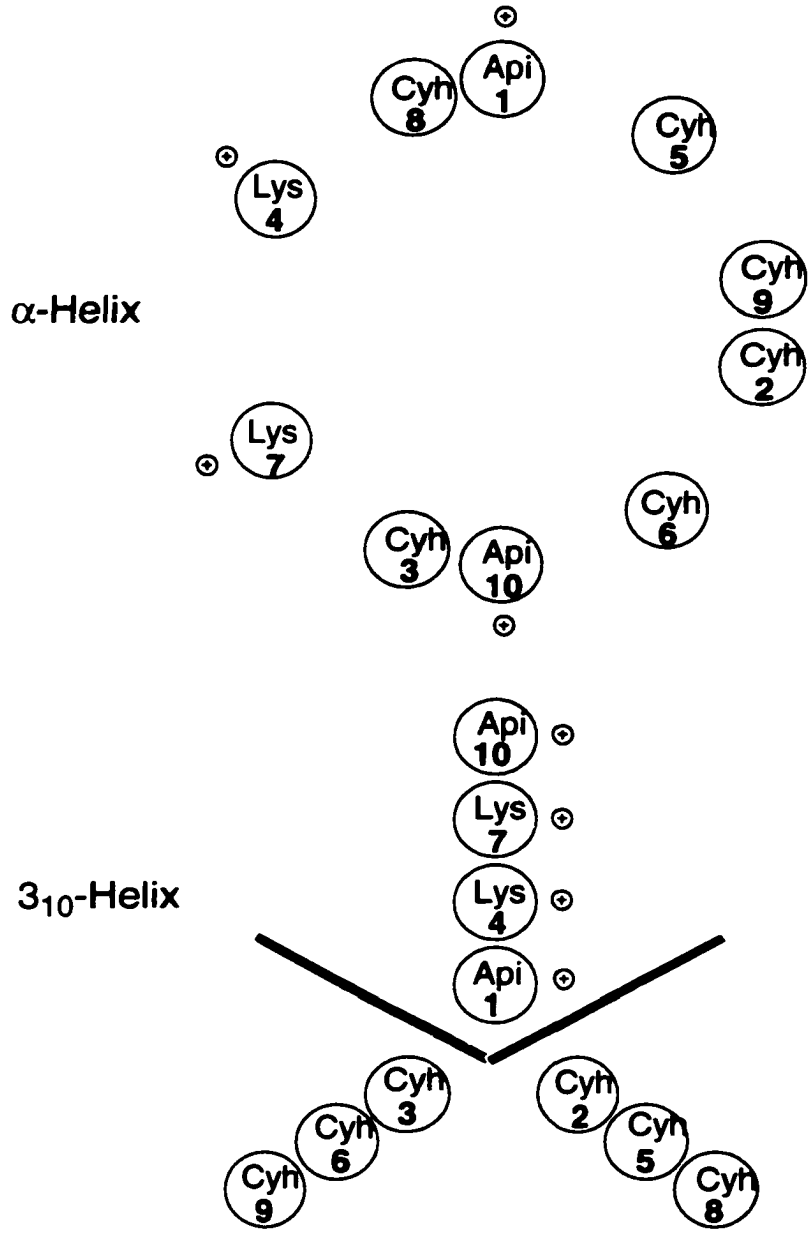

Ich-10 H-Api-Cyh-Cyh-Lys-Cyh-Cyh-Lys-Cyh-Cyh-Api-NH_2

Figure 3.4. Sequence and α-helix and 3_{10}-helical wheel diagrams for Ich-10.

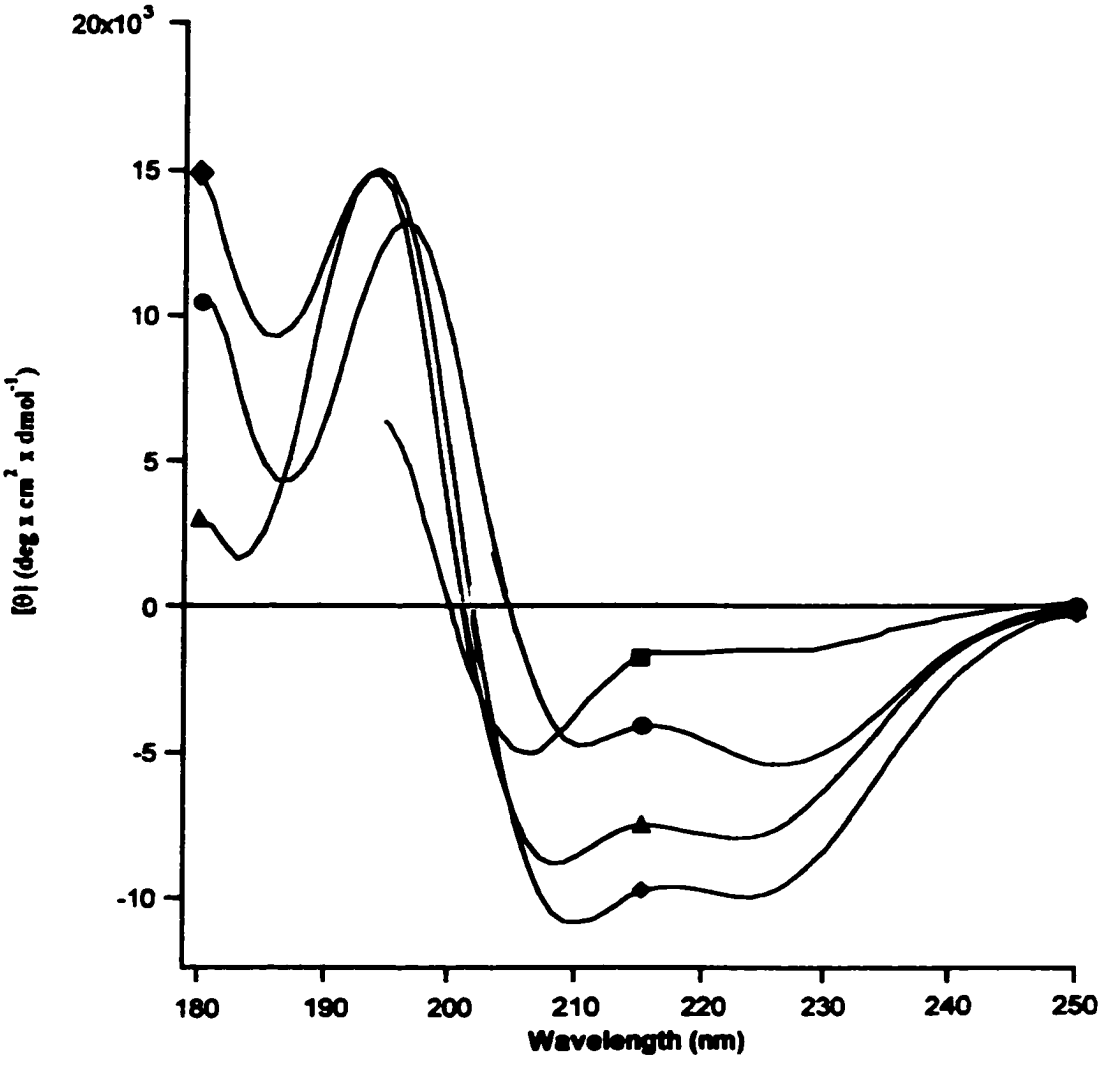

Figure 3.5. CD Spectra of Pi-10 (▲), Ipi-10 (■), Cyh-10 (♦) and Ich-10 (●) in SDS micelles.

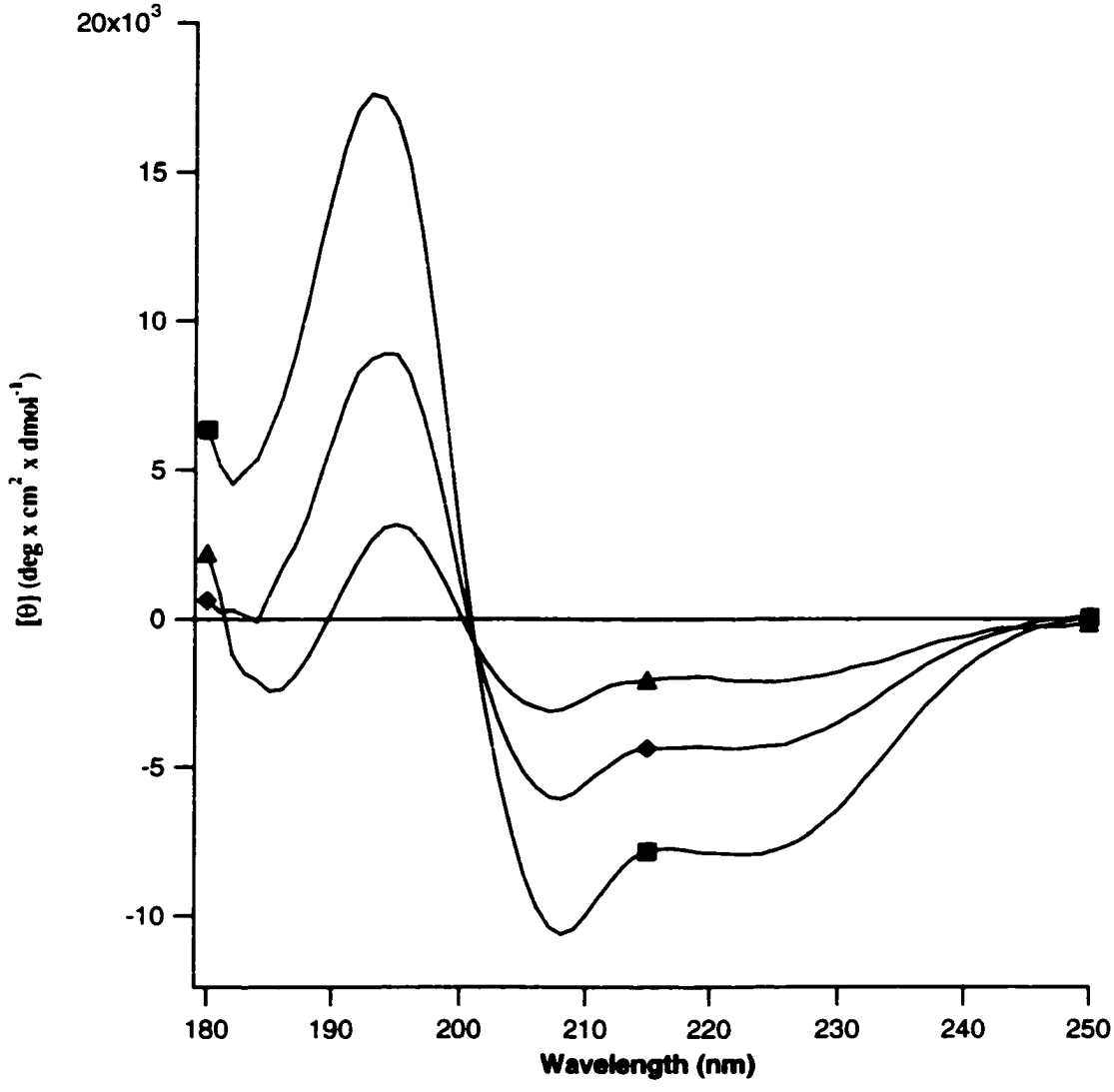

Figure 3.6. CD spectra of Pi-10 in 1:1 CH_3CN-H_2O (▲), 9:1 CH_3CN-H_2O (♦), and 9:1 CH_3CN-TFE (■).

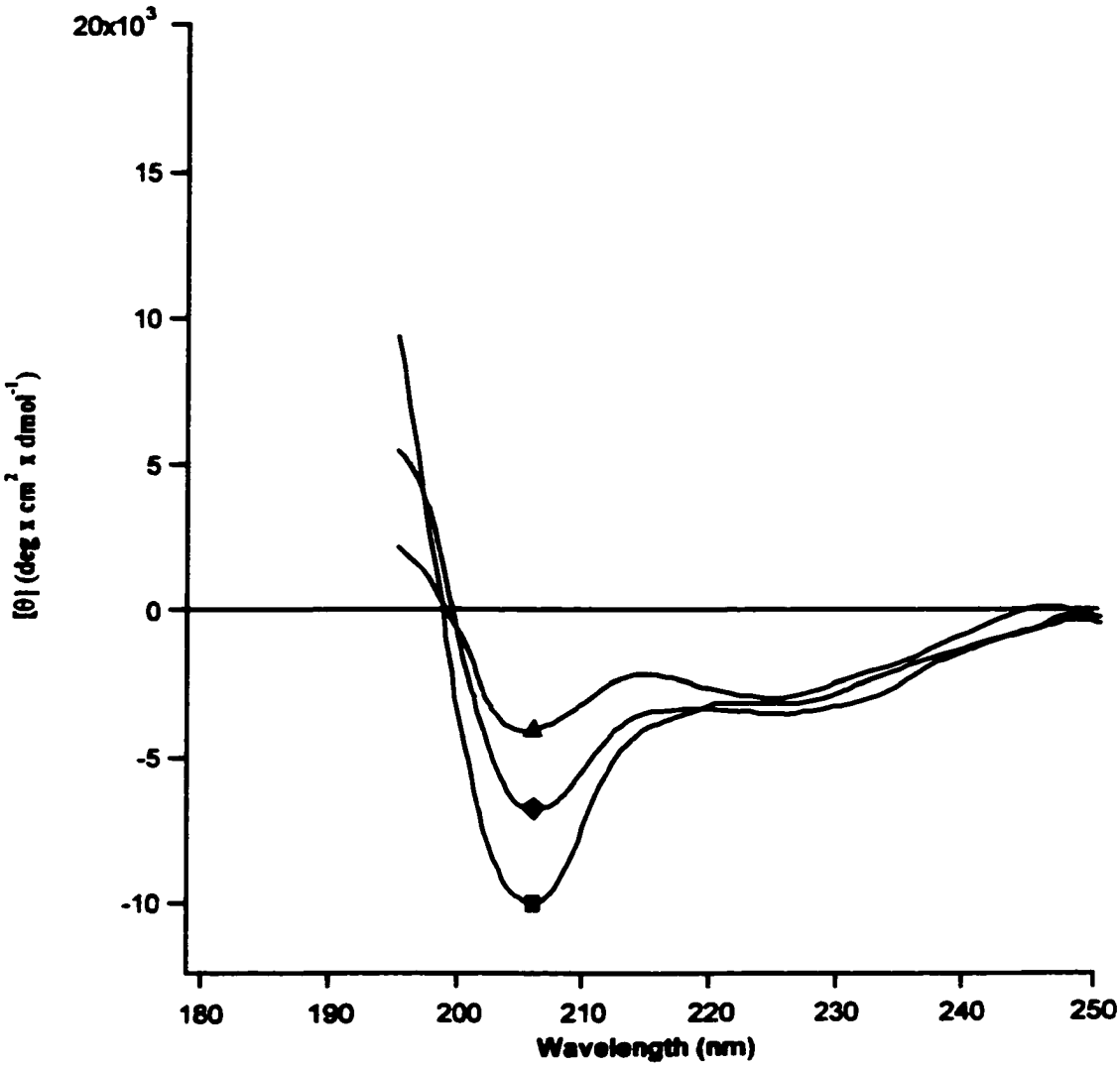

Figure 3.7. CD spectra of Ipi-10 in 1:1 CH_3CN-H_2O (▲), 9:1 CH_3CN-H_2O (♦), and 9:1 CH_3CN-TFE (■).

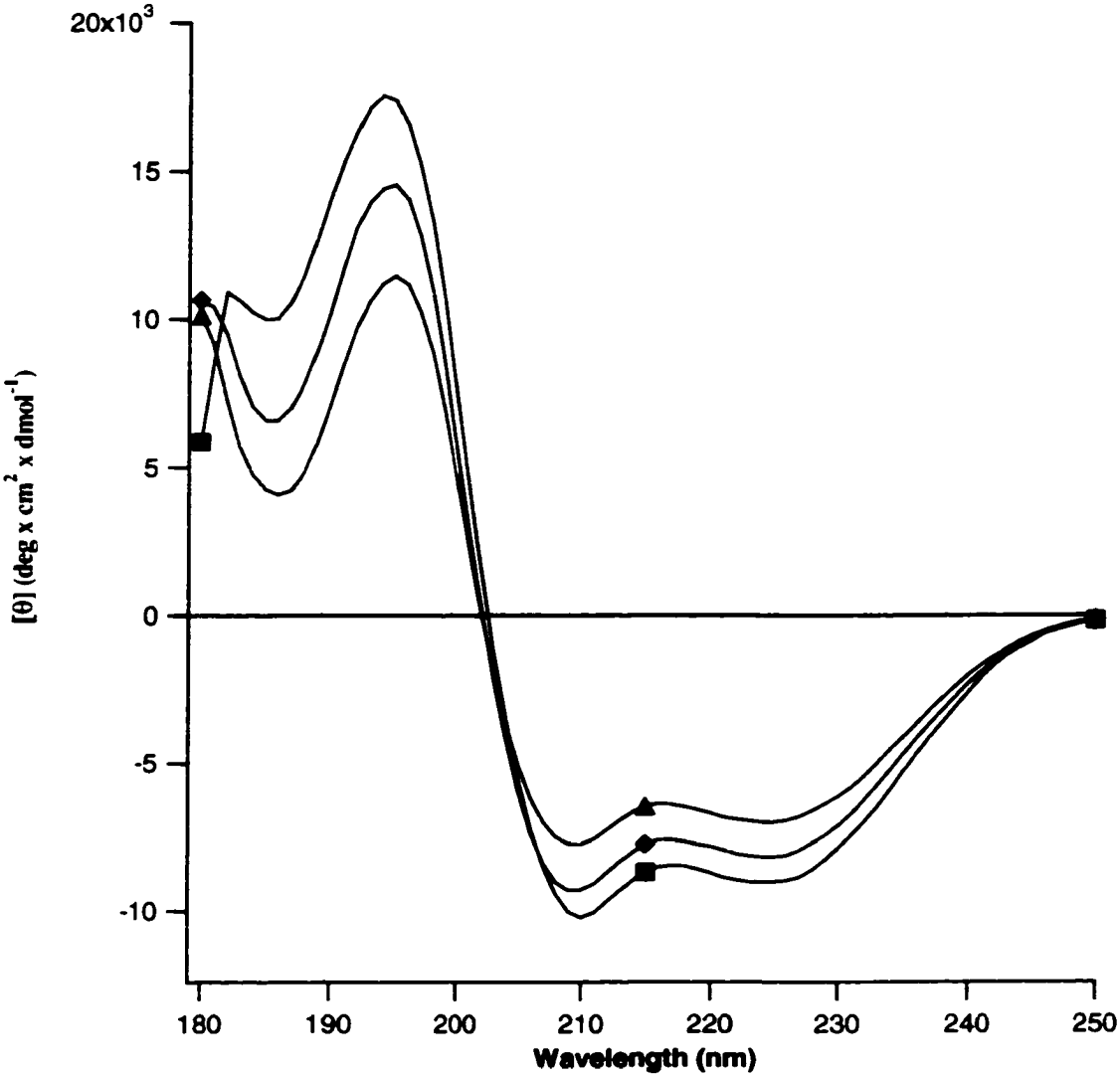

Figure 3.8. CD spectra of Cyh-10 in 1:1 CH_3CN-H_2O (▲), 9:1 CH_3CN-H_2O (♦), and 9:1 CH_3CN-TFE (■).

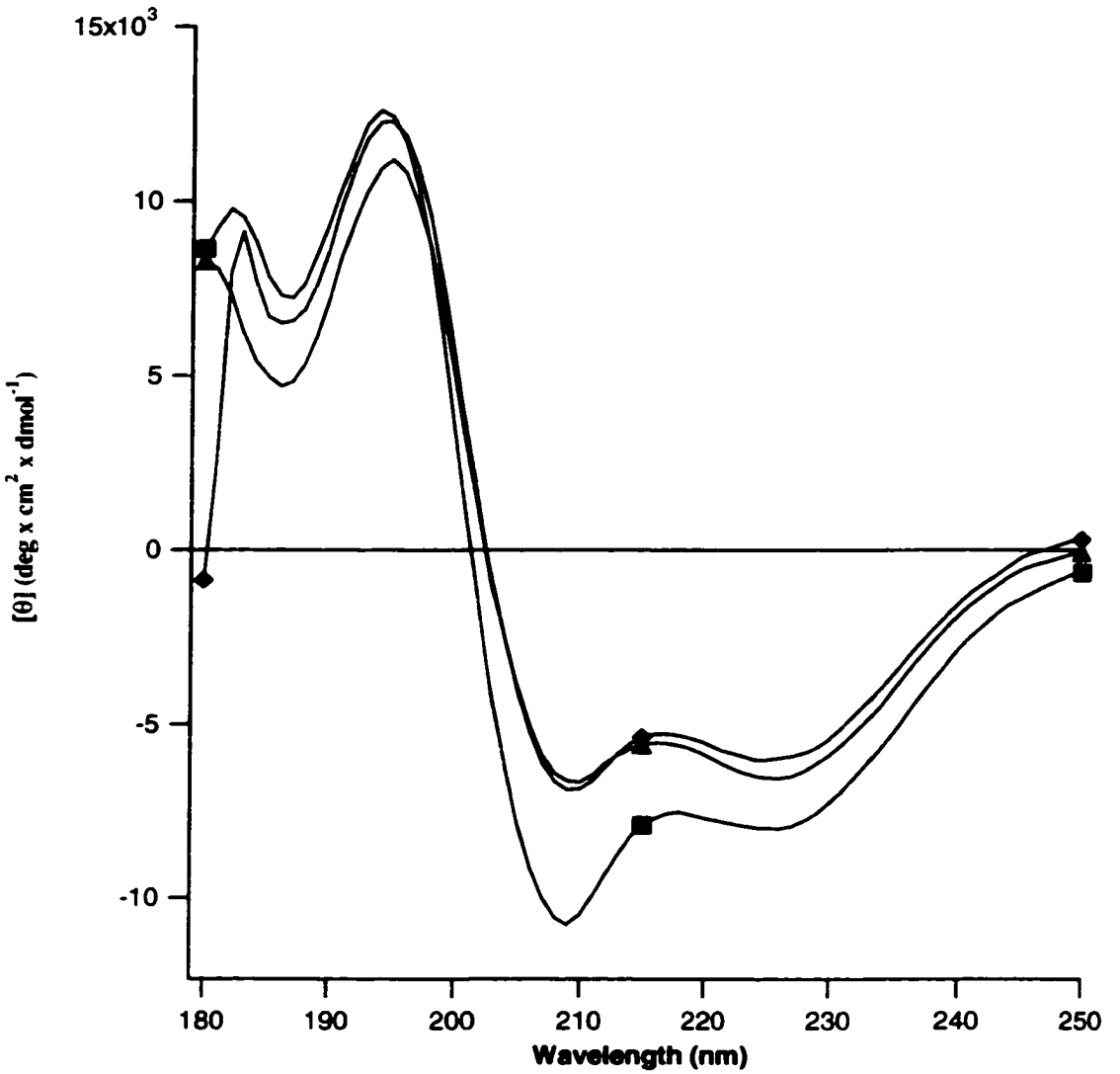

Figure 3.9. CD spectra of Ich-10 in 1:1 CH_3CN-H_2O (▲), 9:1 CH_3CN-H_2O (♦), and 9:1 CH_3CN-TFE (■).

Table 3.1

CD data and calculated structural information for Pi-10.[a]

Solvent	$[\theta]_{\pi\rightarrow\pi^*}$[b,c]	$[\theta]_{n\rightarrow\pi^*}$[b,d]	R	% Helicity
25 mM SDS	-8750	-7930	0.90	33 (α)
9:1 CH_3CN-TFE	-10710	-7930	0.74	33 (α)
9:1 CH_3CN-H_2O	-6180	-4290	0.71	22 (α)
1:1 CH_3CN-H_2O	-3180	-2130	0.66	15 (α)

[a] Peptide concentration was 200 μM.
[b] Units for [θ] are deg cm^2 $dmol^{-1}$.
[c] The minimum for the $[\theta]_{\pi\rightarrow\pi^*}$ band is taken in the range from 205-209 nm.
[d] The minimum for the $[\theta]_{n\rightarrow\pi^*}$ band is taken in the range from 222-225 nm.

Table 3.2

CD data and calculated structural information for Ipi-10.[a]

Solvent	$[\theta]_{\pi\rightarrow\pi^*}$[b,c]	$[\theta]_{n\rightarrow\pi^*}$[b,d]	R	% Helicity
25 mM SDS	-5520	-1750	0.32	25 (3_{10})
9:1 CH_3CN-TFE	-9920	-3150	0.33	33 (3_{10})
9:1 CH_3CN-H_2O	-6740	-3610	0.54	[e]
1:1 CH_3CN-H_2O	-4200	-3120	0.74	19 (α)

[a] Peptide concentration was 200 μM.
[b] Units for [θ] are deg cm^2 $dmol^{-1}$.
[c] The minimum for the $[\theta]_{\pi\rightarrow\pi^*}$ band is taken in the range from 205-209 nm.
[d] The minimum for the $[\theta]_{n\rightarrow\pi^*}$ band is taken in the range from 222-225 nm.
[e] In this solvent, Ipi-10 is probably a mixture of coil structures. The % α-helix is estimated to be 20% and the % 3_{10}-helix is estimated to be 31%.

Table 3.3

CD data and calculated structural information for Cyh-10.[a]

Solvent	$[\theta]_{\pi\rightarrow\pi^*}$[b,c]	$[\theta]_{n\rightarrow\pi^*}$[b,d]	R	% Helicity
25 mM SDS	-10870	-9980	0.92	39 (α)
9:1 CH_3CN-TFE	-10290	-9010	0.88	37 (α)
9:1 CH_3CN-H_2O	-9340	-8190	0.88	34 (α)
1:1 CH_3CN-H_2O	-7850	-7030	0.88	30 (α)

[a] Peptide concentration was 200 μM.
[b] Units for [θ] are deg cm^2 $dmol^{-1}$.
[c] The minimum for the $[\theta]_{\pi\rightarrow\pi^*}$ band is taken in the range from 205-209 nm.
[d] The minimum for the $[\theta]_{n\rightarrow\pi^*}$ band is taken in the range from 222-225 nm.

Table 3.4

CD data and calculated structural information for Ich-10.[a]

Solvent	$[\theta]_{\pi\rightarrow\pi^*}$[b,c]	$[\theta]_{n\rightarrow\pi^*}$[b,d]	R	% Helicity
25 mM SDS	-4790	-5460	1.14	26 (α)
9:1 CH_3CN-TFE	-10960	-8060	0.73	33 (α)
9:1 CH_3CN-H_2O	-6970	-6090	0.87	28 (α)
1:1 CH_3CN-H_2O	-6770	-6580	0.97	29 (α)

[a] Peptide concentration was 200 μM.
[b] Units for [θ] are deg cm^2 $dmol^{-1}$.
[c] The minimum for the $[\theta]_{\pi\rightarrow\pi^*}$ band is taken in the range from 205-209 nm.
[d] The minimum for the $[\theta]_{n\rightarrow\pi^*}$ band is taken in the range from 222-225 nm.

peptides, except Ipi-10, showed CD spectra characteristic of an α-helix (Figure 3.5). As expected, Pi-10 and Cyh-10 are α-helices in all solvent systems (Tables 3.1, 3.3 and Figures 3.6, 3.8). Ipi-10 displays a transition from an α-helix to a 3_{10}-helix as the solvent system increases in organic content (Table 3.2 and Figure 3.7). It was expected that Ich-10 would display this same transition; however as can be seen in Table 3.4 and Figure 3.9, this did not occur. Ich-10 displays an α-helical spectrum in all solvent systems tested.

The percent α-helix was estimated according to the following: percent α-helix = $-100([\theta]_{n\rightarrow\pi^*} + 3000)/33000$, where the minimum for the $[\theta]_{n\rightarrow\pi^*}$ transition is observed in the range 222-225 nm.[3.29] Little work has been done to quantify the percent 3_{10}-helix; therefore, we have used the CD spectrum of H-(Leu-Arg-Leu)$_8$-OH in diphosphatidylcholine liposomes as the model 3_{10}-helix. In this peptide, $[\theta]_{\pi\rightarrow\pi^*}$=-21,500 deg cm^2 dmol^{-1} is defined as 100% 3_{10}-helix.[3.33] Using this model, the above equation is modified to estimate percent 3_{10}-helicity: percent 3_{10}-helix = $-100([\theta]_{\pi\rightarrow\pi^*}/-21500)$.

3.3 Discussion

Factors stabilizing α-helices in many solvent systems have been extensively studied.[3.36-3.38] Coil to α-helix transitions have been observed as solvent systems increase in organic content.[3.39] A similar observation is predicted to occur for 3_{10}-helix/coil transitions.[3.5] One factor used to favor helices over a random coil is the incorporation of helix promoting ααAA's. Usually, incorporation of more than 50% ααAA's favors a 3_{10}-helix in short peptides.[3.16-3.23] However, due to the lack of

charged ααAA's, this factor has not been thoroughly studied as these studies have been limited to organic media. With the advent of a convenient synthesis of the lysine-like ααAA, Api, a polar ααAA can now be readily incorporated into peptides by solid-phase techniques.[3.30, 3.31, 3.40] The use of this positively charged ααAA allows the amphipathic design element to be extended to helical, water-soluble peptides. This will allow CD studies to be performed on peptides in aqueous/organic solvent systems and will allow us to probe the 3_{10}-/α-helix equilibrium in water, which is currently under debate.[3.5, 3.9-3.12, 3.27]

In order to study the stability of the 3_{10}- and α-helices, one needs to be able to distinguish between the two. It was thought that there was no difference in the CD spectra for these two secondary structures.[3.35] Other techniques such as electron spin resonance and NMR are difficult and have met with mixed results, especially with peptides containing ααAA's.[3.5-3.8, 3.41] Toniolo and co-workers have re-visited the issue of using CD to resolve this issue. They conclude that the 3_{10}-helix has an R-value ≤ 0.4 while the R-value for an α-helix is ≅ 1. An additional distinguishing feature is the positive CD band near 195 nm. This band is much weaker in the 3_{10}-helix than in the α-helix. Toniolo shows that his CD spectra for 3_{10}-helices in phospholipid bilayers are in agreement with that predicted by modeling.[3.32, 3.33]

All peptides tested contain 80% ααAA's to induce helicity. Pi-10 and Ipi-10 consisted of 6 Aib residues and 2 Api residues. Cyh-10 and Ich-10 consist of 6 Cyh residues and 2 Api residues. The remaining amino acid residue in each peptide is L-

lysine. This natural amino acid is used to induce a right-handed helix, which will result in a CD signal. The lack of this amino acid would result in no circular dichroism signal as the peptide would have no preference for a right or left-handed helix. The L-lysines are well seperated, near the middle of the sequence, to aid in the synthesis of the peptides.[3.42, 3.43]

In the peptides under study, amphipathy is the only factor used to influence the formation of either a 3_{10}- or α-helix. Pi-10 and Cyh-10 are designed to be α-helical while Ipi-10 and Ich-10 are designed to be 3_{10}-helical. Each of these peptides is less perfectly amphipathic in their alternative helix form (Figures 3.1 to 3.4) The peptides showed minimal structure in water or pH 7.1-7.4, 2.5 mM phosphate buffer. Upon addition of 25 mM SDS micelles to Pi-10, a transition to an α-helix spectrum with R = 0.90 and % α-helix = 33 % (Table 3.1 and Figure 3.5). The CD spectrum of Ipi-10 in 25 mM SDS micelles has an R = 0.32, indicative of a 3_{10}-helix (Table 3.2 and Figure 3.5). The % 3_{10}-helicity is estimated to be 25%. As noted in other studies, the positive CD band near 195 nm is weaker for Ipi-10 than for Pi-10.[3.32-3.34] Cyh-10 displays a typical α-helix CD spectrum in 25 mM SDS micelles with R = 0.92 and % α-helix = 39% (Table 3.3 and Figure 3.5). Ich-10, which was expected to be a 3_{10}-helix, exhibits an α-helical CD spectrum. The R-value for Ich-10 in SDS is 1.14 and % α-helix is 26%. Though Ich-10 is perfectly amphipathic in a 3_{10}-helix, it nevertheless adopted an α-helix structure. In the case of Ich-10, its α-helix structure is not perfectly amphipathic but it is still significantly amphipathic. In this form, the bulky cyclohexyl side chains on Cyh are further apart than in a 3_{10}-helix. In a 3_{10}-helix, these side chains would be in proximity.

CD spectra of all peptides in this study were taken in solvent systems ranging from 100% organic to 1:1 organic/water (Tables 3.1 to 3.4 and Figures 3.6 to 3.8). Pi-10 and Cyh-10 are typical α-helices in each solvent. Interestingly, Pi-10 exhibits an isodichroic point near 201 nm and Cyh-10, near 205 nm. This suggests a cooperative helix/coil transition. An additional observation is the reduction of helicity as organic solvent composition declines. The increase in helicity as the solvent system becomes rich in organic composition has been observed in other monomeric α-helices.[3.28] Others have predicted that peptides with high percentages of ααAA's (≥ 50%), such as Pi-10 and Cyh-10, would be 3_{10}-helical.[3.20, 3.42] In addition, theoretical calculations suggest these peptides would exhibit a shift to a 3_{10}-helix as organic content increases.[3.5] This is not observed in our studies, suggesting that amphipathy is a significant factor in determining helix structure. Ipi-10 behaves as expected, displaying a weak α-helix in 1:1 CH_3CN/H_2O, 3_{10}-helical character in 9:1 CH_3CN/H_2O and stronger 3_{10}-helical character in 9:1 CH_3CN/TFE. Ich-10 displays an α-helix structure in each solvent system. Though still α-helical, the R-value for Ich-10 is lower in 100% organic solvent than the other solvent systems.

The transition of Ipi-10 from an α-helix to a 3_{10}-helix and the lower R-value for Ich-10 in 100% organic solvent agrees with predictions of solvent effects on the 3_{10}-/α-helix equilibrium. It has been shown that peptides rich in Aib favor a 3_{10}-helix in less polar media and an α-helix in water. The increased stability of the 3_{10}-helix in non-polar solvents is due to the extra hydrogen bond formed relative to the α-helix. It is suspected

that α-helices are favored in water because the "extra" carbonyl and amide are able to hydrogen bond with the solvent.[3.5]

For Pi-10, Cyh-10 and Ich-10, a maximum number of 7 hydrogen bonds are possible in the α-helix conformation. For Ipi-10 in the 3_{10}-helical structure, 8 hydrogen bonds are possible. Helix end effects and incomplete micelle binding tend to reduce the absolute helicity of peptides.[3.29, 3.44, 3.45] In the case of Pi-10, Cyh-10 and Ich-10, the three N-terminal amides and the two C-terminal carbonyls do not have internal hydrogen bonding partners. For Ipi-10, the two N-terminal amides and the two C-terminal carbonyls are without internal hydrogen bonding partners. As a result, the peptides may adopt non-ideal structures at the ends to interact with solvent.[3.46] Recently, Toniolo and co-workers reported a short peptide exhibiting significant 3_{10}-helical structure in water.[3.27] The peptide contains the novel azacrowned functionalized amino acid, 2-amino-3-[1-(1,4,7-triazacyclononane)] propionic acid.

As stated previously, a sufficient database of 3_{10}-helix structures does not yet exist. As a result, estimation of % 3_{10}-helicity is difficult. It has been suggested that the CD bands of a 3_{10}-helix will be highly dependent on the ϕ and ψ torsion angles in the peptide backbone. 3_{10}-Helical peptides comprised of ααAA's have different ϕ and ψ angles than 3_{10}-helical peptides comprised only of natural amino acids.[3.20-3.23, 3.32] Toniolo and co-workers synthesized Ac-(αMeVal)$_8$-OtBu which exhibited significant 3_{10}-helical structure.[3.33, 3.34] Recently, Toniolo reported an additional short peptide exhibiting 3_{10}-helical structure in water.[3.27] Conflicting % 3_{10}-helix content can be

calculated based on which peptide is considered to be a definitive 3_{10}-helix. Clearly, more work needs to be done to resolve this issue.

3.4 Experimental

3.4.1 Peptide Synthesis

Cyh-10 and Ich-10 were synthesized as previously reported.[3.30, 3.31] The first 3 residues were manually coupled onto PAL-PEG-PS solid support. The couplings were done by gently refluxing 8 equivalents of the Fmoc-acid fluoride, 3 equivalents of DIEA and the resin in methylene chloride. The couplings were allowed to gently reflux until an acceptable yield was determined by quantitative Fmoc test.[3.47] After the first three residues were coupled to the resin, the remainder of the peptide was synthesized using a Milligen 9050 peptide synthesizer on the PAL-PEG-PS solid support using 8 equivalents of preformed Fmoc-acid fluorides, 3 equivalents of DIEA and a 1.5 h recycling time. Residues were double coupled when they were third in a series of α,α-disubstituted amino acids. A solution of 20% piperidine/2% 1,8-diazabicyclo[4.5.0]undec-7-ene (DBU) in DMF was used for Fmoc removal. The peptides were simultaneously cleaved from the resin and side-chain deprotected using reagent B (8.8 : 0.2 : 0.5 : 0.5, trifluoroacetic acid (TFA) : triisopropylsilane : water : phenol).[3.48] The resulting acidic solution was diluted with cold 30% acetic acid, washed with ethyl ether 94 x 50 mL), and lyophilized. The crude peptides were purified by preparative reverse-phase HPLC on a Waters 15 μM Deltapak C_4 column using a water (0.05% TFA) and acetonitrile (0.05% TFA) gradient system. The gradient was run from 10% to 50% organic and the absorption monitored at 222 nm. Purity of the peptides was checked on a Vydac 5 μM

C_{18} column using the same conditions. Matrix assisted laser desorption ionization (MALDI) mass spectrometry was used to verify the peptide masses. Cyh-10 and Ich-10, 1276 $(M+H)^+$.

3.4.2 Circular Dichroism

Circular dichroism measurements were taken on a (+)-camphor sulfonic acid calibrated Aviv 60DS spectrophotometer at 5°C. The measurements were recorded over 250-180 nm using a 0.1 cm pathlength quartz cell, 1 nm bandwith, 10 nm/min scan speed and a 5 second time constant. Background spectra were acquired prior to each sample spectrum and the two subtracted. Three repetitive scans were recorded and averaged to improve signal to noise. The reported mean residue ellipticity $[\theta]$ (deg cm^2 $dmol^{-1}$) is derived from the observed ellipticity, $[\theta]_{obs}$ (millidegrees), using the formula $[\theta] = [\theta]_{obs}$ (MRW/10*lc*). MRW is the mean residue molecular weight of the peptide (molecular weight of the peptide divided by the number of peptide bonds), *l* is the pathlength (cm) and *c* is the peptide concentration (mg/mL).

Final peptide concentrations of 0.2 mM were used for all experiments. The peptides were dissolved in: trifluoroethanol for spectra taken in 9:1 CH_3CN:TFE; pH 7.1-7.4, 2.5 mM phosphate buffer for spectra taken in SDS; and doubly distilled water for the aqueous/organic spectra. For representative aqueous/organic experiments, pH 7.1, 2.5 mM buffer was also used as the aqueous component and the resulting spectra were nearly identical to the pure H_2O/CH_3CN spectra.

3.5 References

3.1 Scholtz, J.M. and Baldwin, R.L., *Annu. Rev. Biophys. Biomol. Struct.*, **1992,** *21*, 95-118.

3.2 Hecht, M.H., *Proc. Natl. Acad. Sci. USA*, **1994,** *91*, 8729-8730.

3.3 Betz, S.F., Raleigh, D.P., and DeGrado, W.F., *Curr. Opin. Struct. Biol.*, **1993,** *3*, 601-610.

3.4 Barlow, D.J. and Thornton, J.M., *J. Mol. Biol.*, **1988,** *201*, 601-619.

3.5 Smythe, M.L., Nakaie, C.R., and Marshall, G.R., *J. Am. Chem. Soc.*, **1995,** *117*, 10555-10562.

3.6 Millhauser, G.L., *Biochemistry*, **1995,** *34*, 3874-3877.

3.7 Miick, S.M., Martinez, G.V., Fioro, W.R., Todd, A.P., and Millhauser, G.L., *Nature*, **1992,** *359*, 653-655.

3.8 Hanson, P., Martinez, G., Millhauser, G., Formaggio, F., Crisma, M., Toniolo, C., and Vita, C., *J. Am. Chem. Soc.*, **1996,** *118*, 271-272.

3.9 Basu, G., Kitao, A., Hirata, F., and Go, N., *J. Am. Chem. Soc.*, **1994,** *116*, 6307-6316.

3.10 Otoda, K., Kitagawa, Y., Kimura, S., and Imanishi, Y., *Biopolymers*, **1993,** *33*, 1337-1345.

3.11 Tirado-Rives, J., Maxwell, D.S., and Jorgensen, W.L., *J. Am. Chem. Soc.*, **1993,** *115*, 11590-11593.

3.12 Smythe, M.L., Huston, S.E., and Marshall, G.R., *J. Am. Chem. Soc.*, **1993,** *115*, 11594-11595.

3.13 Toniolo, C. and Benedetti, E., *Trends Biochem. Sci.*, **1991,** *16*, 350-353.

3.14 Gerstein, M. and Chothia, C., *J. Mol. Biol.*, **1991,** *220*, 133-149.

3.15 McPhalen, C.A., Vincent, M.G., Picot, D., Jansonius, J.N., Lesk, A.M., and Chothia, C., *J. Mol. Biol.*, **1992,** *227*, 197-213.

3.16 Prasad, B.V.V. and Balaram, P., *CRC Crit. Rev. Biochem.*, **1984,** *16*, 307-348.

3.17 Balaram, P., *Curr. Opin. Struct. Biol.*, **1992,** *2*, 845-851.

3.18 Marshall, G.R., Hodgkin, E.E., Langs, D.A., Smith, G.D., Zabrocki, J., and Leplawy, M.T., *Proc. Natl. Acad. Sci. USA*, **1990,** *87*, 487-491.

3.19 Augspurger, J.D., Bindra, V.A., Scheraga, H.A., and Kuki, A., *Biochemistry*, **1995,** *34*, 2566-2576.

3.20 Karle, I.L. and Balaram, P., *Biochemistry*, **1990,** *29*, 6747-6756.

3.21 Karle, I.L., *Acta Crystallogr. B*, **1992,** *48*, 341-356.

3.22 Karle, I.L., Flippen-Anderson, J.L., Gurunath, R., and Balaram, P., *Biopolymers (Protein Sci.)*, **1994,** *4*, 1547-1555.

3.23 Kennedy, D.F., Crisma, M., Toniolo, C., and Chapman, D., *Biochemistry*, **1991,** *30*, 6541-6548.

3.24 Marqusee, S. and Baldwin, R.L., *Proc. Natl. Acad. Sci. USA*, **1987,** *84*, 8898-8902.

3.25 Marqusee, S., Robbins, V.H., and Baldwin, R.L., *Proc. Natl. Acad. Sci. USA*, **1989,** *86*, 5286-5290.

3.26 Scholtz, J.M., Marqusee, S., Baldwin, R.L., York, E.J., Stewart, J.M., Santoro, M., and Bolen, D.W., *Proc. Natl. Acad. Sci. USA*, **1991,** *88*, 2854-2858.

3.27 Rossi, P., Felluga, F., Tecilla, P., Formaggio, F., Crisma, M., Toniolo, C., and Scrimin, P., *J. Am. Chem. Soc.*, **1999,** *121*, 6948-6949.

3.28 Stewart, J.M., *The Amphipathic Helix*, ed. R.M. Epand. 1993. Boca Raton, FL: CRC Press. 21-37.

3.29 Javadpour, M.M., Juban, M.M., Lo, W.-C.J., Bishop, S.M., Alberty, J.B., Cowell, S.M., Becker, C.L., and McLaughlin, M.L., *J. Med. Chem.*, **1996,** *39*, 3107-3113.

3.30 Wysong, C.L., Yokum, T.S., Morales, G.A., Gundry, R.L., McLaughlin, M.L., and Hammer, R.P., *J. Org. Chem.*, **1996,** *61*, 7650-7651.

3.31 Yokum, T.S., Elzer, P.H., and McLaughlin, M.L., *J. Med. Chem.*, **1996,** *39*, 3603-3605.

3.32 Manning, M. and Woody, R.W., *Biopolymers*, **1991,** *31*, 569-586.

3.33 Iwata, T., S., L., Oishi, O., Aoyagi, H., Ohno, M., Anzai, K., Kirino, Y., and Sugihara, G., *J. Biol. Chem.*, **1994,** *269*, 4928-4933.

3.34 Toniolo, C., Polese, A., Formaggio, F., Crisma, M., and Kamphuis, J., *J. Am. Chem. Soc.*, **1996,** *118*, 2744-2745.

3.35 Sudha, T.S., Vijayakumar, E.K.S., and Balaram, P., *Int. J. Pept. Protein Res.*, **1983,** *22*, 464-468.

3.36 Lau, S.Y.M., Taneja, A.K., and Hodges, R.S., *J. Biol. Chem.*, **1984,** *259*, 13253-13261.

3.37 Hu, J.C., O'Shea, E.K., Kim, P.S., and Sauer, R.T., *Science*, **1990,** *250*, 1400-1403.

3.38 DeGrado, W.F., Wasserman, Z.R., and Lear, J.D., *Science*, **1989,** *243*, 622-628.

3.39 Nelson, J.W. and Kallenbach, N.R., *Proteins*, **1986,** *1*, 211-217.

3.40 Hammarström, L.G.J. and McLaughlin, M.L., *Organic Synthesis*, Submitted for publication.

3.41 Millhauser, G.L., Stenland, C.J., Hanson, P., Bolin, K.A., and van de Ven, F.J.M., *J. Mol. Biol.*, **1997,** *267*, 963-974.

3.42 Basu, G., Bagchi, K., and Kuki, A., *Biopolymers*, **1991,** *31*, 1763-1774.

3.43 Basu, G. and Kuki, A., *Biopolymers*, **1993,** *33*, 995-1000.

3.44 Vijayakumar, E.K.S., Sudha, T.S., and Balaram, P., *Biopolymers*, **1984,** *23*, 877-886.

3.45 Shalongo, W., Dugad, L., and Stellwagen, E., *J. Am. Chem. Soc.*, **1994,** *116*, 8288-8293.

3.46 Bindra, V.A. and Kuki, A., *Int. J. Peptide Prot. Res.*, **1994,** *44*, 539-548.

3.47 Fields, G.B., Tian, Z., and Barany, G., *Synthetic Peptides: A User's Guide*, ed. G.A. Grant. 1992, USA: W. H. Freeman and Co.

3.48 Van Abel, R.J., Tang, Y., Rao, V.S.V., Dobbs, C.H., Tran, D., Barany, G., and Selsted, M.E., *Int. J. Pept. Protein Res.*, **1995,** *45*, 401-409.

Chapter 4

Synthesis of a Beta Sheet Promoting Amino Acid

4.1 Introduction

Next to the α-helix, the most common and readily identifiable secondary structure in proteins is the β-sheet.[4.1] The basic unit of a β-sheet is the β-strand, a polypeptide that is almost fully extended. This extended conformation is not particularly stable because there are no favorable intra-strand interactions as are found in the α- and 3_{10}-helices. The β-strand is stabilized when it is incorporated into a β-sheet, where hydrogen bonds are formed between the peptide groups on adjacent strands. Adjacent strands can be parallel or anti-parallel. Figures 4.1 and 4.2 show each of these structures. Anti-parallel sheets are thought to be more stable than parallel sheets although this is not always the case. Side chains from adjacent residues of the same strand protrude from opposite sides of the sheet and do not interact with each other, but they can have significant interactions with the side chains of neighboring strands.[4.1]

The study of the β-sheet has recently gained interest due to the suspected involvement of the β-sheet in diseases such as Alzheimer's disease (AD), Creutzfeldt-Jacob disease (CJD) and bovine spongiform encephalopathy (mad cow disease). Despite the fact that the β-sheet occurs almost as often as the α-helix among secondary structures found in proteins, relatively little is known about the factors that stabilize the β-sheet. The synthesis of small peptides to study the β-sheet structure has proven elusive. Often, these peptides have a propensity to self-associate into large, generally insoluble, quaternary β-sheet structures.[4.2, 4.3] As a result, most recent studies have

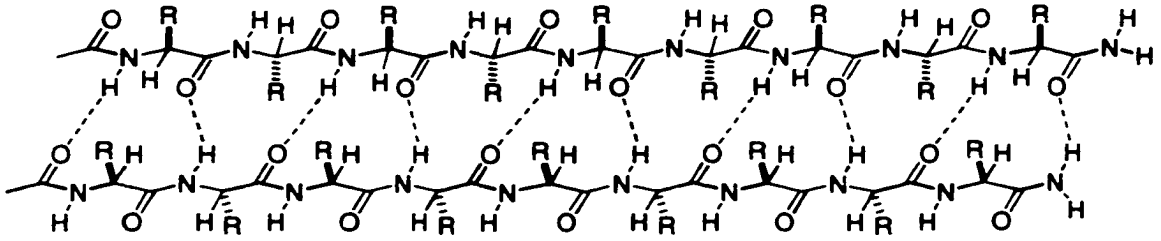

Figure 4.1. Parallel beta sheet.

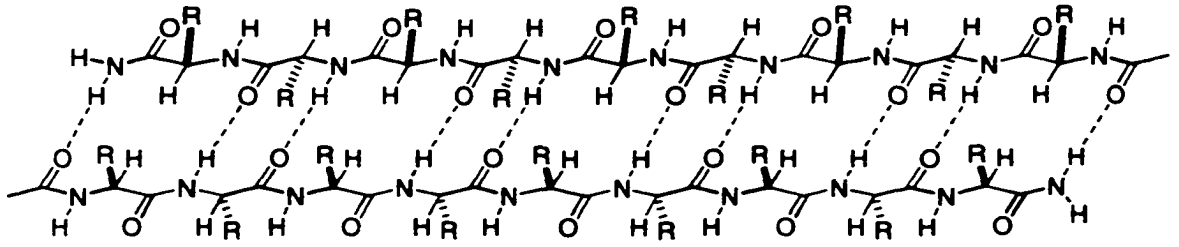

Figure 4.2. Anti-parallel beta sheet.

focused on synthesizing a novel amino acid which serves as a β-turn to nucleate β-sheet formation. These β-sheet structures are intramolecular and are not a completely regular structure because segments of the peptide that connect the strands (i.e. turns) must adopt different conformations.[4.1, 4.4, 4.5] Therefore, it would be beneficial to assemble a β-sheet that is intermolecular. The strands are not covalently linked and would be free to aggregate to form the β-sheet. No alteration of conformation would be needed to accommodate the amino acid making the turn. One problem with this approach is the possibility of large-scale aggregation. Too many strands aggregating to form the β-sheet

could lead to an insoluble protein. This problem could be avoided if the β-sheet could be limited to a small number of strands, possibly as little as two strands.

A two-stranded β-sheet has two distinctly different amide hydrogen and α-carbon hydrogen environments. The endo amide hydrogens, labeled H_a in Figure 4.3, form an inter-strand hydrogen bond (H-bond) to complementary amide oxygens. The endo α-carbon pro-R position, labeled H_b is sterically congested by a convergent H_b from the anti-parallel strand. Therefore, only a proton is tolerated in that position. The exo amide hydrogen, labeled H_c, lacks a specific complementary hydrogen bond partner and could be replaced without disruption of the two-stranded β-sheet. Doig and co-workers have replaced the H_c-like hydrogens of a three-stranded β-sheet with methyl groups, thereby preventing further H-bond mediated oligomerization.[4.6] Figure 4.3 also shows that the exo α-carbon pro-R position, labeled H_d, is not sterically congested so this position can also be substituted without disruption of the two-stranded β-sheet. Replacement of H_c and H_d with cyclic tethers should stabilize two-stranded β-sheet model systems as shown in Figure 4.4.

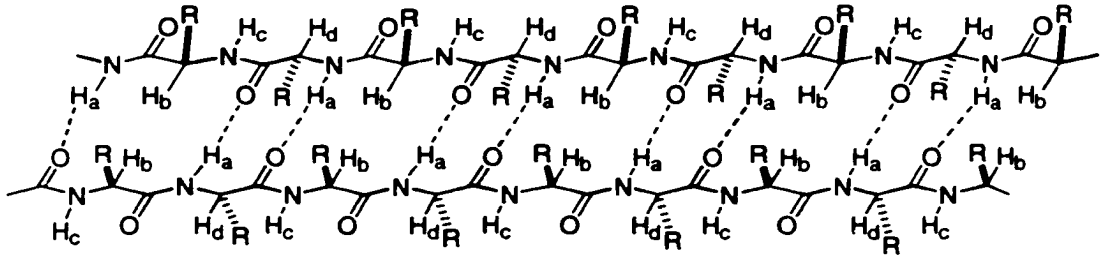

Figure 4.3. Two stranded beta sheet with exo and endo positions shown.

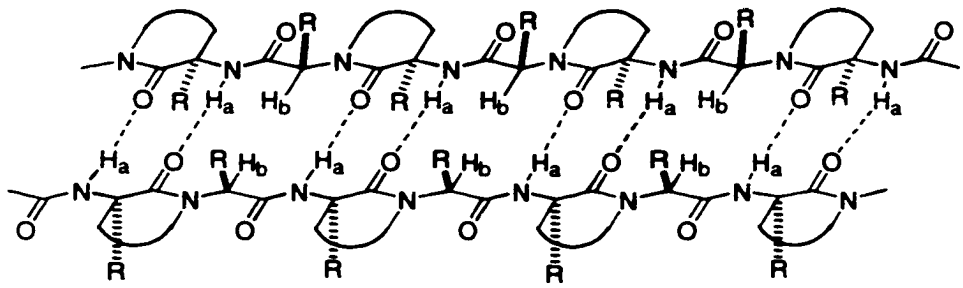

Figure 4.4. Two stranded beta sheet with cyclic tether shown.

Most *de novo* β-sheet models use natural or artificial β-turns or linkers to initiate intramolecular β-sheet dimers.[4.6-4.12] By incorporating lactam-constrained amino acids as well as α-amino acids, it should be possible to synthesize a peptide that is pre-organized to have extended-like conformations. Unlike the hairpin model systems discussed above, these individual extended conformation strands should spontaneously self-assemble into β-sheet dimers when a minimum peptide length is reached. The use of lactam-constrained amino acids, like Doig's approach, should inhibit further H-bond mediated oligomerization because the amide H_c atoms are replaced.

In order to determine the correct tether for the lactam-constrained amino acid, selected distances in several peptides having protons in H_c- and H_d-like environments were measured using Sybyl. The average distance between H_c and H_d is 2.25 Å. Plane angles were then calculated from the HN-amide and pro-R α-CH-carbonyl. The relative plane angle differences were between 12° to 20°. The *i*th C-H_d and *i*th + 1 H-N_c are held close to parallel to each other in the extended conformation. The distance between the *i*th C-H_d and *i*th + 1 N-H_c bonds is almost perfectly spanned by a 3-carbon tether, resulting in a six-membered lactam-constrained dipeptide (Figure 4.5).

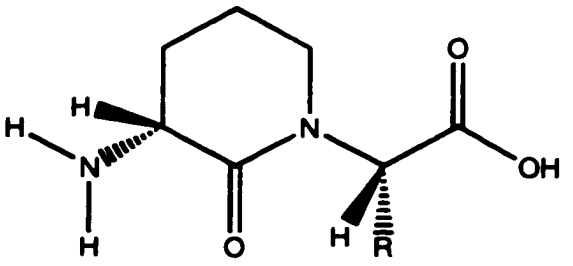

Figure 4.5. Six-membered lactam-constrained dipeptide amino acid.

It is important to note the replacement of the pro-*R* H_d position with a 3-carbon tether requires the D-amino acid configuration. Pro-*S* amino acid side chains alternate pointing up and down in the *i*th +1 and *i*th constrained lactam amino acids in Figure 4.4. In the proposed model, the hydrogen is pointing down in the *i*th pro-*S* amino acid position and pseudo axial on the six-membered lactam. The sterically larger amino group occupies a pseudo equatorial position on the six-membered lactam. This configuration should favor the extended conformation in peptides incorporating the proposed constrained lactam amino acid.

The control of conformation with six-membered rings is well documented. The earliest known synthesis of a lactam-constrained amino acid was reported by Freidinger and co-workers.[4.13] He reports the synthesis of a glycine-like six-membered lactam-constrained dipeptide derivative (Figure 4.6A). Others have since worked to synthesize similar lactam-constrained dipeptide amino acids for study.[4.14-4.18] Zydowsky and co-workers synthesized glycine- and phenylalanine-like lactam-constrained dipeptide amino acids that were α,α-disubstituted at the α-carbon of the lactam (Figure 4.6B). They further report modest coupling yields of the amino acids (68-92%) in the synthesis of a peptide dimer.[4.19] Moss and co-workers report the synthesis of a ureido-based

peptidomimetic inhibitor of a herpes simplex virus enzyme. Their inhibitor contains a lactam-constrained dipeptide amino acid. However, the synthesis of the lactam-constrained dipeptide amino acid involves a lengthy and expensive procedure to obtain an aldehyde intermediate.[4.20] Here we report an improved route to a novel lactam-constrained amino acid that is incorporated, in high yields, in a peptide pre-designed to form a β-sheet dimer.

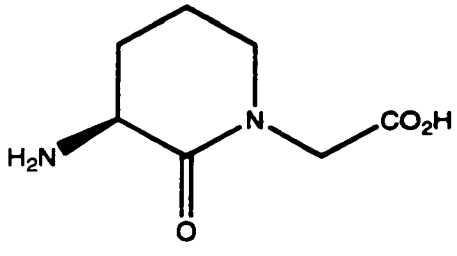

A

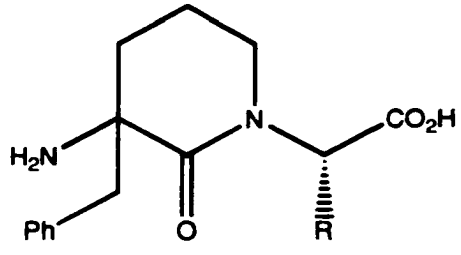

R = methyl or methylphenyl

B

Figure 4.6. Freidinger (a) and Zydowsky (b) constrained lactam amino acids.

4.2 Results and Discussion

The general structure of the target amino acid is shown in Figure 4.5. The amino acid is constructed from a six-membered ring backbone previously shown to promote an extended conformation.[4.13] Specifically, we sought to synthesize the valine derivative of a constrained dipeptide amino acid (Figure 4.7) because valine is known to promote the β-sheet structure.[4.21-4.23] The valine moiety is introduced via a reductive amination. The reductive amination step is likely adaptable to constrained dipeptide amino acids.

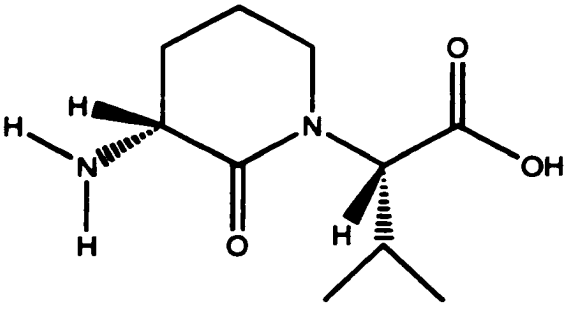

Figure 4.7. Target constrained dipeptide amino acid.

The key to the synthesis of the constrained dipeptide amino acid unit (DPU) is the synthesis of an α-amino acid semialdehyde. The synthesis of the aldehyde is based on a synthetic route developed by Martín and co-workers.[4.24] Figure 4.8 outlines the steps involved in the aldehyde synthesis. The synthesis begins with the esterification of D-glutamic acid, **4.1**, with dry allyl alcohol, under argon, in the presence of trimethylsilylchloride (TMS-Cl, 4.4 equivalents) to yield the diester after 3 days. Triethylamine (6.5 equivalents) and Boc anhydride (1.1 equivalents) were added sequentially and the reaction mixture was stirred overnight. Removal of the allyl alcohol followed by trituration with diethyl ether and filtration through a celite pad gave compound **4.2** in quantitative yield. The presence of the product was verified by FAB-MS (328, $M+H^+$). In addition, ^1H NMR and ^{13}C NMR verified the presence of the Boc and allyl groups by appearance of t-butyl and allyl protons and carbons, respectively. This reaction is versatile in that the scale can be varied greatly (1 gram to 15 grams) with little effect on purity or yield.

The α-nitrogen in **4.2** is still quite nucleophilic, especially towards an aldehyde.[4.20] As a result, the nitrogen must be doubly protected prior to introduction of the aldehyde. A simple way to achieve this protection is to introduce another Boc group. Compound

4.2 is dissolved in dry acetonitrile along with *N, N*-dimethylaminopyridine (DMAP, 0.2 equivalents) followed by Boc anhydride (1.1 equivalents). After two hours, an additional 0.2 equivalents of DMAP and 0.5 equivalents of Boc anhydride are added. The red solution is allowed to stir overnight, after which the solvent is removed. The residue is taken up in a minimum volume of hexanes/ethyl acetate (7:3) and is purified via flash column chromatography over silica gel to give **4.3** in 95% yield. The presence of the product was verified by FAB-MS (428, $M+H^+$). The product was also verified by a slight change in the chemical shift of the protons and carbons in the Boc group as determined by ^1H and ^{13}C NMR.

With the fully protected D-glutamic acid, the key aldehyde intermediate can be synthesized. Compound **4.3** is dissolved in dry diethyl ether under argon. Diisobutyl aluminum hydride (DIBAL, 1.0M solution in hexanes, 1.5 equivalents) is added drop wise at -78° C. The reaction is stirred at -78° C for 30 minutes at which time it is quenched with methanol and 10% sodium bisulfate. After extraction with 10% sodium bisulfate, the organic layer is dried and evaporated to give **4.4** in 98% yield. The presence of the product was verified by FAB-MS (372, $M+H^+$). The product was further verified by the disappearance of one group of allyl protons and carbons and the appearance of the characteristic aldehyde proton and carbon as shown in ^1H and ^{13}C NMR.

It should be noted that the selective reduction of only the side-chain ester is vital to the success of this synthetic scheme. DIBAL is a common reagent used in the reduction of esters to aldehydes. Martín and co-workers reported the selective reduction of the side-chain methyl ester over the main chain ester.[4.24] However, great care had to be taken to

limit the reaction time to 5 minutes so as not to reduce the main chain ester as well. In addition, the temperature must be kept at -78° C or over reduction to the alcohol will result.[4.24] The stability of the aluminum-oxygen complex at this temperature is the key in the reduction to the aldehyde. Premature release of the aldehyde as a result of the collapse of the aluminum-oxygen complex will result in reduction to the alcohol in the presence of hydride. Initially, we sought to repeat Martín's technique by synthesizing the fully protected dimethyl ester of D-glutamic acid. The synthesis was easily accomplished and variations in the conditions of the selective ester reduction confirmed its extreme sensitivity towards over reduction. We encountered difficulties in hydrolyzing the methyl ester, the next step in our synthetic scheme to the DPU. At this point, we decided to make the diallyl ester instead. The selective reduction was carried out as before and we were pleasantly surprised to discover that it was much more robust than previously observed. The reduction time can be extended and the temperature can be varied without any apparent over reduction. We believe the allyl ester provides additional steric hindrance on the main chain ester resulting in exclusive attack of the DIBAL on the side- chain ester.

With the fully protected semi-aldehyde in hand, the synthetic route of the constrained dipeptide amino acid can be altered to accommodate virtually any amino acid via reductive amination.[4.25] In our case, we chose to use L-valine to continue the synthesis (Figure 4.9). Compound **4.4** and L-Val-OtBu·HCl (1 equivalent) were stirred in dry 1,2-dichloroethane (DCE). Triethylamine (TEA, 1.1 equivalents) was added followed by sodium triacetoxyborohydride (1.4 equivalents). The solution was stirred

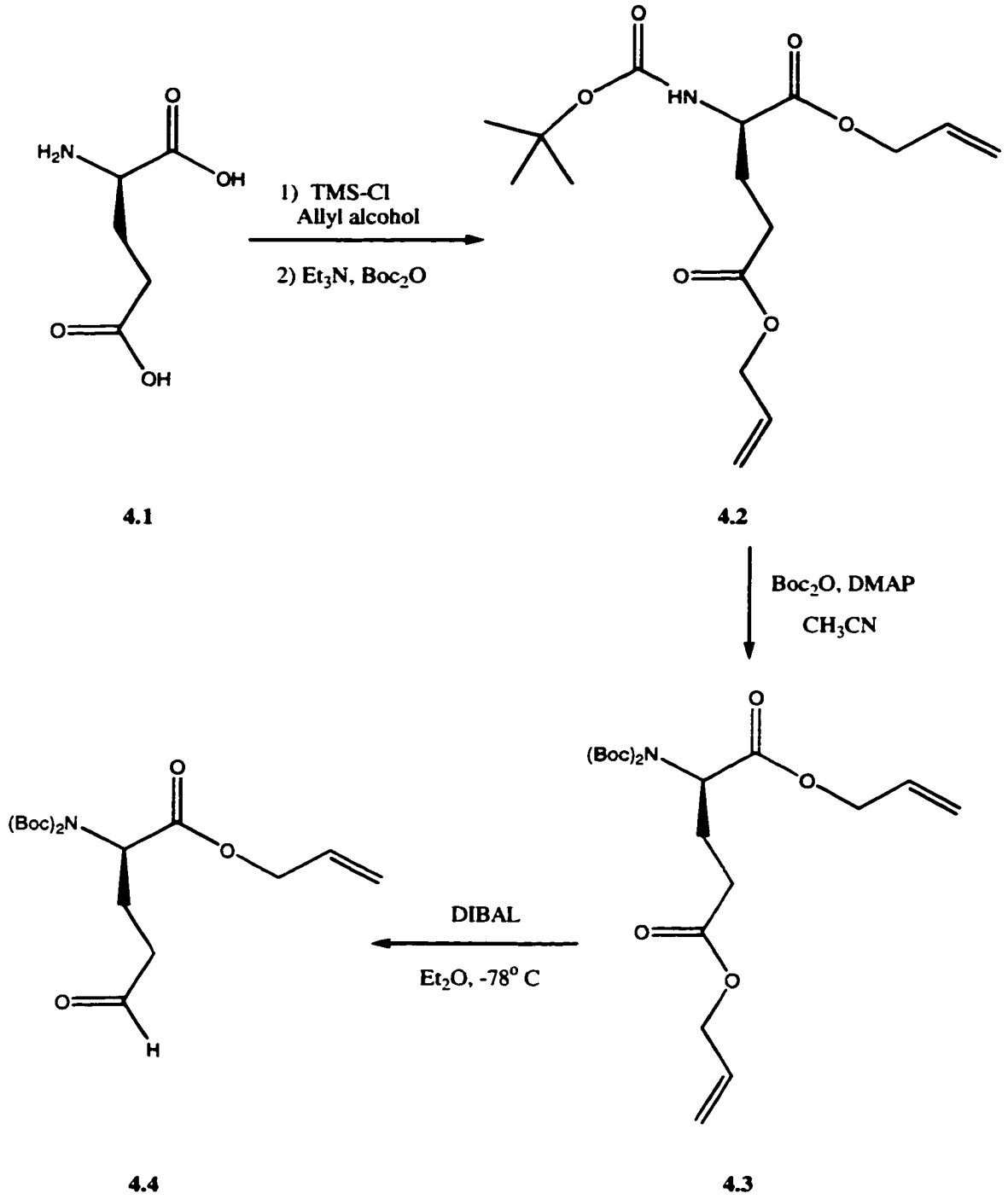

4.1 4.2 4.3 4.4

Figure 4.8. Synthetic route to the key aldehyde intermediate.

overnight, after which it was washed with saturated sodium bicarbonate. The organic layer was dried and evaporated to provide **4.5** in 90% yield. The presence of the product was verified by FAB-MS (529, $M+H^+$). In addition, ^1H and ^{13}C revealed the presence of the valine side-chain methyl groups as well as the t-butyl ester.

Cyclization of **4.5** will yield the constrained dipeptide amino acid. In order to accomplish this step, the allyl ester must be removed. Acid hydrolysis of the ester is not prudent, as the t-butyl ester on the valine moiety will also be removed. Base hydrolysis proved to be too slow to be feasible. A logical alternative is the palladium-catalyzed removal of allyl groups.[4.26, 4.27] Compound **4.5** is dissolved in dry dichloromethane (DCM) under argon. Morpholine (10 equivalents) is added, followed by palladium tetrakistriphenylphosphine (0.1 equivalents). After 30 minutes, the reaction mixture is washed with 1N hydrochloric acid and the organic solvent is dried and removed. The crude product is taken up in ethanol/DCM (9:1) and purified by flash column chromatography to give **4.6** in 85% yield. The presence of the product is verified by FAB-MS (490, $M+H^+$). Further evidence of the removal of the allyl ester is provided by the absence of the allyl protons and carbons as shown in ^1H and ^{13}C NMR spectra of the product.

Compound **4.6** can be cyclized to the constrained dipeptide amino acid by an intramolecular amide bond formation. Compound **4.6** is dissolved in dry acetonitrile to which is added HATU (1 equivalent) and diisopropylethylamine (DIEA, 2.1 equivalents). After stirring for 2 hours, the solvent is removed, the residue taken up in DCM and washed with 10% sodium bisulfate. The DCM is dried and evaporated to yield 77% of cyclized product, **4.7**. The presence of the product is verified by FAB-MS

(472, $M+H^+$) as well as an X-ray crystal structure of the product (Figure 4.10). Tables 4.1 to 4.3 give the bond distances, bond angles and torsion angles, respectively for **4.7**. The ψ angle in **4.7** is 150.3°, which compares favorably to the ideal angle of 135° in an antiparallel β-sheet.

The Boc protecting groups and t-butyl ester must be removed in order to prepare the DPU for coupling. This is easily accomplished by treating **4.7** with approximately 5 mL of DCM/TFA (1:1) for 15 minutes. The DCM/TFA mixture is then removed under vacuum. To prepare the amino acid for coupling, the α-nitrogen must be protected. A convenient protecting group is the Fmoc group. Two routes have been utilized to introduce this protecting group. Figure 4.11 shows both synthetic routes. The first is a method used by Lapatsanis and co-workers.[4.28] In this method, the residue is taken up in sufficient 9% sodium carbonate to give a solution with pH 9. The reaction mixture is cooled to 0° C and a solution of Fmoc-OSu (1.05 equivalents) in dioxane is added. After stirring for 2 hours, the reaction mixture is diluted with water and extracted with diethyl ether followed by ethyl acetate. The aqueous phase is cooled in an ice bath and acidified to pH 2 with concentrated hydrochloric acid. The Fmoc-protected amino acid is extracted with ethyl acetate, which is then dried and evaporated. The crude product is purified by flash column chromatography to give **4.8** in 51% yield. The presence of the product is verified by FAB-MS (437, $M+H^+$). Proton and carbon NMR spectra verify the removal of the Boc groups and the t-butyl ester. The Fmoc protecting group is verified by the appearance of aromatic hydrogens and carbons in the respective spectra.

An alternative procedure to introduce the Fmoc protecting group was developed by Bolin

and co-workers.[4.29] The residue from the Boc-group and t-butyl ester removal is suspended in DCM. TMS-Cl (2.5 equivalents) is added to the ice cooled reaction mixture followed by DIEA (3.0 equivalents) and Fmoc-Cl (1.1 equivalents). This procedure is convenient as it solubilizes the amino acid by neutralizing the free amino function with DIEA and forms the silyl ester with TMS-Cl in neat organic media. The neutral, organic-soluble amino acid is reacted with Fmoc-Cl to yield the protected amino acid. The product is purified via silica gel chromatography to give **4.8** in 85% yield.

With the fully protected constrained lactam amino acid in hand, a peptide designed to prefer an extended conformation can now be synthesized. The peptide under study, Ac-Lys-Lys-Lys-DPU-DPU-Lys-Lys-NH_2, was assembled using a Milligen 9050 peptide synthesizer on PAL-PEG-PS solid support. The couplings were done in N, N-dimethylformamide (DMF) using a four-fold excess of the Fmoc-amino acids, three equivalents of DIEA, four equivalents of HATU and a one-hour recycling time. Fmoc removal was accomplished by treatment with a solution of 2% 1,8-diazobicyclo[4.5.0]undec-7-ene (DBU), 20% piperidine in DMF. Acetylation of the peptide was carried out by treating the resin bound peptide with a 0.2M solution of acetic anhydride in 0.28M DIEA solution in DMF for 40 minutes. Side-chain and resin cleavage was done by treatment with TFA, triisopropylsilane, water, phenol (8.8:0.2:0.5:0.5) (reagent B) for 2 hours.[4.30] The peptide was purified by preparative reverse-phase HPLC on a C_4 column using a gradient of water and acetonitrile with 0.05% TFA in each. Molecular weight and amino acid composition were verified by

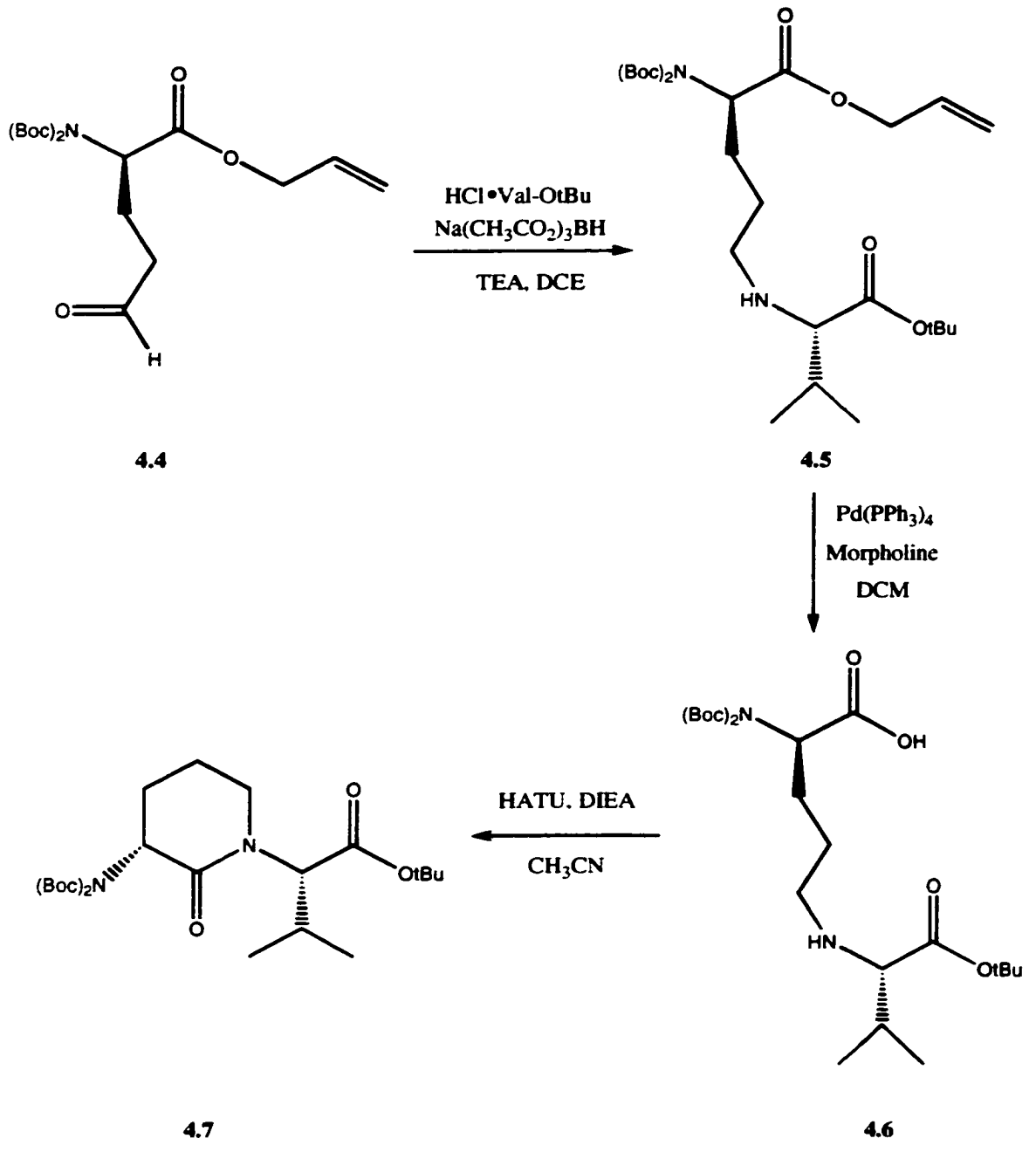

Figure 4.9. Synthetic route to Boc-protected constrained lactam amino acid.

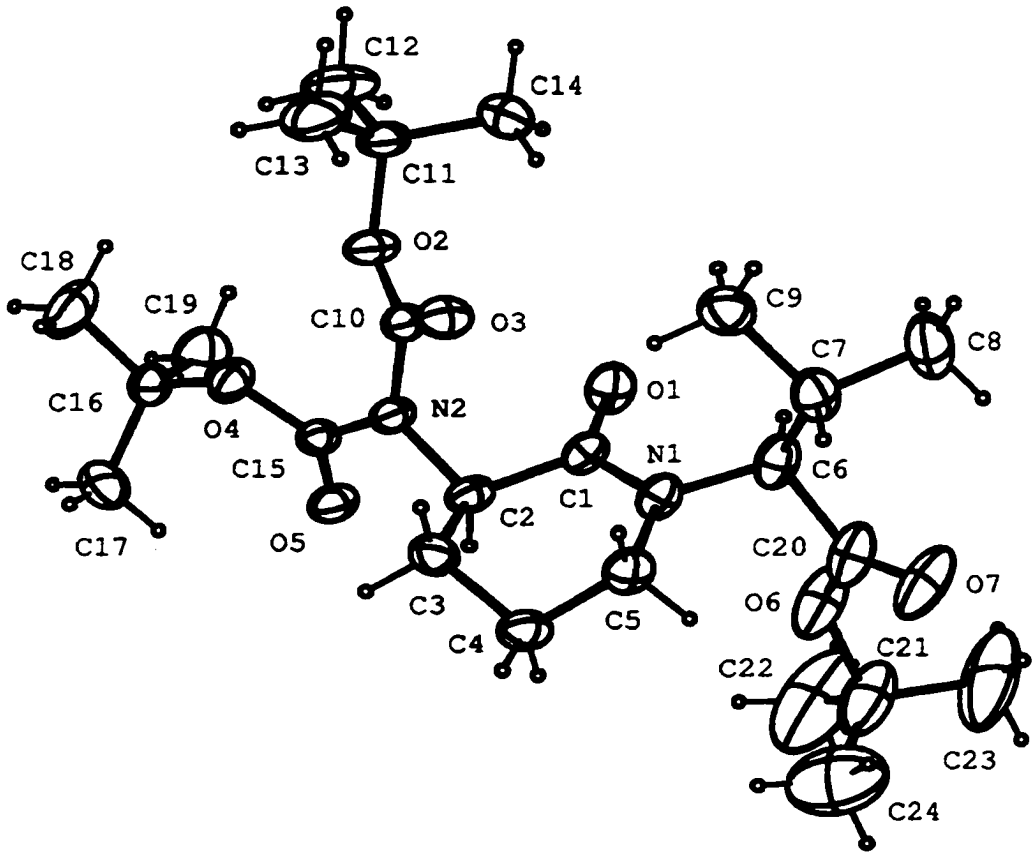

Figure 4.10. ORTEP of **4.7**.

Table 4.1

Bond distances (Å) for **4.7**.[a]

Atom 1	Atom 2	Distance	Atom 1	Atom 2	Distance
O1	C1	1.213(2)	C1	C2	1.522(2)
O2	C10	1.317(3)	C2	C3	1.527(3)
O2	C11	1.484(3)	C3	C4	1.504(4)
O3	C10	1.201(3)	C4	C5	1.499(3)
O4	C15	1.319(3)	C6	C7	1.534(5)
O4	C16	1.470(3)	C6	C20	1.526(4)
O5	C15	1.201(3)	C7	C8	1.523(4)
O6	C20	1.324(4)	C7	C9	1.528(5)
O6	C21	1.480(6)	C11	C12	1.519(5)
O7	C20	1.189(4)	C11	C13	1.468(4)
N1	C1	1.361(3)	C11	C14	1.511(4)
N1	C5	1.471(3)	C16	C17	1.506(5)
N1	C6	1.453(2)	C16	C18	1.497(5)
N2	C2	1.463(3)	C16	C19	1.513(4)
N2	C10	1.404(3)	C21	C22	1.510(1)
N2	C15	1.389(3)	C21	C23	1.563(6)

[a]Numbers in parentheses are estimated standard deviations in the last digits.

Table 4.2

Bond angles (°) for **4.7**.[a]

Atom 1	Atom 2	Atom 3	Angle	Atom 1	Atom 2	Atom 3	Angle
C10	O2	C11	121.3(2)	C6	C7	C9	111.4(2)
C15	O4	C16	121.6(2)	C8	C7	C9	127.1(2)
C20	O6	C21	123.8(3)	O2	C10	O3	127.1(2)
C1	N1	C5	123.9(2)	O2	C10	N2	111.6(2)
C1	N1	C6	118.7(2)	O3	C10	N2	121.2(2)
C5	N1	C6	117.0(2)	O2	C11	C12	102.4(2)
C2	N2	C10	115.9(2)	O2	C11	C13	111.1(2)
C2	N2	C15	117.2(2)	O2	C11	C14	108.9(2)
C10	N2	C15	126.8(2)	C12	C11	C13	111.3(3)
O1	C1	N1	122.3(2)	C12	C11	C14	110.3(2)
O1	C1	C2	120.2(2)	C13	C11	C14	112.3(3)
N1	C1	C2	117.3(2)	O4	C15	O5	126.3(2)

[a]Numbers in parentheses are estimated standard deviations in the last digits.

Table 4.2 (cont'd)

Atom 1	Atom 2	Atom 3	Angle	Atom 1	Atom 2	Atom 3	Angle
N2	C2	C1	109.7(2)	O4	C15	N2	111.6(2)
N2	C2	C3	113.0(2)	O5	C15	N2	121.9(2)
C2	C3	C4	109.9(2)	O4	C16	C18	102.2(2)
C3	C4	C5	108.6(2)	O4	C16	C19	108.6(2)
N1	C5	C4	113.8(2)	C17	C16	C18	113.2(2)
N1	C6	C7	114.0(2)	C17	C16	C19	109.8(3)
N1	C6	C20	108.0(2)	C18	C16	C19	111.3(3)
C7	C6	C20	112.6(2)	O6	C20	O7	124.7(3)
C6	C7	C8	110.5(3)	O6	C20	C6	110.4(3)
O7	C20	C6	124.8(3)	O6	C21	C23	106.4(5)
O6	C21	C22	99.0(5)	C22	C21	C23	107.0(5)

Table 4.3

Torsion angles (°) for **4.7**.[a]

Atom 1	Atom 2	Atom 3	Atom 4	Angle
C11	O2	C10	O3	1.28(0.33)
C11	O2	C10	N2	-175.31(0.17)
C10	O2	C11	C12	178.42(0.21)
C10	O2	C11	C13	-62.62(0.31)
C10	O2	C11	C14	61.57(0.27)
C16	O4	C15	O5	-8.58(0.31)
C16	O4	C15	N2	175.24(0.17)
C15	O4	C16	C17	58.21(0.29)
C15	O4	C16	C18	179.37(0.23)
C15	O4	C16	C19	-62.93(0.29)
C21	O6	C20	O7	4.48(0.57)
C21	O6	C20	C6	-174.12(0.33)
C20	O6	C21	C22	-171.81(0.48)
C20	O6	C21	C23	-60.97(0.57)
C20	O6	C21	C24	64.13(0.58)
C5	N1	C1	O1	172.66(0.21)
C5	N1	C1	C2	-11.78(0.32)
C6	N1	C1	O1	0.36(0.33)

[a]Numbers in parentheses are estimated standard deviations in the last digits.

Table 4.3 (cont'd)

Atom 1	Atom 2	Atom 3	Atom 4	Angle
C6	N1	C1	C2	175.92(0.21)
C1	N1	C5	C4	27.59(0.33)
C6	N1	C5	C4	-159.99(0.23)
C1	N1	C6	C7	106.98(0.24)
C1	N1	C6	C20	-127.04(0.23)
C5	N1	C6	C7	-65.85(0.27)
C5	N1	C6	C20	60.13(0.30)
C10	N2	C2	C1	-47.58(0.23)
C10	N2	C2	C3	82.25(0.22)
C15	N2	C2	C1	131.26(0.18)
C15	N2	C2	C3	-98.91(0.22)
C2	N2	C10	O2	151.48(0.17)
C2	N2	C10	O3	-25.34(0.28)
C15	N2	C10	O2	-27.23(0.27)
C15	N2	C10	O3	155.94(0.20)
C2	N2	C15	O4	156.79(0.16)
C2	N2	C15	O5	-19.58
C10	N2	C15	O4	-24.51(0.26)

Table 4.3 (cont'd)

Atom 1	Atom 2	Atom 3	Atom 4	Angle
C10	N2	C15	O5	159.12(0.19)
O1	C1	C2	N2	-34.09(0.27)
O1	C1	C2	C3	-162.77(0.20)
N1	C1	C2	N2	150.25(0.19)
N1	C1	C2	C3	21.57(0.29)
N2	C2	C3	C4	-173.99(0.20)
C1	C2	C3	C4	-46.94(0.28)
C2	C3	C4	C5	61.24(0.28)
C3	C4	C5	N1	-51.48(0.29)
N1	C6	C7	C8	-169.13(0.22)
N1	C6	C7	C9	-46.98(0.26)
C20	C6	C7	C8	67.32(0.29)
C20	C6	C7	C9	-170.52(0.22)
N1	C6	C20	O6	58.24(0.31)
N1	C6	C20	O6	-120.36(0.33)
C7	C6	C20	O6	-174.93(0.24)
C7	C6	C20	O7	6.47(0.41)

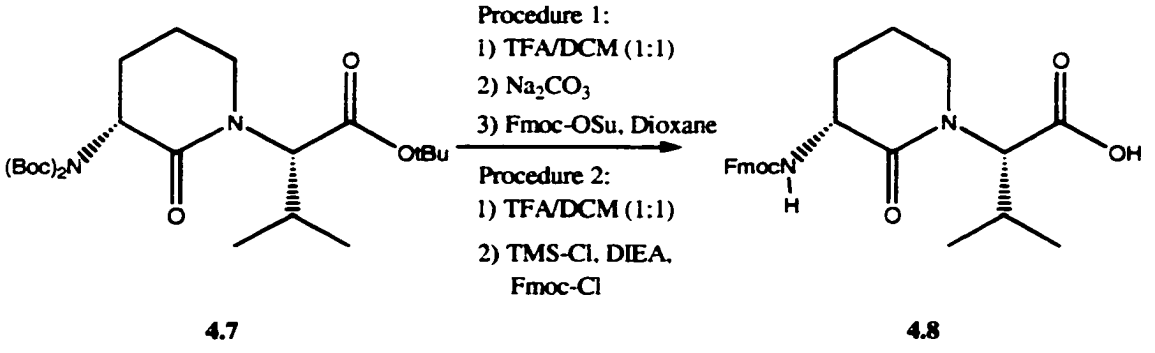

Figure 4.11. Synthetic routes to Fmoc protecting group introduction.

MALDI mass spectrometry and amino acid analysis, respectively. Figures 4.12 to 4.14 are representative examples of crude analytical and preparative scale HPLC chromatograms. Figure 4.15 shows the chromatogram of the purified peptide run on a C18 column. It should be noted that throughout the HPLC process, multiple peaks containing exact masses were obtained. We believe that this is indicative of peptide aggregation on the HPLC columns. Figures 4.16 and 4.17 show MALDI mass spectra of the crude and pure peptide, respectively.

Once the peptide was purified, circular dichroism spectroscopy was used to determine which secondary structure, if any, was present. Specifically, we were looking for a β-

sheet structure. β-Sheet peptides exhibit a minimum near 217 nm and a maximum near 195 nm representing $n \rightarrow \pi^*$ and $\pi \rightarrow \pi^*$ transitions, respectively. CD spectra were acquired in a variety of solvent conditions: 100% trifluoroethanol and 7mM phosphate buffer (at several pH's) to determine the solvent effect on secondary structure. In addition, the concentration of the peptide was varied from 50 μM to nearly 300 mM to see if there was a concentration dependence on structure. Representative CD spectra are shown in Figure 4.18. At relatively low peptide concentrations (50 to 500 μM), the peptide adopted a random coil conformation, regardless of solvent, pH or peptide concentration (Figures 4.20 and 4.21). In a random coil, a peptide exhibits a minimum near 197 nm ($\pi \rightarrow \pi^*$) and a maximum near 217 nm ($n \rightarrow \pi^*$). At relatively high peptide concentrations, no useful CD spectra were obtained; however, as the peptide concentration was lowered, a return to a random coil spectrum was observed (Figure 4.19). Clearly, a β-sheet dimer was not obtained using this peptide. It is possible that the large number of lysine residues relative to the number of DPU residues could disrupt the dimer formation due to the positive charge on the side-chain amino groups. However, when the pH was adjusted above the pKa of these amino groups, no observable shift to a β-sheet structure was observed. Another possibility is that the minimum number of DPU residues needed to nucleate β-sheet dimer formation has not been reached. If this were the case, other peptides would need to be synthesized, with increasing numbers of DPU residues, until the β-sheet dimer is observed. An interim solution would be to synthesize a small peptide that incorporates a β-turn. This would result in the formation of an intramolecular dimer rather than the desired intermolecular dimer, but it would provide useful information to characterize the β-sheet dimer.

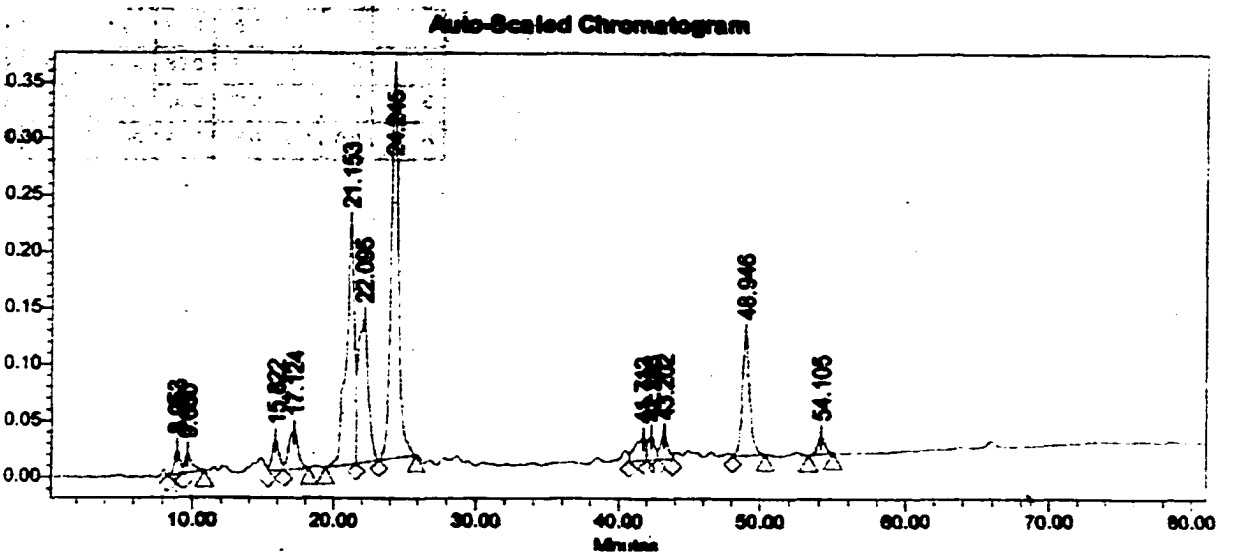

Figure 4.12. Analytical scale HPLC chromatogram of crude target peptide prior to ether wash.

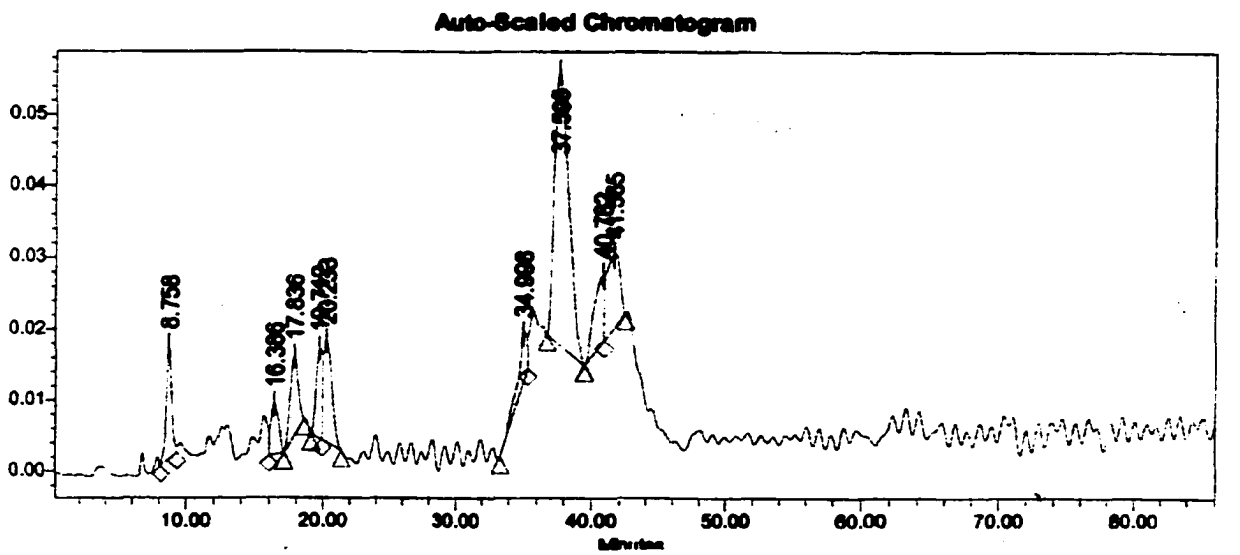

Figure 4.13. Analytical scale HPLC chromatogram of crude target peptide.

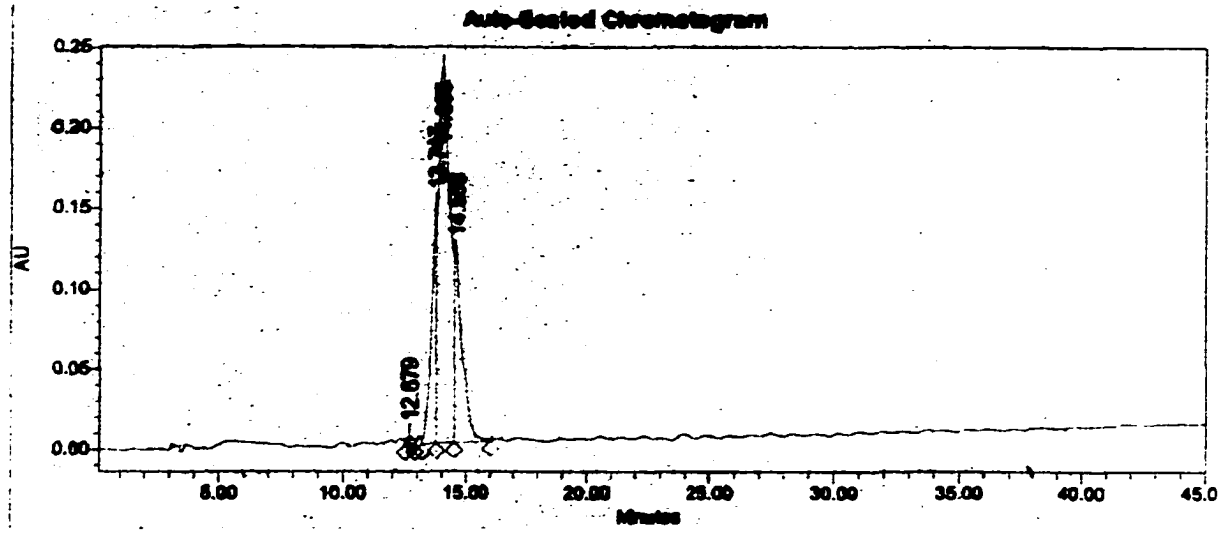

Figure 4.14. Preparative scale HPLC chromatogram of crude target peptide.

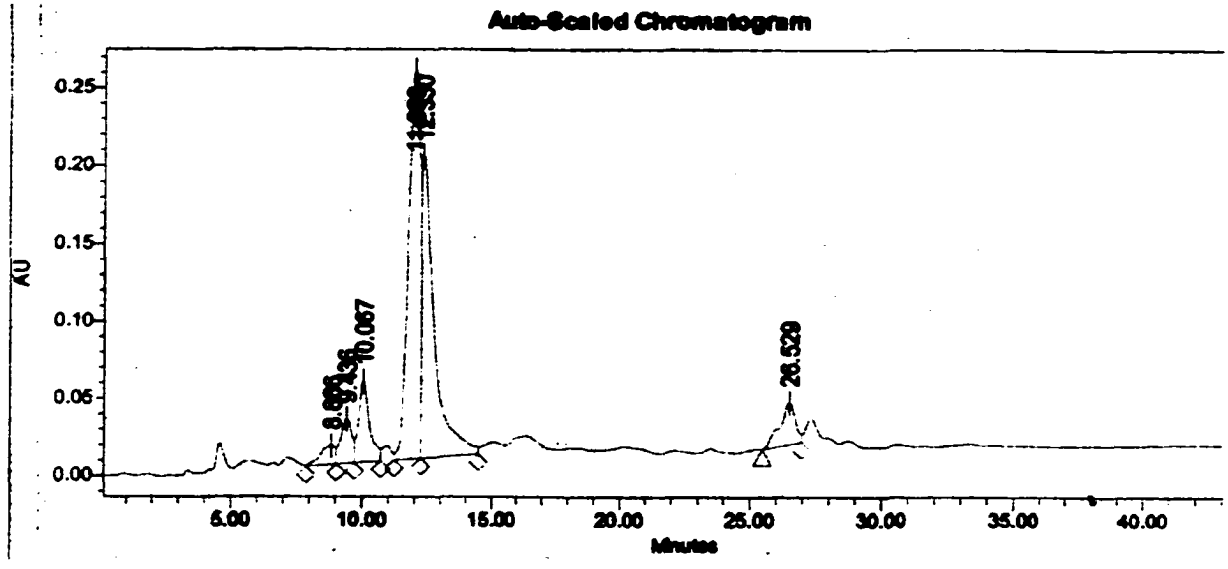

Figure 4.15. Analytical scale HPLC chromatogram of pure target peptide.

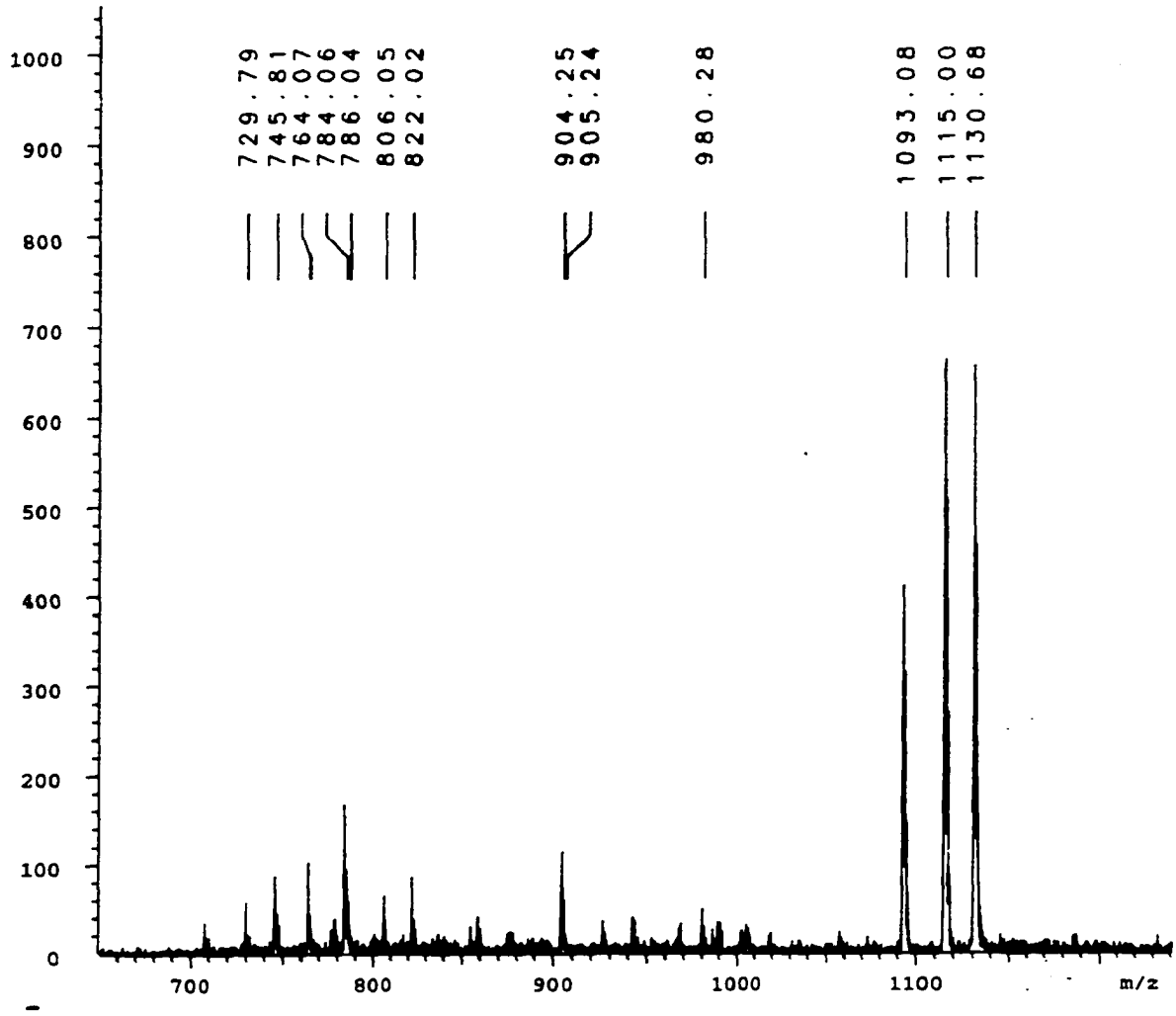

Figure 4.16. MALDI mass spectrum of crude target peptide.

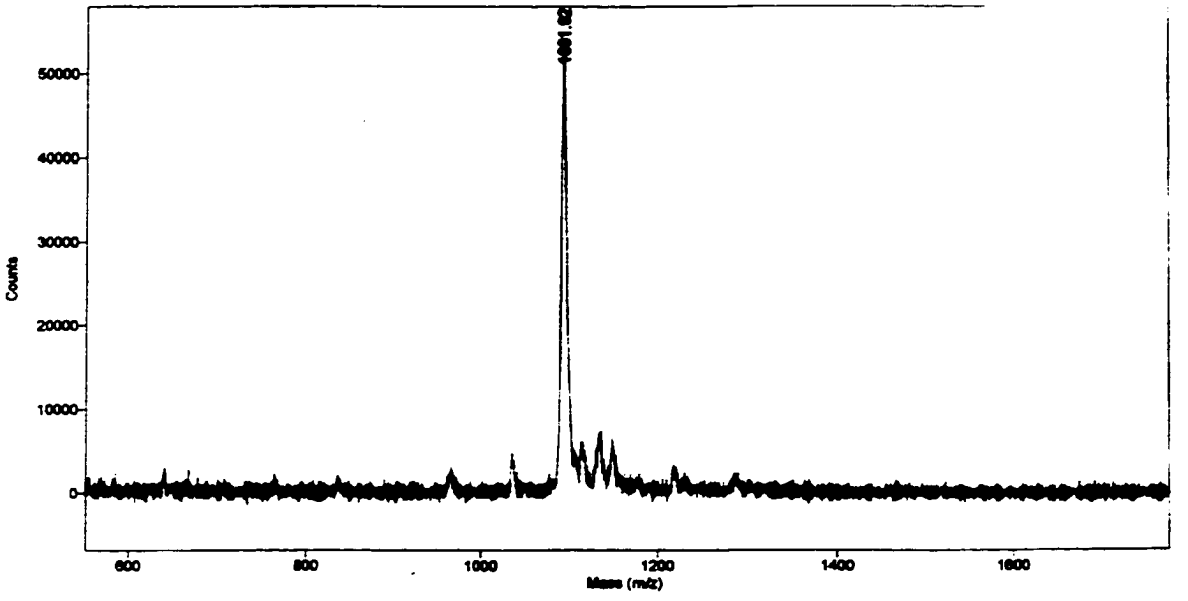

Figure 4.17. MALDI mass spectrum of pure target peptide.

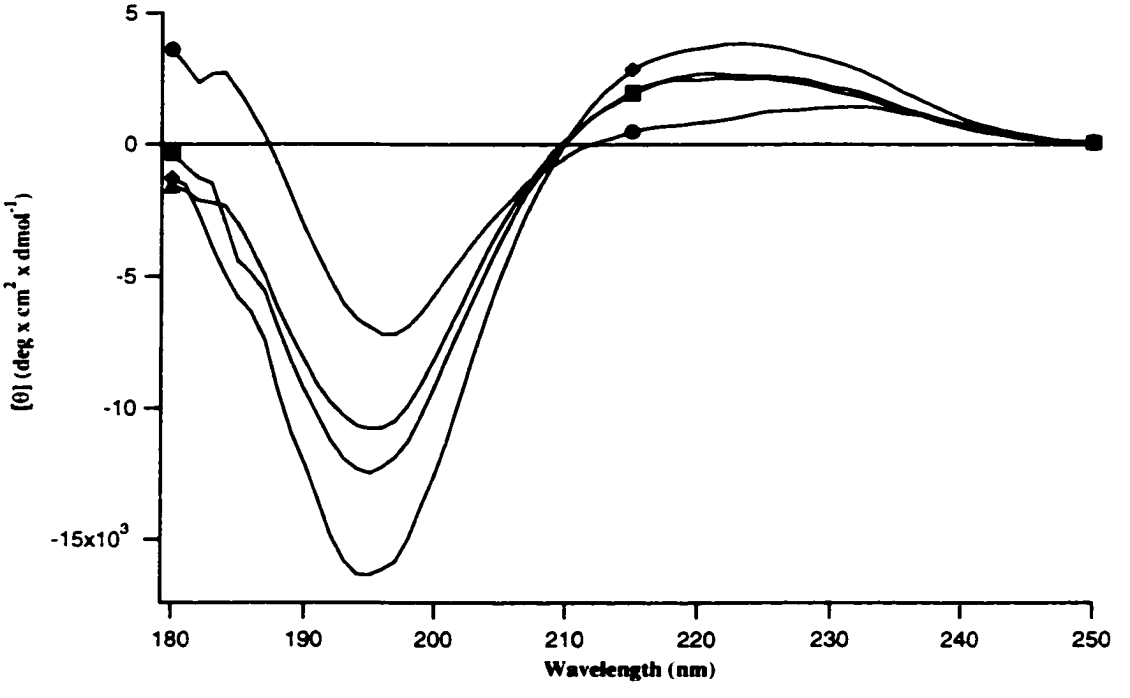

Figure 4.18. CD spectra of target peptide (200μM) in TFE (●), pH 7 phosphate buffer (■), pH 10 phosphate buffer (▲) and pH 10.5 phosphate buffer (♦).

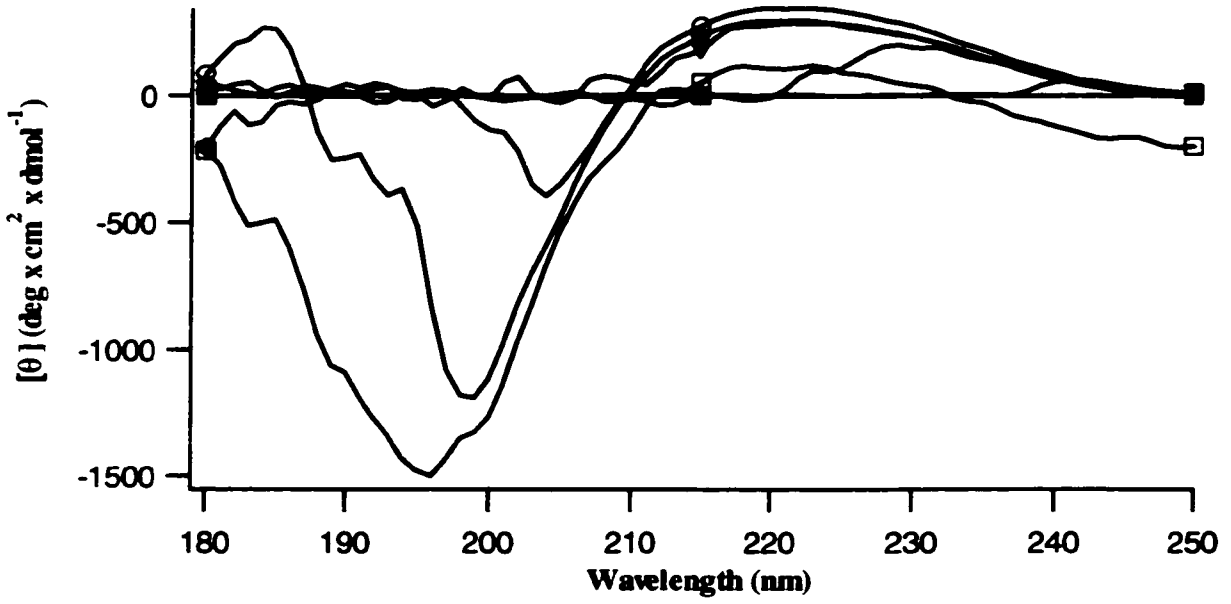

Figure 4.19. CD spectra of target peptide in water at 280mM (●), 140mM (■), 50mM (▲), 25mM (▼), 12mM (♦), 6mM (○), 3mM (□).

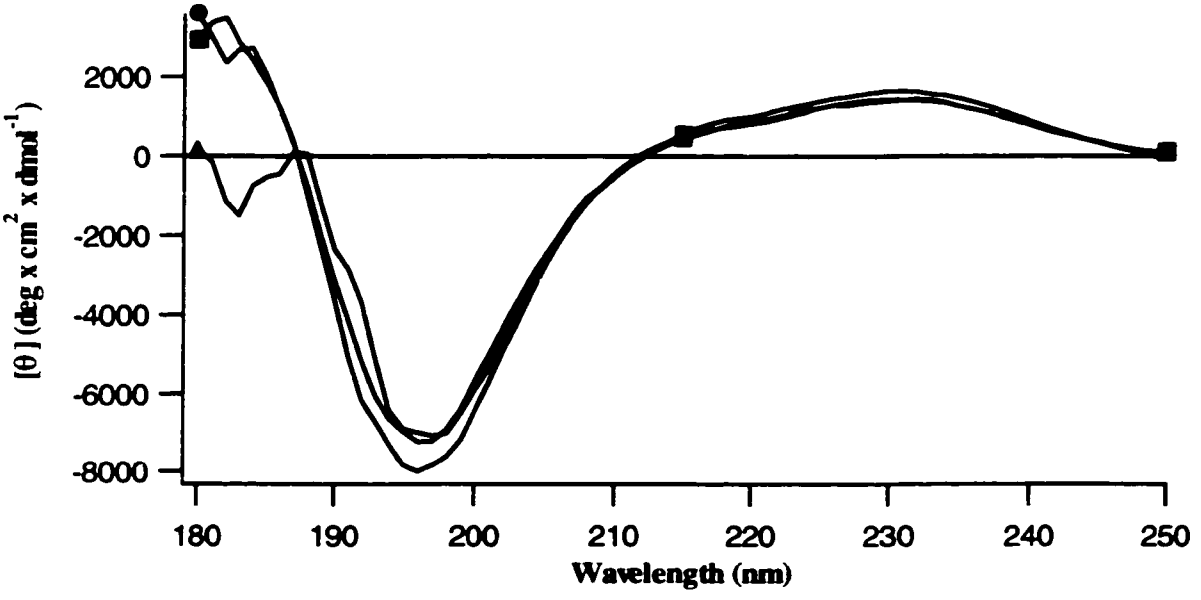

Figure 4.20. CD spectra of target peptide in TFE at 595μM (▲), 297μM (■), 200μM (●).

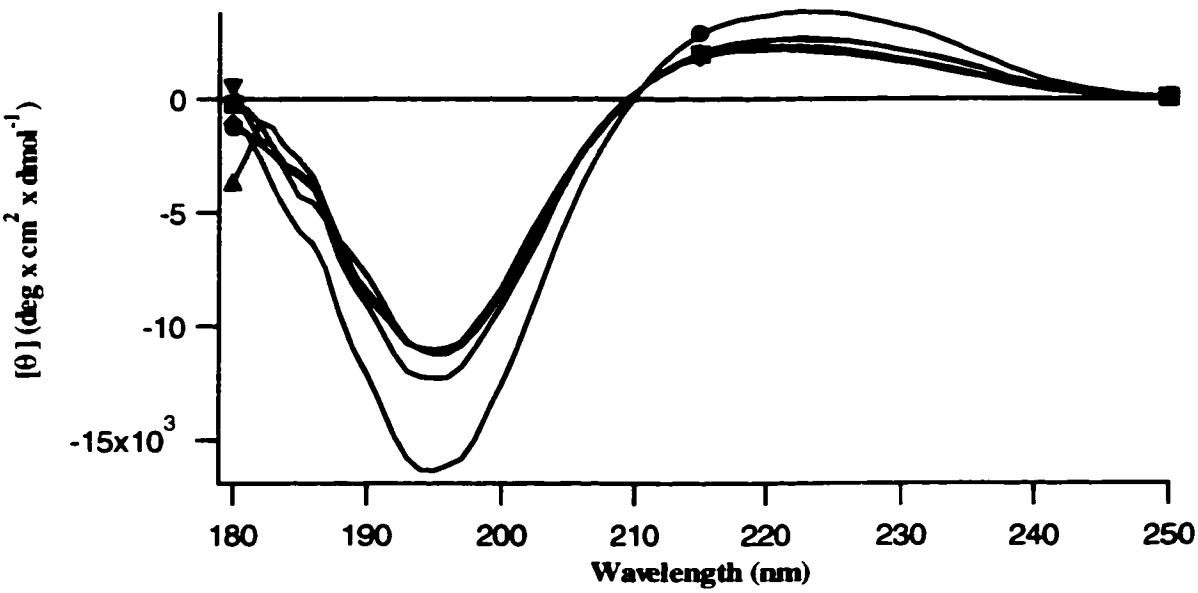

Figure 4.21. CD spectra of target peptide in pH 10.5 phosphate buffer at 400μM (♦), 350μM (▼), 300μM (▲), 250μM (■), 200μM (●).

4.3 Experimental

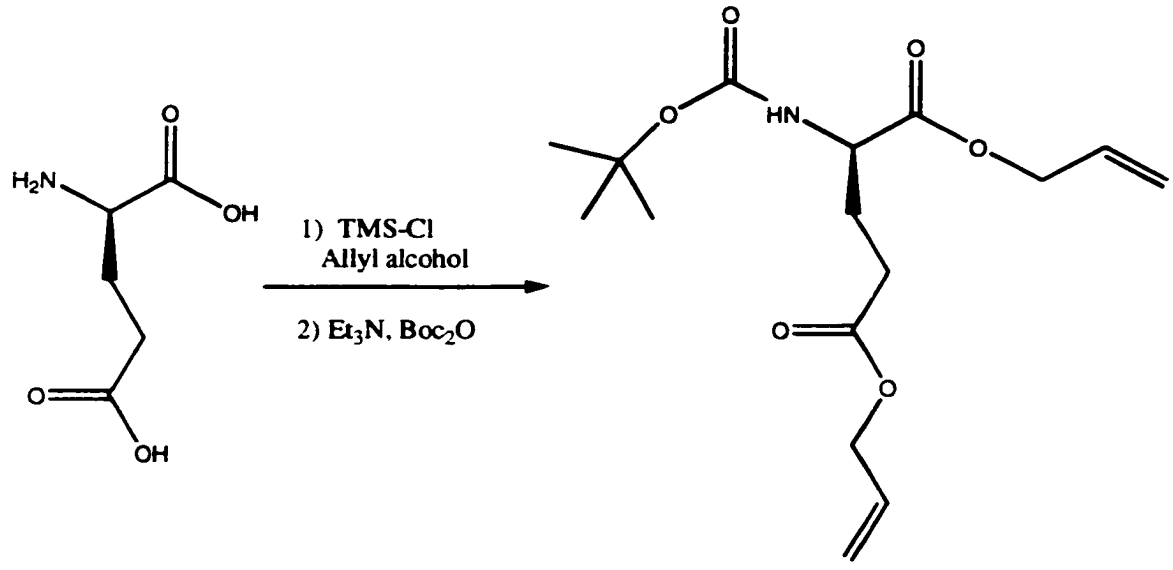

4.1 4.2

4.3.1 diallyl (R)-2-*tert*-butoxycarbonylaminopentanedioate (4.2)

To an ice cold stirred suspension of D-glutamic acid (**4.1**) in dry allyl alcohol (150 mL) was slowly added TMS-Cl (17.3 mL, 136 mmol, 4.4 equiv.). After the addition was completed, the ice bath was removed and the reaction was stirred at room temperature for three days. Triethylamine (31 mL, 221 mmol, 6.5 equiv.) and Boc_2O (8.2 g, 37.4 mmol, 1.1 equiv.) were added sequentially and the reaction mixture was stirred overnight. The solvent was removed under reduced pressure, the residue triturated with ethyl ether and filtered through a Celite pad. The solvent was evaporated yielding a yellow oil as the pure product (11.1 g, 100%). ^{1}H NMR (250 MHz, $CDCl_3$) δ 1.43 (s, 9H), 1.99 (m, 2H), 2.19 (m, 2H), 2.47 (m, 1H), 4.58 (d, 2H), 4.63 (d, 2H), 5.29 (m, 4H), 5.55 (d, 1H), 5.90 (m, 1H), 5.92 (m, 1H). ^{13}C NMR (62.5 MHz, $CDCl_3$) δ 27.19, 28.03, 30.01, 52.76, 64.95, 65.58, 79.41, 117.92, 118.38, 131.48, 131.94, 155.24, 171.66, 172.03. FAB-MS 328 $(M+H)^+$.

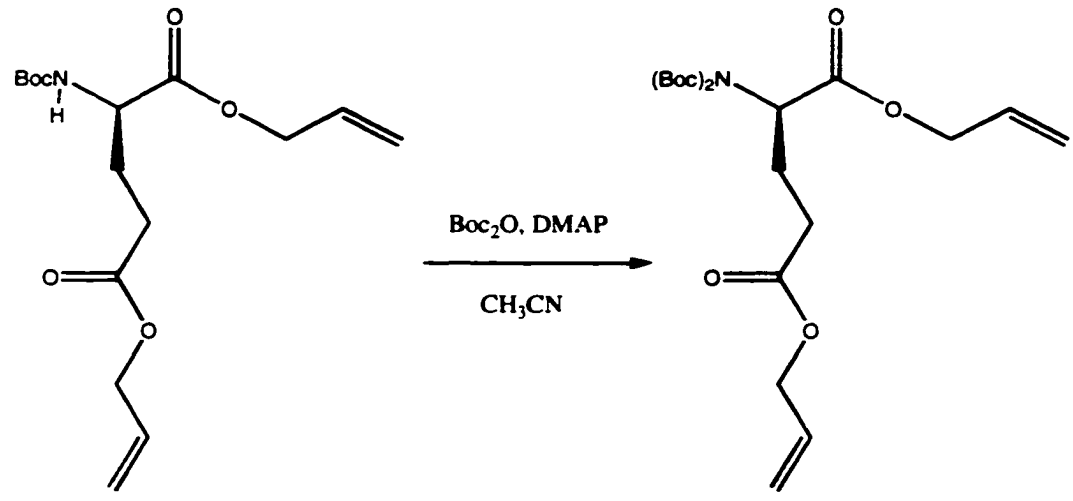

4.2 4.3

4.3.2 diallyl (2R)-2-*N*-[bis (*tert*-butyl)oxycarbonyl]amino}-pentanedioate (4.3)

To a stirred solution of **4.2** (5 g, 15.3 mmol) and DMAP (379 mg, 3.1 mmol, 0.2 equiv.) in dry acetonitrile (50 mL) was added Boc_2O (3.67 g, 16.8 mmol, 1.1 equiv.) at room temperature. After two hours, an additional 1.35 g Boc_2O and 379 mg DMAP were added and the red solution was allowed to stir overnight. The solvent was removed under reduced pressure and the residue taken up in hexanes/ethyl acetate (7:3). The crude product was purified by flash column chromatography to yield the pure product, **4.3**, as a yellow oil (6.17 g, 95%). ^1H NMR (250 MHz, $CDCl_3$) δ 1.49 (s, 18H), 2.20 (m, 2H), 2.45 (t, 1H), 2.50 (m, 2H), 4.58 (d, 2H), 4.61 (d, 2H), 5.28 (m, 4H), 5.88 (m, 1H), 5.93 (m, 1H). ^{13}C NMR (62.5 MHz, $CDCl_3$) δ 25.05, 28.08, 30.86, 57.52, 65.34, 65.88, 83.43, 118.27, 118.33, 131.86, 132.31, 152.11, 170.15, 172.44. FAB-MS 428 $(M+H)^+$. Anal. calcd for $C_{21}H_{33}NO_8$: C, 59.02; H, 7.73; N, 3.28. Found: C, 59.18; H, 7.70; N, 3.45.

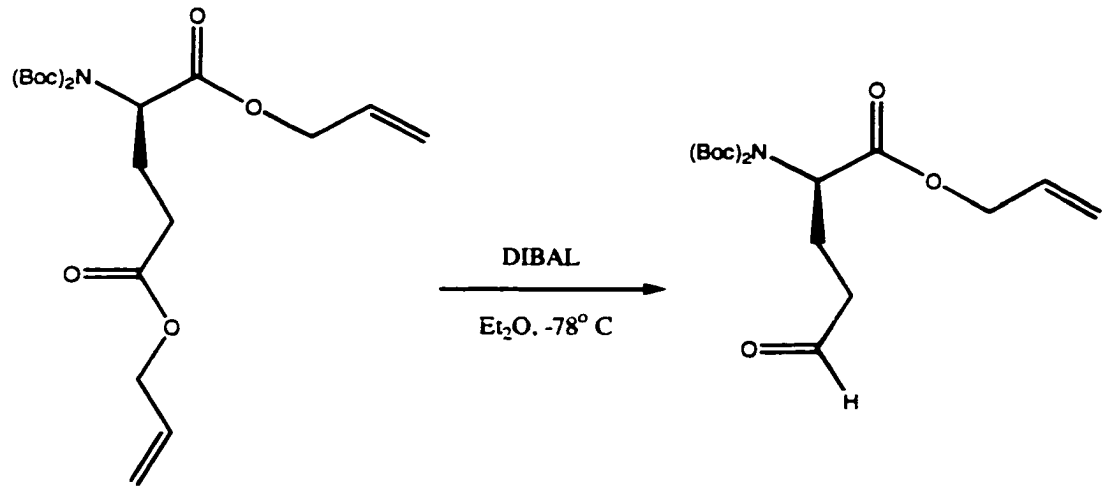

4.3 4.4

4.3.3 allyl (2R)-2-*N*-[bis (*tert*-butyl)oxycarbonyl]-amino}-5-oxopentanoate (4.4)

A solution of **4.3** (1 g, 2.34 mmol) in dry Et_2O was cooled to -78° C. DIBAL (3.51 mL, 1.0M in hexanes, 3.51 mmol, 1.5 equiv.) was slowly added over 10 minutes. The reaction was stirred for 30 minutes after the addition was completed and quenched with methanol (4 mL) and 10% $NaHSO_4$ (2mL). The mixture was stirred at room temperature for 30 minutes then extracted with 10% $NaHSO_4$ and the solvent evaporated to yield the product, **4.4**, as a yellow oil (0.84 g, 98%). ^1H NMR (200 MHz, $CDCl_3$) δ 1.49 (s, 18H), 2.18 (m, 2H), 2.54 (m, 2H), 2.56 (t, 1H), 4.62 (m, 2H), 4.91 (m, 1H), 5.27 (m, 2H), 9.78 (t, 1H). ^{13}C NMR (50 MHz, $CDCl_3$) δ 22.45, 28.09, 40.61, 57.55, 65.93, 83.57, 118.34, 131.84, 152.16, 170.07, 201.01. FAB-MS 372 $(M+H)^+$.

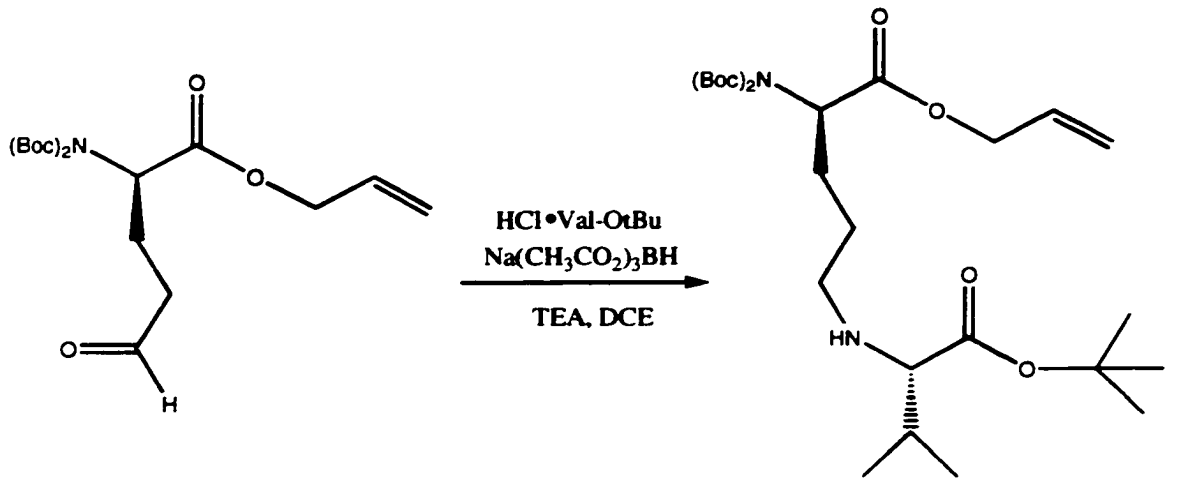

4.4 4.5

4.3.4 *tert*-butyl (2S)-2-*N*-1-[(5-allylcarboxylate)-(4R)-bis(*N'*, *N'*-*tert*-butyloxycarbonylamino)pentyl]-2-amino-3-methyl-butanoate (4.5)

Compound **4.4** (2 g, 5.39 mmol) and L-valine-OtBu (1.13 g, 5.39 mmol, 1 equiv.) were dissolved in dry DCE (100 mL) under argon. TEA (0.83 mL, 5.93 mmol, 1.1 equiv.) was added followed by sodium triacetoxyborohydride (0.97 g, 7.55 mmol, 1.4 equiv.). The mixture was stirred overnight then washed with saturated $NaHCO_3$ (3 x 50 mL). The organic layer was dried over Na_2SO_4 and evaporated. The residue was taken up in hexanes:ethyl acetate (4:1) and purified by flash column chromatography to yield **4.5**, a yellow oil (2.56 g, 90%). ^1H NMR (250 MHz, $CDCl_3$) δ 0.92 (d, 6H), 1.47 (s, 9H), 1.49 (s, 18H), 2.10 (m, 7H), 2.45 (t, 1H), 2.80 (d, 1H), 4.60 (d, 2H), 4.62 (m, 1H), 5.27 (m, 2H), 5.90 (m, 1H). ^{13}C NMR (62.5 MHz, $CDCl_3$) δ 18.92, 19.31, 27.21, 27.56, 28.13, 28.33, 31.84, 48.25, 58.29, 65.72, 68.08, 80.86, 83.11, 119.09, 132.03, 152.31, 170.71, 174.82. FAB-MS 529 $(M+H)^+$. Anal. calcd for $C_{27}H_{48}N_2O_8$: C, 59.34; H, 9.16; N, 5.13. Found: C, 59.34, H, 8.76; N, 5.05.

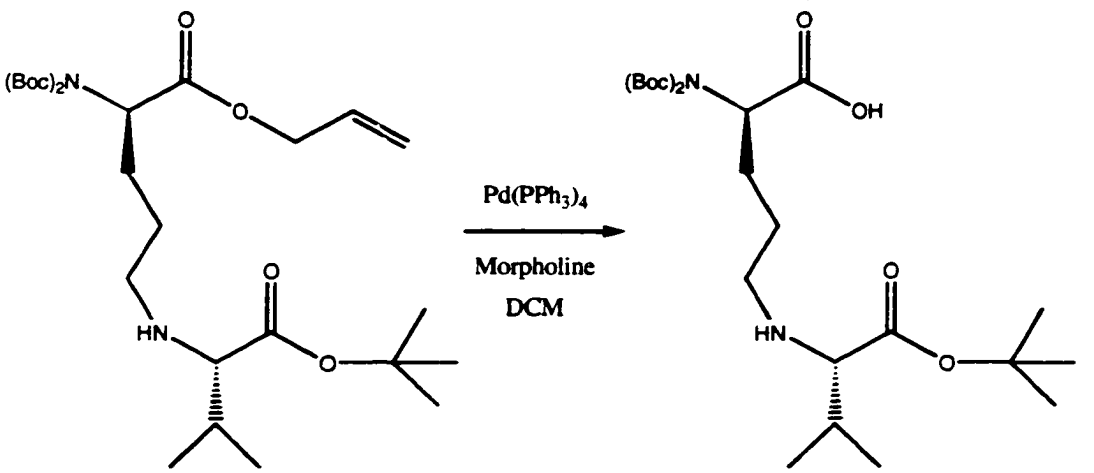

4.5 4.6

4.3.5 *tert*-butyl (2S)-2-*N*-1-[(5-carboxy)-(4R)-bis(*N'*, *N'-tert*-butyloxycarbonylamino) pentyl]-2-amino-3-methyl-butanoate (4.6)

Compound **4.5** (1.77 g, 3.35 mmol) was dissolved in dry DCM (30 mL) under argon. Morpholine (2.92 mL, 33.5 mmol, 10 equiv.) was added followed by $Pd(PPh_3)_4$ (0.42 g, 0.335 mmol, 0.1 equiv.). The solution was stirred for 30 minutes and then was washed with 1N HCl (2 x 50 mL). A precipitate formed which was kept with the organic layer. The organic layer is dried over Na_2SO_4 and evaporated to yield a yellow residue. The residue is taken up in $CHCl_3$:MeOH (9:1) and purified by flash column chromatography to yield **4.6**, a yellow oil (1.39 g, 85%). ^1H NMR (250 MHz, $CDCl_3$) δ 0.98 (m, 6H), 1.47 (s, 9H), 1.48 (s, 18H), 1.62 (m, 1H), 2.18 (m, 6H), 2.66 (m, 2H), 3.12 (d, 1H), 4.66 (m, 1H). ^{13}C NMR (62.5 MHz, $CDCl_3$) δ 18.27, 19.56, 26.37, 28.22, 28.34, 28.49, 30.93, 47.74, 50.92, 59.28, 66.96, 82.24, 82.76, 152.76, 172.08, 176.34. FAB-MS 489 $(M+H)^+$.

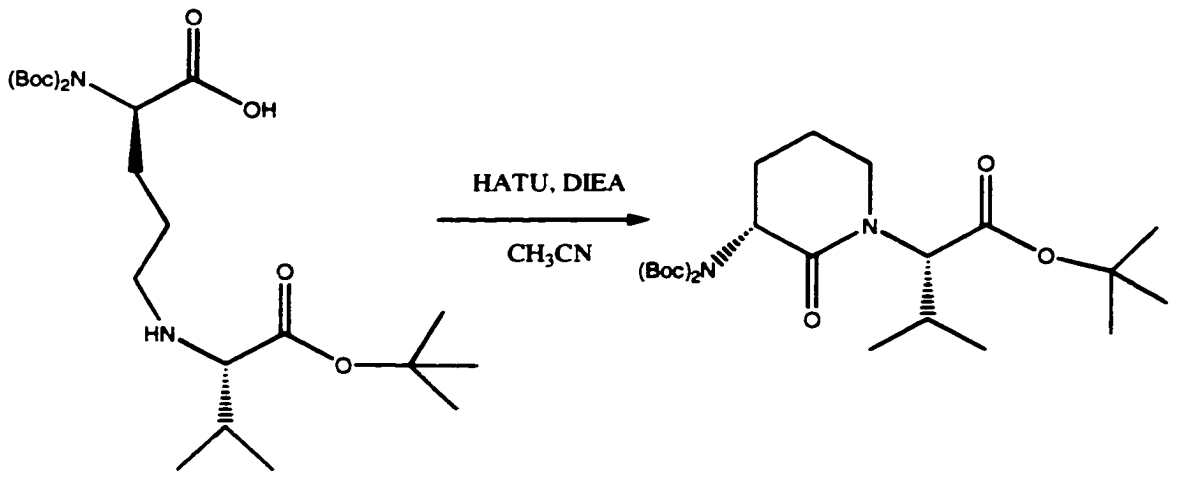

4.6 4.7

4.3.6 3-(R)-*N'*,*N'*-[1,1-dimethylethoxy)carbonyl]-amino-1-[1-(S)-methylethylethanoic acid]-2-piperidinone (4.7)

Compound **4.6** (1.05 g, 2.15 mmol) was dissolved in dry CH_3CN (15 mL) and kept under argon. HATU (0.82 g, 2.15 mmol, 1 equiv.) was added, followed by DIEA (0.79 mL, 4.52 mmol, 2.1 equiv.). The solution was stirred for 2 hours after which the solvent was removed under reduced pressure. The residue was taken up in hexanes:ethyl acetate (3:1) and purified by flash column chromatography to give **4.7** as a white solid (0.78 g, 77%). ^{1}H NMR (250 MHz, $CDCl_3$) δ 0.98 (m, 6H), 1.44 (s, 9H), 1.49 (s, 18H), 1.69 (m, 1H), 1.84 (m, 2H), 2.15 (m, 2H), 3.28 (m, 1H), 3.56 (m, 1H), 4.78 (m, 1H), 4.92 (d, 1H). ^{13}C NMR (62.5 MHz, $CDCl_3$) δ 19.49, 19.96, 22.84, 27.10, 27.94, 28.31, 43.85, 57.06, 61.99, 81.42, 82.71, 152.97, 168.45, 170.73. FAB-MS 472 (M+H)+. Anal. calcd for $C_{24}H_{42}N_2O_7$: C, 61.24; H, 9.00; N, 5.95. Found: C, 61.03; H, 8.65; N, 6.02.

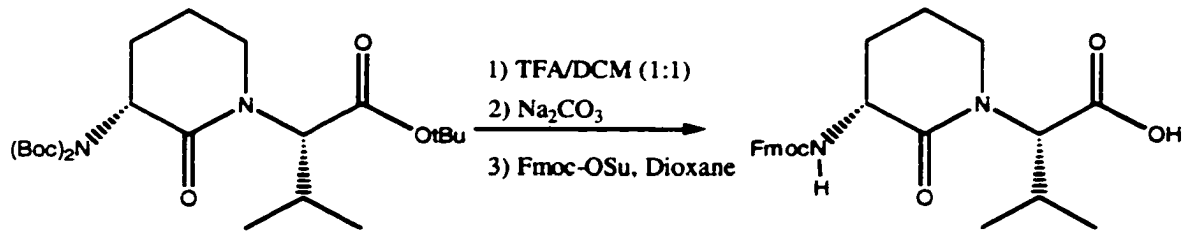

4.7 4.8

4.3.7 3-(R)-*N'*-[(9H-fluoren-9-ylmethoxy)carbonyl]-amino-1-[1-(S)-methylethylethanoic acid]-2-piperidinone

Compound **4.7** (1.32 g, 2.80 mmol) was treated with TFA/DCM (1:1, 5 mL) and stirred for 15 minutes. The solvent was evaporated and the resulting yellow oil was taken up in sufficient 9% Na_2CO_3 to give a solution with pH 9. The solution was cooled in an ice bath and a solution of Fmoc-OSu (0.99 g, 2.94 mmol, 1.05 equiv.) in dioxane (10 mL) was added. The solution was allowed to stir at room temperature for 2 hours after which the reaction mixture was diluted with water (100 mL). The reaction mixture was extracted with ether (1 x 50 mL) then with ethyl acetate (2 x 50 mL). The aqueous phase was cooled to 0° C, acidified to pH 2 with concentrated hydrochloric acid and then extracted with ethyl acetate (4 x 50 mL). The organic layer was dried over Na_2SO_4 and evaporated. The remaining clear oil is taken up in 1% acetic acid in $CHCl_3$/MeOH (9:1) and purified by flash column chromatography. The solvent was evaporated to yield **4.8** as an off white solid (0.62 g, 51%). ^{1}H NMR (250 MHz, $CDCl_3$) δ 0.96 (d, 3H), 1.09 (d, 3H), 1.28 (m, 1H), 2.07 (m, 2H), 2.45 (m, 2H), 3.47 (m, 2H), 4.26 (m, 3H), 4.41 (d, 1H), 5.86 (m, 1H), 7.52 (m, 8H). ^{13}C NMR (62.5 MHz, $CDCl_3$) δ 19.17, 19.99, 20.49, 26.61, 27.15, 45.08, 47.09, 51.79, 64.78, 67.08, 119.89, 125.16, 127.05, 127.65, 141.26, 143.81, 143.91, 156.34, 171.38, 173.43. FAB-MS 437 $(M+H)^+$.

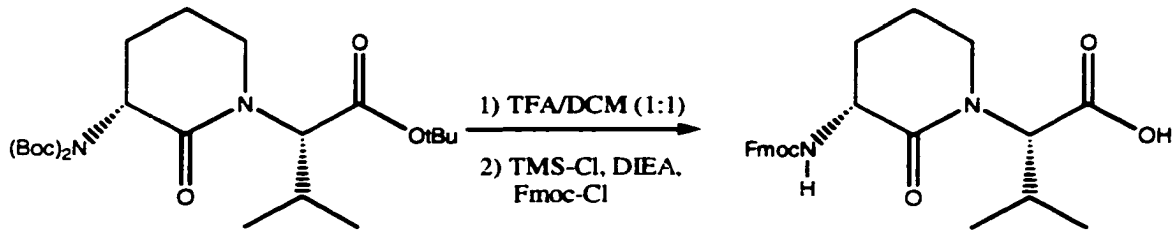

4.7 4.8

Alternative procedure for **4.8**. Compound **4.7** (1.72 g, 3.65 mmol) was treated with TFA/DCM (1:1, 5 mL) and stirred for 15 minutes. The solvent was evaporated and the resulting yellow oil was dissolved in dry DCM (30 mL). DIEA (1.97 mL, 11.3 mmol, 3.1 equiv.) was added and the solution cooled to 0° C. TMS-Cl (0.92 mL, 7.28 mmol, 2.0 equiv.) was added and the solution stirred for 2 hours. The solution was again cooled to 0° C and Fmoc-Cl (0.94 g, 3.64 mmol, 1.0 equiv.) dissolved in dry DCM (10 mL) was added. The reaction was stirred for 4 hours at room temperature after which the DCM was evaporated. The residue was taken up in 2.5% Na_2CO_3 (25 mL) and washed with ether (2 x 50 mL). The aqueous layer was cooled to 0° C and acidified to pH 2 using concentrated hydrochloric acid. The precipitated product is extracted with ethyl acetate (4 x 50 mL). The organic layer is dried over Na_2SO_4 and the solvent removed to yield a clear oil. The crude product is taken up in 1% acetic acid in $CHCl_3$/MeOH (9:1) and purified by flash column chromatography. The solvent was evaporated to yield **4.8** as an off white solid (1.37 g, 85%).

4.3.8 Peptide Synthesis

The peptide under study was synthesized via solid-phase peptide synthesis using a Milligen 9050 peptide synthesizer on PAL-PEG-PS solid support. Four equivalents of each amino acid, 3 equivalents of DIEA, 4 equivalents of HATU and a one-hour recycling time were used for the couplings. A solution of 20% piperidine/2% 1,8-diazobicyclo[4.5.0]undec-7-ene (DBU) in DMF was used for Fmoc removal. The peptide was acetylated on the solid support by treatment with a 0.2M solution of acetic anhydride in 0.28M DIEA in DMF for 40 minutes. The peptide was simultaneously cleaved from the resin and side-chain deprotected using reagent B, TFA, triisopropylsilane, water, phenol (8.8:0.2:0.5:0.5).[4.30] The resulting acidic solution was diluted with 30% acetic acid, washed with ether (4 x 50 mL) and lyophilized. The crude peptide was purified by preparative reverse-phase HPLC on a Waters 15 μM Deltapak C_4 column using a water (0.05% TFA) and acetonitrile (0.05% TFA) gradient system. The gradient was run from 10% to 70% organic and the absorption monitored at 222 nm. Purity of the peptide was checked on a Vydac 5 μM C_{18} column using the same conditions. Matrix assisted laser desorption ionization (MALDI) mass spectrometry was used to verify peptide mass, 1093 $(M+H)^+$.

4.4 References

4.1 Creighton, T.E., *Proteins*. 1993, New York: W. H. Freeman and Company.

4.2 Brack, A. and Orgel, L.E., *Nature*, **1975,** *256*, 383-385.

4.3 DeGrado, W.F. and Lear, J.D., *J. Am. Chem. Soc.*, **1985,** *107*, 7684-7691.

4.4 McWilliams, K. and Kelly, J.W., *J. Org. Chem.*, **1996,** *61*, 7408-7414.

4.5 Tsang, K.Y., Diaz, H., Graciani, N., and Kelly, J.W., *J. Am. Chem. Soc.*, **1994,** *116*, 3988-4005.

4.6 Doig, A.J., *Chem. Commun.*, **1997**, 2153-2154.

4.7 Chitnumsub, P., Fiori, W.R., Lasheul, H.A., Diaz, H., and Kelly, J.W., *Bioorg. Med. Chem.*, **1999,** *7*, 39-59.

4.8 Sharman, G.J. and Searle, M.S., *J. Am. Chem. Soc.*, **1998,** *120*, 5291-5300.

4.9 Stranger, H.E. and Gellman, S.H., *J. Am. Chem. Soc.*, **1998,** *120*, 4236-4237.

4.10 Tsai, J.H., Waldman, A.S., and Nowick, J.S., *Bioorg. Med. Chem.*, **1999,** *7*, 29-38.

4.11 Soth, M.J. and Nowick, J.S., *J. Org. Chem.*, **1999,** *64*, 276-281.

4.12 Gellman, S.H., *Curr. Opin. Chem. Biol.*, **1998,** *2*, 717-725.

4.13 Freidinger, R.M., Perlow, D.S., and Veber, D.F., *J. Org. Chem.*, **1982,** *47*, 104-109.

4.14 Estiarte, M.A., de Sousa, M.V.N., del Rio, X., Dodd, R.H., Rubiralta, M., and Diez, A., *Tetrahedron*, **1999,** *55*, 10173-10186.

4.15 Piro, J., Rubiralta, M., Giralt, E., and Diez, A., *Tet. Lett.*, **1999,** *40*, 4865-4868.

4.16 Griesbeck, A.G., Heckroth, H., and Schmickler, H., *Tet. Lett.*, **1999,** *40*, 3137-3140.

4.17 Semple, J.E., *Tet. Lett.*, **1998,** *39*, 6645-6648.

4.18 Wyss, C., Batra, R., Lehmann, C., Sauer, S., and Giese, B., *Angwe. Chem. Int. Ed. Engl.*, **1996,** *35*, 2529-2531.

4.19 Zydowsky, T.M., Dellaria, J.F., and Nellans, H.N., *J. Org. Chem.*, **1988,** *1988*, 5607-5616.

4.20 Moss, N., Beaulieu, P., Duceppe, J.-S., Ferland, J.-M., Gauthier, J., Ghiro, E., Goulet, S., Guse, I., Llinas-Bruntet, M., Plante, R., Plamondon, L., Wernic, D., and Deziel, R., *J. Med. Chem.*, **1996,** *39*, 2178-2187.

4.21 Chou, P.Y. and Fasman, D.G., *Adv. Enzymol.*, **1978,** *47*, 45-148.

4.22 Kim, C.A. and Berg, J.M., *Nature*, **1993,** *362*

4.23 Smith, C.K. and Regan, L., *Science*, **1995,** *270*, 980-982.

4.24 Padron, J.M., Kokotos, G., Martin, T., Markidis, T., Gibbons, W.A., and Martin, V.S., *Tetrahedron Assym.*, **1998,** *9*, 3381-3394.

4.25 Abdel-Magid, A.F., Carson, K.G., Harris, B.D., Maryanoff, C.A., and Shah, R.D., *J. Org. Chem.*, **1996,** *61*, 3849-3862.

4.26 Waldmann, H. and Kunz, H., *Angew. Chem. Int. Ed. Engl.*, **1984,** *23*, 71-73.

4.27 Kunz, H. and Marz, J., *Angew. Chem. Int. Ed. Engl.*, **1988,** *27*, 1375-1377.

4.28 Lapatsanis, L., Milias, G., Froussios, K., and Kolovos, M., *Synthesis*, **1983**, 671-673.

4.29 Bolin, D.R., Sytwu, I.-I., Humiec, F., and Meinenhofer, J., *Int, J. Pept. Protein Res.*, **1989**, 353-359.

4.30 Van Abel, R.J., Tang, Y., Rao, V.S.V., Dobbs, C.H., Tran, D., Barany, G., and Selsted, M.E., *Int. J. Pept. Protein Res.*, **1995,** *45*, 401-409.

Chapter 5

Summary and Future Studies

5.1 Summary and Future Studies

This dissertation focused on the synthesis and studies of helical peptides and the synthesis of an amino acid designed to nucleate β-sheet dimer formation. The short, helical peptides were rich in α, α-disubstituted amino acids (ααAA's) and designed to be amphipathic. Helix preferences of the peptides in several solvent systems were studied as was antimicrobial activity. A peptide utilizing the constrained lactam dipeptide amino acid was synthesized and studied for β-sheet dimer formation.

Chapter 2 outlined the synthesis of short, amphipathic helical peptides. The helix type and percent helicity of the peptides was determined using circular dichroism spectroscopy. In addition, *in vivo* and *in vitro* studies were done to determine the effectiveness of the peptides in eliminating intracellular pathogens. The peptides were synthesized to determine if short, amphipathic peptides would exhibit increased biological activity against bacteria versus mammalian cells. It has been shown that shorter peptides are more selective and more helical peptides are more active.[5.1-5.4]

To increase the helicity of the peptides, ααAA's were used.[5.5-5.7] Pre-formed acid fluorides of α-aminoisobutyric acid (Aib), 1-aminocyclohexanecarboxylic acid (Cyh) and 4-aminopiperidine-4-carboxylic acid (Api) were used in the synthesis.[5.8-5.9] The use of Api allowed a polar ααAA to be used on the polar face of the amphipathic peptides. Once synthesized, the peptides were tested *in vitro* for direct antimicrobial activity against *E. coli* and *S. aureus*. All of the peptides showed good activity against *E.*

coli while the more hydrophobic peptides, Cyh-10 and Ich-10 had excellent activity against *S. aureus*. Several of the peptides were tested against macrophages infected with intracellular pathogens. *In vivo* and *in vitro* studies were done to evaluate the effectiveness of several peptides in eliminating these pathogens. *B. abortus* and *M. chelonei* were used as representative intracellular pathogens. Pi-10 and Ich-10 significantly reduced the *B. abortus* load in BALB/c mice. Pi-10 showed a 90% *B. abortus* reduction with a single dose of 500 μg whereas Ich-10 showed an 82% *B. abortus* reduction with a single dose of 25 μg.

Brucella abortus expressing a green fluorescent protein and *Mycobacterium chelonei* were used to test if Pi-10 is selective in destroying only infected macrophages. Using these bacteria, infected macrophages can be visualized easily. Trypan blue exclusion identifies dead macrophages. Test results were promising. Further studies need to be done to improve control over the number of macrophages infected. In addition, fluorescently labeled peptides should be synthesized to determine the binding affinity of the peptides for infected versus non-infected macrophages.

Chapter 3 outlines the solvent effects on the helix preferences of a series of amphipathic peptides. Pi-10 and Cyh-10 were designed to be amphipathic α-helical peptides while Ipi-10 and Ich-10 were designed to be amphipathic 3_{10}-helical peptides. All peptides contained 80% ααAA's.

According to the literature, Pi-10 and Cyh-10 should display CD spectra typical for a 3_{10}-helix in SDS micelles due to their high ααAA content and the position of the proteinogenic amino acids.[5.5, 5.10] Instead, both peptides formed an α-helix in SDS micelles, demonstrating the importance of amphipathy in determining helix preference.

Ipi-10, a sequence permutation isomer of Pi-10, showed the expected 3_{10}-helix spectrum. Ich-10, a sequence permutation isomer of Cyh-10, did not display a 3_{10}-helix spectrum as anticipated. Instead, a spectrum indicative of an α-helix was observed. It is theorized that the side-chains of the cyclohexyl amino acid residues are sterically congested in a 3_{10}-helix, forcing the peptide to adopt an α-helix conformation.

Various organic and aqueous/organic solvent systems were studied to determine the effects on helix preferences. Pi-10 and Cyh-10 displayed α-helix spectra in all solvent systems. As expected, Ipi-10 adopted a 3_{10}-helix structure in 100% organic solvent but shifted to an α-helix as the water content increases. As in SDS micelles, Ich-10 adopted an α-helix conformation in all solvent systems tested. The demonstration that amphipathy, rather than ααAA content, controls helix preference can be further investigated by altering the sequence of Ich-10 to reduce the steric hinderance of the side-chains.

Chapter 4 described the synthesis of 3-(R)-*N'*-[(9H-fluoren-9-ylmethoxy)carbonyl]-amino-1-[1-(S)-methylethylethanoic acid]-2-piperidinone, a constrained lactam dipeptide amino acid. The amino acid was synthesized to incorporate into peptides designed to form intermolecular β-sheet dimers. The amino acid was synthesized beginning with the complete allyl esterification and double nitrogen protection of D-glutamic acid. The key step in the sequence is the selective DIBAL reduction of the side-chain allyl ester to the aldehyde.[5.11] A reductive amination with L-valine-OtBu is carried out followed by removal of the remaining allyl ester. Cyclization of the amino acid followed by removal of the α-nitrogen protecting groups and *tert*-butyl

ester on the valine moiety yielded the free constrained lactam dipeptide amino acid. Protection of the α-nitrogen with the Fmoc group gives the target amino acid ready for peptide synthesis.

The target amino acid was incorporated into a peptide pre-designed to form a β-sheet dimer. The structure of the peptide was studied in various solvents, pH levels and concentrations. Unfortunately, only random coil spectra were observed. It is possible that the minimum number of constrained lactam dipeptide amino acids has not been reached. Future studies should concentrate on synthesizing a series of peptides, each with increasing numbers of constrained lactam dipeptide amino acid residues. These peptides can then be studied to determine the minimum number of constrained lactam dipeptide amino acid residues needed to nucleate β-sheet dimer formation. It would also prove helpful to synthesize a peptide containing a β-turn. D-proline-glycine is a known β-turn.[5.12, 5.13] Using this β-turn would result in an intramolecular β-sheet dimer, rather than intermolecular, but it would aid greatly in the characterization of a β-sheet dimer.

5.2 References

5.1 Javadpour, M.M., Juban, M.M., Lo, W.J., Bishop, S.M., Alberty, J.B., Cowell, S.C., Becker, C.L., and McLaughlin, M.L., *J. Med. Chem.*, **1996,** *39*, 3107-3113.

5.2 Bessalle, R., Gorea, A., Shalit, I., Metzger, J.W., Dass, C., Desiderio, D.M., and Fridkin, M., *J. Med. Chem.*, **1993,** *36*, 1203-1209.

5.3 Andreu, D., Ubach, J., Boman, A., Wahlin, B., Wade, D., Merrifield, R.B., and Boman, H.G., *FEBS Lett.*, **1992,** *296*, 190-193.

5.4 Blondelle, S.E. and Houghten, R.A., *Biochemistry*, **1992,** *31*, 12688-12694.

5.5 Karle, I.L. and Balaram, P., *Biochemistry*, **1990,** *29*, 6747-6756.

5.6 Benedetti, E., *Biopolymers (Peptide Sci.)*, **1996,** *40*, 3-44.

5.7 Balaram, P., *Curr. Opin. Struct. Biol.*, **1992,** *2*, 845-851.

5.8 Wenschuh, H., Beyermann, M., Krause, E., Brudel, M., Winter, R., Schumann, M., Carpino, L., and Bienert, M., *J. Org. Chem.*, **1994,** *59*, 3275-3280.

5.9 Wenschuh, H., Beyermann, M., Haber, H., Seydel, J.K., Krause, E., Bienert, M., Carpino, L., El-Faham, A., and Albericio, F., *J. Org. Chem.*, **1995,** *60*, 405-410.

5.10 Basu, G., Bagchi, K., and Kuki, A., *Biopolymers*, **1991,** *31*, 1763-1774.

5.11 Padron, J.M., Kokotos, G., Martin, T., Markidis, T., Gibbons, W.A., and Martin, V.S., *Tetrahedron Assym.*, **1998,** *9*, 3381-3394.

5.12 Das, C., Raghothama, S., and Balaram, P., *J. Am. Chem. Soc.*, **1998,** *120*, 5812-5813.

5.13 Stranger, H.E. and Gellman, S.H., *J. Am. Chem. Soc.*, **1998,** *120*, 4236-4237.

Vita

Ted Joseph Gauthier was born on November 7, 1963, in Cottonport, Louisiana. After graduating as valedictorian from Plaucheville High School in 1981, he attended Louisiana State University where he earned a bachelor's degree in 1985, majoring in finance. After working for a year in the banking field, he returned to Louisiana State University to complete work on a master's degree, also in finance. He worked in the banking industry in Texas, Louisiana and Florida for five years before returning to Louisiana State University to pursue a career in chemistry. In 1995, he completed his bachelor's degree in chemistry and started his work in a doctoral program. After receiving the degree of Doctor of Philosophy, he will be employed by Rohm and Haas in Spring House, Pennsylvania.

DOCTORAL EXAMINATION AND DISSERTATION REPORT

Candidate: Ted Gauthier

Major Field: Chemistry

Title of Dissertation: Structure and Function Studies of De Novo Peptides Containing Novel Amino Acids

Approved:

Major Professor and Chairman

Dean of the Graduate School

EXAMINING COMMITTEE:

Date of Examination:

July 14, 2000